Natural Resources Canada | Ressources naturelles Canada

GEOLOGICAL SURVEY OF CANADA
OPEN FILE 8931

Current research on slow-moving landslides in the Thompson River valley, British Columbia (IMOU 5170 annual report)

D. Huntley, D. Rotheram-Clarke, R. Cocking, J. Joseph, and P. Bobrowsky

2022

Canada

ISSN 2816-7155
ISBN 978-0-660-46252-3
Catalogue No. M183-2/8931E-PDF

GEOLOGICAL SURVEY OF CANADA
OPEN FILE 8931

Current research on slow-moving landslides in the Thompson River valley, British Columbia (IMOU 5170 annual report)

D. Huntley[1], D. Rotheram-Clarke[1], R. Cocking[1], J. Joseph[1], and P. Bobrowsky[2]

[1]Geological Survey of Canada, 1500-605 Robson Street, Vancouver, British Columbia
[2]Geological Survey of Canada, 9860 West Saanich Road, Sidney, British Columbia

2022

Permanent link: https://doi.org/10.4095/331175

This publication is available for free download through GEOSCAN (https://geoscan.nrcan.gc.ca/).

Recommended citation

Huntley, D., Rotheram-Clarke, D., Cocking, R., Joseph, J., and Bobrowsky, P., 2022. Current research on slow-moving landslides in the Thompson River valley, British Columbia (IMOU 5170 Annual Report); Geological Survey of Canada, Open File 8931, 67 p. https://doi.org/10.4095/331175

Publications in this series have not been edited; they are released as submitted by the author.

Abstract

Interdepartmental Memorandum of Understanding (IMOU) 5170 between Natural Resources Canada (NRCAN), the Geological Survey of Canada (GSC) and Transport Canada Innovation Centre (TC-IC) aims to gain new insight into slow-moving landslides, and the influence of climate change, through testing conventional and emerging monitoring technologies. IMOU 5107 focuses on strategically important sections of the national railway network in the Thompson River valley, British Columbia (BC), and the Assiniboine River valley along the borders of Manitoba (MN) and Saskatchewan (SK). Results of this research are applicable elsewhere in Canada (e.g., the urban-rural-industrial landscapes of the Okanagan Valley, BC), and around the world where slow-moving landslides and climate change are adversely affecting critical socio-economic infrastructure. Open File 8931 outlines landslide mapping and change-detection monitoring protocols based on the successes of IMOU 5170 and ICL-IPL Project 202 in BC. In this region, ice sheets, glaciers, permafrost, rivers and oceans, high relief, and biogeoclimatic characteristics contribute to produce distinctive rapid and slow-moving landslide assemblages that have the potential to impact railway infrastructure and operations. Bedrock and drift-covered slopes along the transportation corridors are prone to mass wasting when favourable conditions exist. In high-relief mountainous areas, rapidly moving landslides include rock and debris avalanches, rock and debris falls, debris flows and torrents, and lahars. In areas with moderate to low relief, rapid to slow mass movements include rockslides and slumps, debris or earth slides and slumps, and earth flows. Slow-moving landslides include rock glaciers, rock and soil creep, solifluction, and lateral spreads in bedrock and surficial deposits. Research efforts lead to a better understanding of how geological conditions, extreme weather events and climate change influence landslide activity along the national railway corridor. Combining field-based landslide investigation with multi-year geospatial and *in-situ* time-series monitoring leads to a more resilient railway national transportation network able to meet Canada's future socioeconomic needs, while ensuring protection of the environment and resource-based communities from landslides related to extreme weather events and climate change. InSAR only measures displacement in the east-west orientation, whereas UAV and RTK-GNSS change-detection surveys capture full displacement vectors. RTK-GNSS do not provide spatial coverage, whereas InSAR and UAV surveys do. In addition, InSAR and UAV photogrammetry cannot map underwater, whereas boat-mounted bathymetric surveys reveal information on channel morphology and riverbed composition. Remote sensing datasets, consolidated in a geographic information system, capture the spatial relationships between landslide distribution and specific terrain features, at-risk infrastructure, and the environmental conditions expected to correlate with landslide incidence and magnitude. Reliable real-time monitoring solutions for critical railway infrastructure (e.g., ballast, tracks, retaining walls, tunnels, and bridges) able to withstand the harsh environmental conditions of Canada are highlighted. The provision of fundamental geoscience and baseline geospatial monitoring allows stakeholders to develop robust risk tolerance, remediation, and mitigation strategies to maintain the resilience and accessibility of critical transportation infrastructure, while also protecting the natural environment, community stakeholders, and Canadian economy. We propose a best-practice solution involving three levels of investigation to describe the form and function of the wide range of rapid and

slow-moving landslides occurring across Canada that is also applicable elsewhere. Research activities for 2022 to 2025 are presented by way of conclusion.

Keywords
Geological Hazards, Climate Change, Landslide Monitoring, Railway Infrastructure, Disaster Risk Reduction, Thompson River, British Columbia, Assiniboine River, Manitoba-Saskatchewan

1. Introduction

Historically, Canada's national railway network has been the dominant mode for exporting natural resources (e.g., coal, oil, grain, potash, forest products) to deep-water marine terminals; and for intermodal goods entering continental North America from global markets. Unfortunately, across much of the continent (**Figure 1**), railway infrastructure and operations are confined to transportation corridors with slopes susceptible to a broad range of landslide processes (Geertsema et al. 2009a, b; Bobrowsky and Dominguez 2012). Landslide form and function are dependent upon regional physiographic setting (montane belts, high plateaus, prairies, lowlands), environmental conditions (past and present), and local geology (solid and drift). Regionally, the diverse bedrock geology, wide range of surficial deposits, along with high relief in mountains, plateaus and deeply incised valleys (**Figure 1**) favours a broad range of rapid- to slow-moving landslides (**Table 1**). Where transportation corridors traverse unstable slopes, varying degrees of damage to infrastructure, or service delays caused by landslides have potential local and national economic, social, and environmental consequences. A landslide-resilient national transportation railway network requires sustainable, cost-effective management of service operations to meet future socioeconomic needs while protecting the natural environment and public. In a scenario of future extreme weather events and climate change, railway infrastructure and operations are expected to face unique challenges in design, monitoring, adaptation, mitigation, reclamation and restoration. An understanding of the geographic distribution and temporal range of earth materials and geological hazards is fundamental to effective hazard management and risk reduction safety (cf. Jespersen-Groth et al. 2009; Laimer 2017).

Because of its socioeconomic primacy, GSC Open File 8931 focuses on landslide processes adversely affecting the national railways connecting the deep-water ports of Vancouver and Squamish in southwestern British Columbia (BC) to the rest of Canada (**Figure 2**). From these coastal ports, the Canadian National (CN) and Canadian Pacific (CP) railways traverse mountainous and rolling plateau terrain, running through deeply incised valleys and along the steep shorelines of fjords and lakes (**Figure 2a-c**). CN and CP railway transportation corridors in this region are usually <1 km from river channels, fjord coastlines, and lakeshores to maintain an optimal grade (**Figure 2d-f**). Located so, railway tracks and associated infrastructure are prone to damage by landslides, floods, wildfires, and other natural hazards. Local physiography, weather conditions, geological hazards, and land-use activities present local and national economic, social, and environmental challenges (cf. Schuster and Fleming 1986; Haque et al. 2016; Blais-Stevens 2020). The strategic importance of these vital corridors, along with the need to understand and manage the safety risks related to landslides, make on-site investigations a strategic priority for governments, academia, and the rail industry (Bunce and Chadwick 2012; Hendry et al. 2015). Combining

field-based landslide investigation with multi-year geospatial and *in-situ* time-series monitoring leads to a more resilient railway national transportation network able to meet Canada's future socioeconomic needs, while ensuring protection of the environment and resource-based communities from landslides related to extreme weather events and climate change.

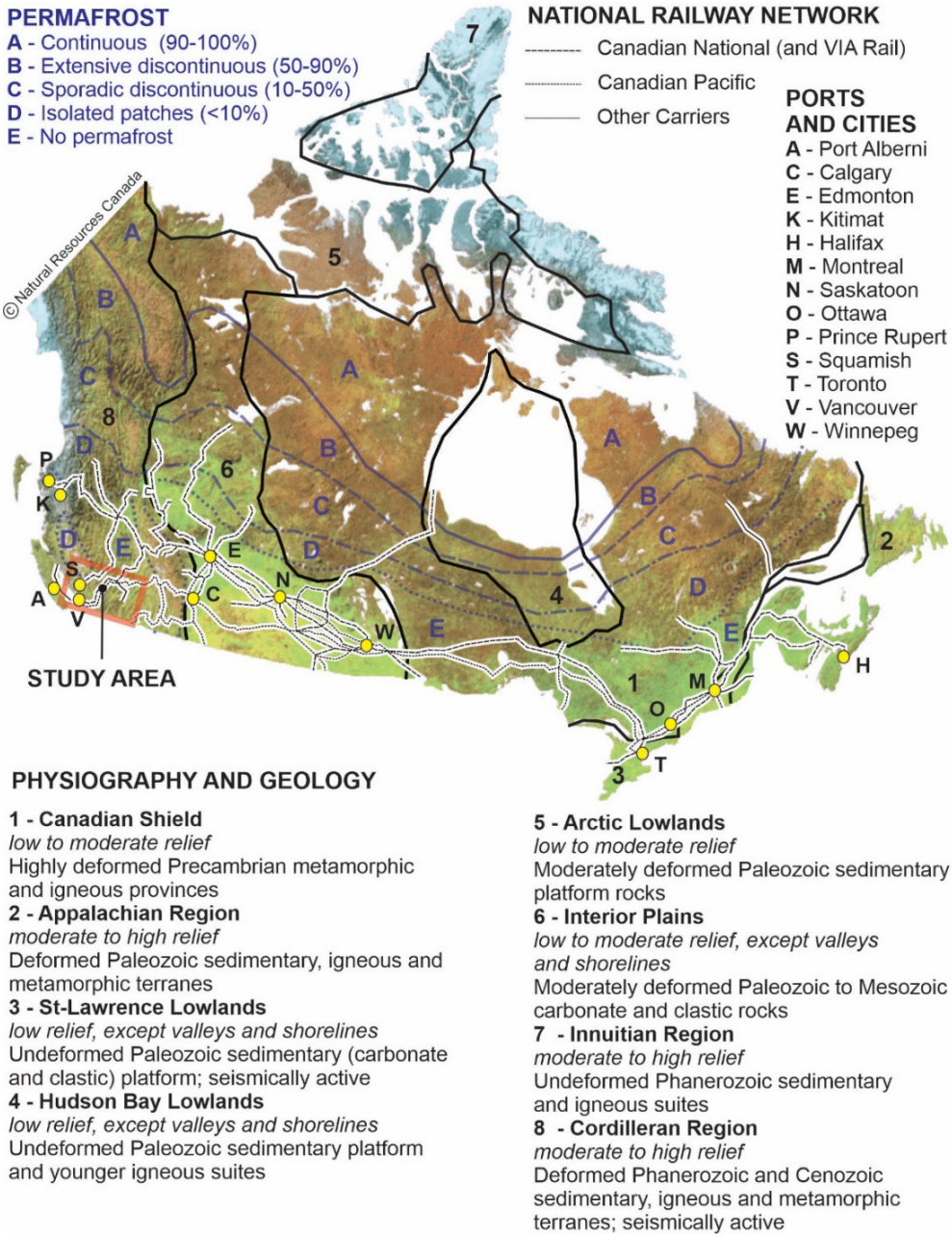

Figure 1. Physiographic and topography of Canada, showing extent of national railway network, major ports, population centres, and location of Thompson River valley landslide study area in south-central BC (after Bostock 2014).

Table 1. Surficial materials and landslides of Canada (classification after Howes and Kenk 1997; Highland and Bobrowsky 2008). See **Figure 2** for terrain code legend (after Deblonde et al. 2018).

Landslide type	Physiographic Region							
	Canadian Shield	Appalachians	St-Lawrence Lowlands	Hudson Bay Lowlands	Arctic Lowlands	Interior Plains	Inuitian Region	Cordilleran Region
Rapid mass movement (annual displacement = m yr^{-1} to km yr^{-1})								
Rock avalanche		R					R	R
Debris avalanche		C, GF, GL, T					C, T	C, GF, GL, T
Rock fall + Topple	R	R					R	R
Debris fall		C, GF, T					C, GF, T	C, GF, T
Debris flow	A, LG, WG	A, C, GL, T	A, LG, WG	A, LG, WG	A, LG, WG	A, C, GL, T	C, GL, WG, T	C, GL, WG, T
Debris torrent		A, C, GL, GF						A, C, GL, GF
Lahar								R, C, T, GF
Rapid to slow mass movement (annual displacement = cm yr^{-1} to m yr^{-1})								
Rock slide + slump		R				R	R	R
Debris / Earth slide + slump		C, GF, GL, T	GF, GL, WG, T	GF, GL, WG, T	C, GF, GL, T	C, GF, GL, T	C, T	C, GF, GL, T
Earth flow		C, GF, GL, T	GF, GL, WG, T	GF, GL, WG, T	GF, GL, WG, T	C, GF, GL, T	C, GF, GL, WG, T	C, GF, GL, T
Active layer detachment + Thaw flow	A, GL, WG, T			A, GL, WG, T	A, GL, WG, T		A, GL, WG, T	
Slow mass movement (annual displacement = mm yr^{-1} to m yr^{-1})								
Rock creep + Rock glaciers		R, C					R, C	R, C
Soil creep + Solifluction	A, C, L, W, GF, GL, WG, T	A, C, T, GF, GL	A, C, GF, GL, WG, T	A, C, L, W, GF, GL, WG, T	A, C, L, W, GF, GL, WG, T	A, C, GF, GL, T,	A, C, L, W, GF, GL, WG, T	A, C, GF, GL, WG, T
Lateral spreading (bedrock & earth)	GL, WG, T	R, C, T	GL, WG, T	GL, WG, T	GL, WG, T	R, C, GL, T	R, C, WG, T	R, C, GL, WG, T

1.1 Geoscience for public safety and socioeconomic security

A core mandate of Natural Resources Canada (NRCAN) is to provide fundamental science information on geological hazards. Across Canada (**Figure 1**), railway infrastructure and services are vulnerable to damage and loss as consequence of a wide range of landslides, whose form and function are dependent upon regional physiographic setting (montane belts, high plateaux, prairies, lowlands), environmental conditions (past and present), and local geology (solid and drift) (Huntley 2008; Geertsema et al. 2009a, b; Spooner et al. 2013). National railways are expected to face unique challenges in design, monitoring, adaptation, mitigation, reclamation and restoration in a scenario of future extreme weather events and climate change. An understanding of the geographic distribution and temporal range of earth materials and geological

hazards, and their potential responses to climate change is essential for a resilient and accessible transportation network, but also to protect the natural environment, local communities, land-use practices, and the national economy.

Here, we present a suite of monitoring best practices for railway disaster risk-reduction that meets Canada's obligations under the International Programme on Landslides and the Kyoto Landslide Commitment. This monitoring framework incorporates: 1) fundamental spatial and temporal information on geological, geophysical, and geotechnical properties of landslides at national, regional and local scales; with 2) site-specific benchmark monitoring acquired using an array of remote sensing platforms; and 3) *in situ* change-detection monitoring technologies and methodologies. We demonstrate an effective landslide change-detection mapping protocol, combining: 1) Georeferenced satellite (SENTINEL-1 [S1] and RADARSAT Constellation Mission [RCM]) interferometric synthetic aperture radar (InSAR) analysis. 2) Uninhabited aerial vehicle (UAV) change-detection photogrammetry. 3) Field-based monitoring of slope displacement using a real-time kinematic global navigation satellite system (RTK-GNSS). 4) And, instrumental measurement of climate and hydrological variables (precipitation, temperature, seasonal changes in river discharge).

2. Regional landslide types in Canada

Landslides involve the downslope movement of bedrock fragments, surficial materials, snow and ice, often mixed with vegetation debris under the influence of gravity (Howes and Kenk 1997). Conventionally, landslides are classified according to the type of mass movement and material(s) involved, and rate of displacement (cf. Cruden and Varnes 1996; Highland and Bobrowsky 2008). Landslides range in volume from 10s of m^3 (e.g., tension cracks, rock falls and thaw flow slides) to 10s of km^3 (e.g., rock avalanches, debris slides and earth flows). In general, smaller landslides occur with greater frequency (annual to decadal) than larger mass movements (centurial to millennial). Rapid landslides move by falling, rolling, sliding or flowing of dry, moist or saturated debris derived from bedrock, surficial materials and soils. Slow mass movement of cohesive or non-cohesive bedrock and surficial materials occurs by creep, flow or sliding (Howes and Kenk 1997). Due to differences in biogeoclimatic controls across the continent, bedrock and earth materials and soils in the nine physiographic regions of Canada each have distinctive assemblages of slow moving to rapid landslides, varying in magnitude and frequency (Mollard 1977; **Table 1**).

Over the next 50 years, temperature, precipitation, and other climatic factors are expected to change across Canada as a result of climate change (Weaver 2004; IPCC 2014; IPCC 2022). Depending on location, climate change will trigger positive or negative feedback in: groundwater recharge, river flow, flooding and stream erosion, the extent and duration of wildfires, the magnitude and frequency of landslides, the distribution of permafrost, and the distribution of wildlife and vegetation (Bruce and Cohen 2004; Smith and Burgess 2011; Weaver 2004; IPCC 2014; IPCC 2022). Increases in magnitude and frequency of landslides and other geohazards are expected as a response to rising precipitation amounts (as rain and snow), greater seasonal ranges in temperature and more extensive wildfires (cf. Heginbottom et al. 1995; Evans and Clague 1997; Geertsema et al. 2006; Couture and Evans 2006; Wang and Lesage 2007).

Increased erosion rates of exposed sediments is likely if wind strength and duration increases due to changes in storm systems, air pressure gradients, loss of vegetation and wildfires (cf. Wolfe 1997; Wolfe 2001). Increasing precipitation, duration of rainfall, loss of vegetation, and wildfires will lead to an increase in magnitude and frequency of gully erosion on valley sidewalls and riverbanks (cf. Sauchyn and Nelson 1999; Valentin et al. 2005). In addition, rising flood magnitudes and frequency of events will contribute to increased erosion and deposition in rivers and streams adjacent to active landslides (cf. Knox 2000; Chen et al. 2006; St. George 2007; Chen and Grasby 2009).

2.1 Rapid-moving landslides

Rock and debris avalanches are large, extremely rapidly moving unconfined flows, formed when an unstable slope collapses and the resulting fragmented debris is transported away from the slopes at speeds up to 100 m s^{-1} (Cruden and Varnes 1996; Highland and Bobrowsky 2008). This class of landslide occurs primarily in the mountainous glaciated terrain of the Appalachian, Innuitian, and Cordilleran regions, where they involve weathered bedrock (including volcanic rock debris and melted ice as lahars in British Columbia), colluvium and glacial deposits (Shilts et al. 1991; Shugar and Clague 2011; Dufrense and Geertsema 2020). Rock and debris falls are extremely rapid down-slope movements of rock masses and debris that have detached from steep slopes or cliffs, then bounce, break on impact, and roll down colluvial aprons, coming to rest on flatter terrain (Cruden and Varnes 1996; Highland and Bobrowsky 2008). Toppling involves the slow to extremely rapid forward rotation of a mass of bedrock or debris out of a slope. Rock and debris falls, and topples are widespread on bedrock and surficial slopes in the Appalachian, Innuitian and Cordilleran regions, and Canadian Shield where undercutting of bedrock slopes by river erosion, frost weathering, and anthropogenic processes occurs (Cruden et al. 1989; Couture and Evans 2002; Geertsema et al. 2006).

Channelized debris flows are triggered when surficial deposits, rock fragments and organic materials combine with water to form slurries that flow rapidly downslope at speeds up to 50 km hr^{-1} in steep gullies and canyons. Successive debris flows form fans or cone deposits where they run out along valley floors. Debris flows are widespread across all physiographic regions on slopes >18° where slopes are exposed to heavy precipitation or rapid snowmelt that mobilizes and erodes loose earth materials (VanDine and Bovis 2002; Blais-Stevens et al. 2010; Germain et al. 2018). Debris torrents are mass movements that involve water-charged, predominantly coarse-grained debris and organic materials flowing rapidly down steep, confined channels in mountainous terrain of the Cordillera and, to a lesser extent, the Appalachian region (VanDine 1985; Blais-Stevens et al. 2012; Wieczorek et al. 2018).

2.2 Rapid to slow-moving landslides

Rock slides and debris slides involve the slow to rapid movement of rock masses or surficial materials on listric or planar rupture surfaces, or thin zones of intense shear strain (Cruden and Varnes 1996; Highland and Bobrowsky 2008). Rotational slides are characterized by relatively coherent sliding blocks tilting or rotating back toward a head scarp as rock, debris or earth masses move downslope over listric slide planes. In contrast, translational slides move slowly down and outward along relatively planar surfaces with little

rotational movement or back tilting. Slumps involving bedrock and debris are distinguished from slides by having several parallel curved planes of movement (cf. Cruden and Varnes 1996). With increasing velocity, sliding or slumping masses may disintegrate into unconfined open slope debris flows (Geertsema et al. 2005; Brideau et al. 2006; Glastonbury and Fell 2010). Large volume rock and debris avalanches are uncommon in the Canadian Shield where crystalline bedrock is more prone to smaller volume rock slides, rock falls and debris slides. In all other physiographic regions where sedimentary bedrock outcrops, or is buried by layered glacial deposits, slides are triggered by intense and sustained rainfall, or rapid snowmelt which leads to increased groundwater levels within the sliding mass. Other triggers include loss of toe slope support caused by rapid drops in river level following floods, or rising river and lake levels eroding the base of slopes (Porter et al. 2002; Eshraghian et al. 2008). In the Cordillera and St-Lawrence Lowlands, rotational and translational slides can be earthquake-induced (Clague 2002; Urgeles et al. 2002).

Earth flows occur on gentle to moderate slopes (<30°), generally comprising silt and clay rich surficial earth materials, and very weathered, clay-bearing bedrock (Jackson 2002; Blatz et al. 2004; Lévy et al. 2012). Earth flow masses move through plastic or viscous flow with pervasive internal deformation (Bovis 1985; Bovis and Jones 1992). Glaciomarine and marine clays in the St-Lawrence Lowlands and coastal British Columbia are highly susceptible to earth flows (Evans 1982; Geertsema et al. 2006; Quinn et al. 2010; Lévy et al. 2012; Stacey et al. 2020). When disturbed, fine-grained materials experience a change in natural water content and lose all their shear strength, suddenly and catastrophically liquefying. Triggers include the saturation of earth materials and weathered bedrock during prolonged and intense rainfall, and snowmelt. Slow to very rapid earth flows are also triggered by sudden lowering of adjacent water surfaces that result in rapid groundwater drawdown within the slope (Geertsema et al. 2006; Locat et al. 2011; Lévy et al. 2012. Stream erosion at the base of a slope, excavation or excessive loading of slopes, and industrial and seismic ground vibrations will also trigger earth flows (Highland and Bobrowsky 2008). The resulting rapidly moving earth flows increase in size through headscarp retrogression, disturbing larger areas and flowing for several kilometres. Slides and lateral spreads may evolve downslope into earth flows (Gerath and Hungr 1982; Cruden and Varnes 1996).

Confined to the zones of continuous or discontinuous permafrost across the Canadian Shield, Hudson Bay and Arctic lowlands, fine-grained ice-rich glacial deposits on gentle slopes <2° are prone to active-layer detachments and retrogressive thaw flows. Following disturbance by bank erosion, wildfire, or anthropogenic activity, seasonal (active) thaw layers and vegetation mats may detach, then rapidly flow downslope on the underlying frozen sediment as shallow, long, narrow tongues of water-saturated sediment. Over time, active-layer detachments evolve into larger retrogressive thaw flows with steep headwalls that expose frozen earth materials, and a low-angle, lobate tongue of saturated fine-grained sediment. Retrogression continues until displaced vegetation buries and insulates the ice-rich scarp (e.g., Aylsworth et al. 2000; Couture and Riopel 2008; Huntley and Duk-Rodkin 2008).

2.3 Slow-moving landslides

Creep is the extremely slow to very slow, continuous downslope movement of bedrock masses, weathered in situ rock, surficial materials, and soils under the influence of gravity. Creep in bedrock masses occurs chiefly in the higher relief terrain of the Interior Plains, such as along river valleys, and Cordilleran region (Berg et al. 2018; Conway and Vaughn Barrie 2018). In all physiographic regions, creep requires that internal shear stresses continuously exceed the strength of earth materials, and be sufficient to cause slope deformation but not failure. Seasonal changes in precipitation, temperature, and soil moisture trigger cyclical variations in creep rate on slopes (Harris 1973; Tavenas and Leroueil 1981). A progressive increase in rate of creep commonly precedes more rapid and damaging landslides. In anthropogenic environments, poor irrigation and drainage practices, leaking pipes and construction are common contributors to slope creep (Highland and Bobrowsky 2008). In permafrost and alpine terrain (**Figure 1**), the annual thaw of the upper layer of ice-rich, fine-grained earth materials leads to the slow gravitational creep of saturated non-frozen overburden across a frozen or otherwise impermeable substrate (Howes and Kenk 1997; Short et al. 2014). Relict solifluction lobes on preserved on slopes in regions with no permafrost now attest to past climatic changes and landslide processes during paraglaciation (Price 1991; Ballantyne 2002). In the western Cordillera, rock glaciers are perennially frozen masses of ice and coarse debris that creep downslope under the weight of gravity (Luckman and Crockett 1977; Johnson and Lacasse 1988; Charbonneau and Smith 2018). Most rock glaciers are confined to north-facing cirque basins where rock and debris avalanches have buried stagnant glacier ice; and reduced insolation extends montane permafrost to lower elevations.

Lateral spreading occurs on very gentle slopes (<2°) where a stronger upper layer of bedrock or surficial earth material undergoes extension and moves above, and into a softer, underlying weathered layer (Gerath and Hungr 1982; Geertsema et al. 2006; Lévy et al. 2012). Initially, bedrock block spreads are characterized by internal extensional fractures formed as rock masses move over weaker layers, but with no surface expression of rupture. Compression of underlying weak rock units can lead to upward creep of deformed fine-grained material between spreading competent blocks. With continued lateral spreading, tension cracks daylight at the surface, permitting the rapid percolation of precipitation, snowmelt, and surface runoff deep into the failing rock mass (Cruden 1985; Thompson et al. 1997; Jackson 2002). Earth spreads occur when an upper, stable layer extends along a weaker underlying unit that has flowed following liquefaction or plastic deformation (Cruden and Varnes 1996; Highland and Bobrowsky 2008). If the weaker unit is relatively thick, the overlying fractured blocks may subside into it, translate, rotate, disintegrate, liquefy, or flow (Porter et al. 2002; Quinn et al. 2011; Cruden and VanDine 2013). Triggers for spreading are physiographically constrained. Across all regions, lateral spreading is triggered by saturation of underlying weak layers due to changes in pore-pressures (e.g., from precipitation, snowmelt and/or groundwater). In the south-central Interior Platform, localized surface subsidence is a manifestation of plastic deformation and dissolution of unstable bedrock at depth (e.g., potash deposits). In the coastal fjords of the western Cordillera, and the Hudson Bay, Arctic, and St-Lawrence lowlands, liquefaction of underlying sensitive marine clays follows sudden river and coastal erosion events, or anthropogenic excavations at the base of slopes (Geertsema et al. 2006; Lévy et al. 2012; Stacey et al. 2020). Also in the Cordillera and St-Lawrence

Lowlands, earthquake shaking in high seismic risk areas can trigger liquefaction of weak layers (Nastev 2014; https://www.earthquakescanada.nrcan.gc.ca/ [URL 2021]).

3. Landslide hazards along railway corridors in British Columbia

The strategic importance of the CN and CP railway transportation corridors in Cordilleran southwestern BC (**Figure 1**; **Figure 2a**) make it a priority for governments, academia, and the rail industry to understand and manage the safety risks related to landslides (Bunce and Chadwick 2012; Hendry et al. 2015). From coastal ports in Greater Vancouver and Squamish, CN and CP railway corridors in southwestern mainland British Columbia traverse mountainous and rolling plateau terrain, running through deeply incised valleys and along the steep shorelines of fjords and lakes (**Figure 2b-c**). To maintain optimal grades, railway transportation corridors are usually <1 km from river channels, fjord coastlines, and lakeshores, with gentle to steep bedrock slopes mantled by surficial deposits susceptible to a range of rapid to slow-moving landslides triggered by floods, wildfires and other natural hazards (**Figure 2d-f**).

3.1 Physiography and landslide susceptibility

Southwestern BC is divisible into: 1) Low-relief terrain dominated by slopes of 2° or less confined to the Fraser Lowland and major glaciated valleys dissecting mountains and intermontane plateaus, with a low level of landslide susceptibility (**Table 2**, green). 2) Moderate-relief slopes >2°-18° are characteristic of the Interior Plateaus and Okanagan Highlands, although drift-mantled monadnocks rising above the Fraser Lowland are included here; all are moderately susceptible to landslides (**Table 2**, yellow). 3) High-relief terrain in the Coast, Monashee, and Selkirk Mountains, dominated by bedrock and colluvial slopes from 18° to >30° are considered prone to failure if conditions are favourable, are highly susceptible to landslides (**Table 2**, red). Where railway corridors traverse moderate to high-relief terrain, infrastructure and services are prone to disturbance by a wide range of slow moving to rapid landslides on open slopes, or adjacent to rivers, lakeshores and fjord coastlines.

Similar to other linear transportation infrastructure traversing steep, high-relief mountainous terrain (e.g., highways, power transmission lines, and pipelines), railway corridors are vulnerable to a broad range rapid and slow-moving landslides (**Table 2**), often occurring a cascade of events. Common to the Cascade, Coast, Monashee and Selkirk mountains, initiation zones at high elevation (>2000 m asl.) transition to broad run-out zones with low relief and vegetation cover at lower elevation, where avalanching materials may evolve into other landslide types. For example, in montane watersheds with tundra, isolated permafrost, perennial snow and glaciers, progressive, very slow gravitational creep and lateral spreading of steep bedrock slopes can evolve into large-volume rock and debris avalanches that rapidly remobilize bedrock masses, colluvium and glacial deposits along deeply incised river valleys, fjords and lakes. Although occurring at distances greater than a kilometre from railway corridors, melting glaciers, perennial snow packs, and isolated permafrost in mountain watersheds contribute to rock, debris and earth slides and flows that can adversely affect railway infrastructure downstream (**Table 2**).

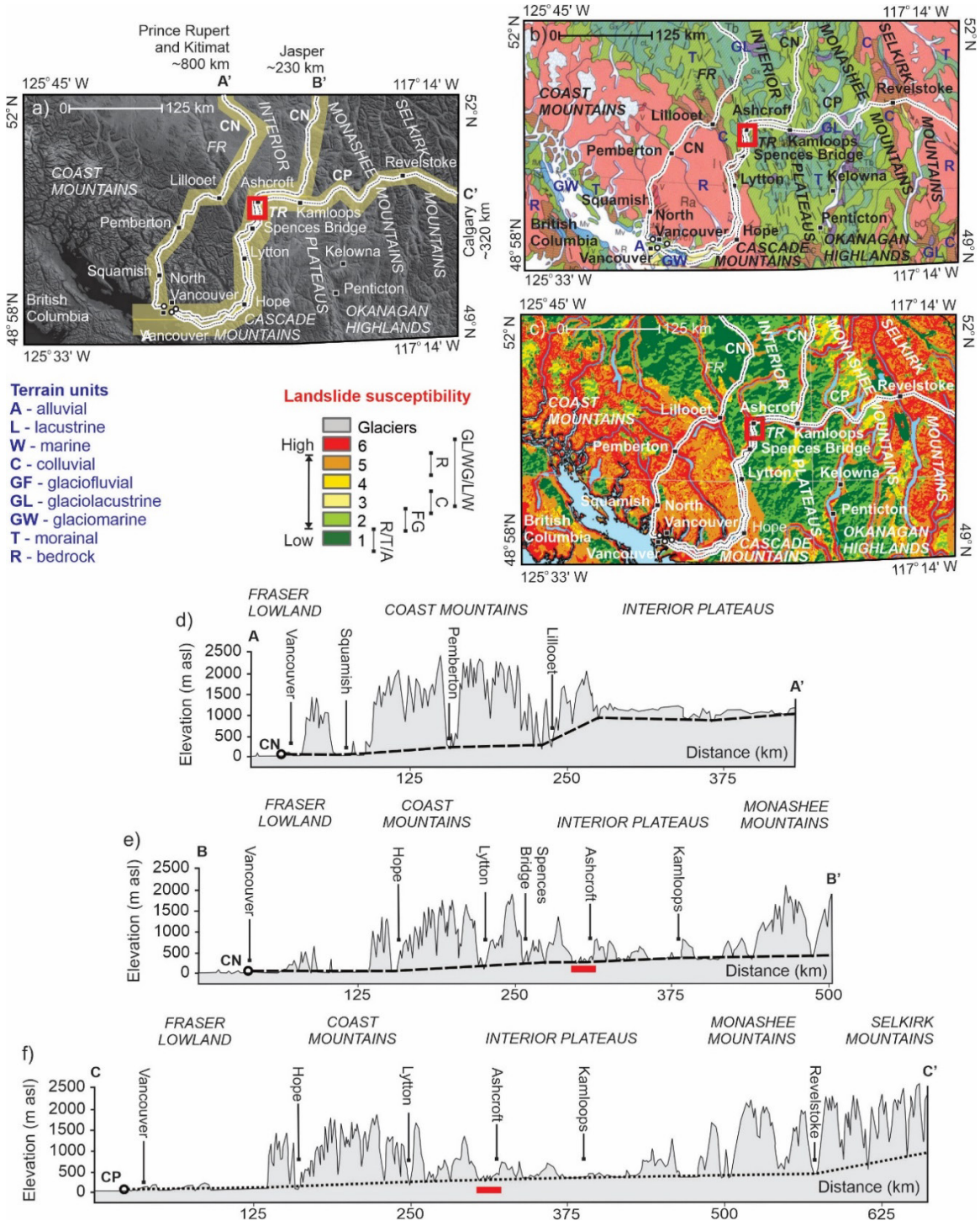

Figure 2. CN and CP railway corridors traversing southwestern BC: a) Topography and physiography, showing location.

Table 2 Landslide susceptibility of southwestern BC (parameter classifications after Howes and Kenk 1997; Highland and Bobrowsky 2008; Bobrowsky and Dominguez 2012; Deblonde et al. 2018).

		Rapid mass movement							Rapid to slow mass movement			Slow mass movement		
		Rock avalanche	Debris avalanche	Rock fall + Topple	Debris fall	Debris flow	Debris torrent	Lahar	Rock slide + slump	Debris slide + slump	Earth flow	Rock creep + glaciers	Soil creep + Solifluction	Lateral spreading
Topography	Relief	H	H	H	H	H L	H L	H	H	H L	H L	H	H L	H L
	Slope (degrees)	>30	>30	>30	>30	>18	>18	>30	>18	>18	>2	>30	>18	>2
	Aspect	S	S	S	S	W	W	S	S	S	S	N	N	S
	Distance from rivers #	H	H	H	H	H L	H L	H	H	H	H L	H	H L	H L
	Distance from lakes #	H	H	H	H	H L	H L	H	H	H	H L	H	H L	H L
	Distance from coast #	H	H	H	H	H L	H L		H	H	H L	H	H L	H L
Environ-ment	Annual ppt (mm) *	H	H	H	H	H L	H L	H	H	H	H L	H	H L	H L
	Isolated permafrost	H	H	H	H	H	H	H	H	H	H	H	H	H
	No permafrost	H	H	H	H	H L	H L	H	H	H	H L	H	H L	H L
Surficial geology	Alluvial					H L	H L			H	H L		H L	
	Colluvial	H	H	H	H	H L	H L	H	H	H	H L	H	H L	H L
	Lacustrine					H L	H L			H	H L			
	Marine					H L	H L			H	H L			
	Glaciofluvial				H	H L	H L			H	H L			
	Glacio-lacustrine				H	H L	H L			H	H L		H L	H L
	Glacio-marine				H	H L	H L			H	H L		H L	H L
	Glacial (moraine)		H		H	H L	H L	H		H	H L		H L	H L
	Bedrock	H	H	H	H			H	H			H		H L
Vegetation and Land use	Snow / Glaciers	H	H	H	H	H	H	H	H	H		H	H L	H L
	Tundra	H	H	H	H	H	H	H	H	H	H L	H	H L	H L
	Wetland / Shrublands	H L	HL			L	L	L						
	Forests / Shrublands	H	HL			H L	H L	L			H L		H L	H L
	Mixed Forest	H	H			H L	H L	H L			H L		H L	H L
	Grasslands										H L		H L	H L
	Croplands					H L	H L	L			H L		H L	H L
	Urban lands			H	H	H L	H L	L	H	H	H L		H L	H L

Relief: **H** – High relief terrain (mountains, valleys, fjords, >1000-500 m); **L** – Low relief terrain (plateaus and coastal lowlands, <500 m). Aspects: **N** – 270°-000°-090°; **S** – 090°-180°-270°; **W** – 180°-270°-000°. # Distance from rivers, lakes and coasts < 1 km. * Annual precipitation >2700 mm.

In the Cascade and Coast Mountains, infrequent volcanic activity, large magnitude earthquakes, and extreme precipitation events trigger lahars, rock and debris avalanches, although anthropogenic activities can also contribute. More frequent, small-volume rock falls, topples, and debris falls occur on steep bedrock and unconsolidated bluffs along railway corridors the deeply incised valleys draining the Coast and Monashee mountains (**Table 2**). Particularly on west-facing (windward) mountain slopes, falling rock masses and colluvial material may transition downslope into debris flows and debris torrents (open slope and channelized) with potential to adversely impact urban and agricultural land-use, in addition to railway and other transportation infrastructure crossing high-gradient streams, talus cones and alluvial fans (**Table 2**).

For railway corridors traversing the Fraser Lowland and Interior Plateaus, low to moderate relieve terrain within a kilometre of river channels, lakeshores, and coastline are moderately or highly susceptible to slow-moving slides, slumps and flows of bedrock and fine-grained earth materials (**Table 2**). In the Fraser Lowland, extreme precipitation events, tidal surges, uncontained irrigation of cropland or urban runoff will trigger shallow debris slumps and earth flows in fine-grained glacial sediments and anthropogenic fill exposed along riverbanks near bridge abutments and rail embankments. Particularly in the semi-arid high relief Fraser and Thompson canyons, weathered igneous and metamorphic bedrock form steep slopes susceptible to slow-moving deep-seated bedrock slides and slumps that adversely affect railway (and highway) infrastructure (VanDine 1983; Bovis and Jones 1992; Macciotta et al. 2017; Donati et al. 2020; **Table 2**). Along the western margin of the Interior Plateaus, glacial terraces in the Thompson River valley, supporting grasslands and croplands, are composed of fine-grained glaciolacustrine deposits and tills overlain by coarser glaciofluvial outwash (Bovis 1985; Porter et al. 2002; Eshraghian et al. 2007; Eshraghian et al. 2008; **Table 2**).

3.2 Landslide susceptibility along the CN railway corridors

Interior and northern British Columbia are serviced by secondary CN tracks connecting North Vancouver to Prince George through Squamish, Pemberton, and Lillooet in the southern Coast Mountains, then north across the Interior Plateaus (**Figure 2a, d**). Faulted intrusive and extrusive igneous rocks, and deformed metamorphic and sedimentary sequences (Journeay et al. 2000); and coarse-grained colluvium are the dominant earth materials exposed on transportation corridor slopes through the Coast Mountains (Fulton 1995; Blais et al. 2012). Coarse and fine-grained glacial sediments mantle lower slopes or form valley terraces incised and draped by alluvial, lake and marine lag deposits. Mountainous sections of the railway corridor to the Fraser River valley have high relief (>1000-500 m) with slopes >30º. Windward slopes with a western aspect receive significant orographic rainfall and snow >2700 mm yr^{-1}; and slopes support dense coniferous and mixed forests below the alpine tundra. To maintain an optimal grade, railway tracks and infrastructure are usually <1 km from river channels, fjord coastlines, and lakeshores. South-facing slopes receive most insolation through the year, and experience the greatest seasonal snowmelt. Isolated

permafrost in bedrock and glacial drift extends to lower elevations on north-facing mountain slopes receiving minimal insolation through the year (**Figure 2b, c)**.

At Lillooet, the CN tracks gain elevation following the Fraser River canyon north before heading east to Clinton and north to Prince George on the Interior Plateaus. From Prince George, a CN corridor runs west to the coastal ports of Kitimat and Prince Rupert in the northern Coast Mountains (**Figure 2a, d**). East of Prince George, a railway corridor runs through the Rocky Mountain Trench to connect with primary CN route to Jasper and eastern Canada. Crossing the fault-bounded Fraser River, the geology of the intermontane plateaus are dominated by less deformed sedimentary bedrock, partly buried by extrusive volcanic sequences, and draped by glacially streamlined boulder-rich till, glaciofluvial outwash deposits, and hillslope colluvium (Fulton 1995; Mathews and Monger 2010; **Figure 2b**). Plateau topography is dominated by rolling terrain with low to moderate relief (<500 m), with slopes between 2º and 18º, although incised valleys and gullies have slopes >30º (**Figure 2d**). Leeward of the Coast Mountains, precipitation falls below 2700 mm yr-1, and open coniferous-dominated forests become interspersed with grasslands prone to disturbance by wildfires.

The main continental route for CN rail freight first travels east from Vancouver to Hope through the Fraser Lowland. This broad coalescent alluvial plain of Fraser River and lower reaches of tributaries draining the Coast and Cascade mountains has low relief (<200 m) and slopes <2º. Alluvial sediments drape glaciomarine, glaciofluvial outwash and tills deposited during higher stands of the Salish Sea at the end of the last glaciation (**Figure 2a, b**). Windward slopes with a south and west aspects receive significant orographic rainfall and snow >2700 mm yr^{-1}. Croplands and urban lands cover much of the lowland. From Hope, the corridor runs north through Coast Mountains along the lower slopes of the deeply dissected Fraser and Thompson valleys to Ashcroft and Kamloops (**Figure 2a, e**). In the Fraser and Thompson canyons, deformed igneous, metamorphic and sedimentary rocks, and coarse-grained colluvium are the dominant earth materials along the transportation corridor, although glacial outwash form fans and valley terraces at lower elevations (Fulton 1995; Mathews and Monger 2010). The CN railway corridor in the Fraser and Thompson valleys has high relief (>1000-500 m) with slopes >30º (**Figure 2e**)

A bioclimatic transition occurs between Hope and Lytton as annual precipitation falls below 2700 mm yr^{-1} in the rain shadow of the Coast Mountains. Sparse mixed forest and grassland replaces dense coniferous cover on mountain slopes and valley sides. Between Lytton to Kamloops, the CN mainline follows a deeply incised Thompson River canyon with over 1000 m of relief and slopes >30º (**Figure 2e**). Between Spences Bridge and Ashcroft, the transportation corridor flanks the western limit of the Interior Plateaus. This portion of the intermontane plateau has moderate to low relief (<500 m), with slopes between 18º and 30º (**Figure 2e**). Annual precipitation falls well below 2700 mm yr^{-1} in the Thompson River valley, where grassland and cropland replaces sparse forest cover on slopes. Deformed igneous, metamorphic and sedimentary rocks and coarse-grained colluvium are the dominant earth materials on steep slopes. Confined to the toe slopes of Thompson River valley, the CN corridor cuts across bedrock, outwash fans and valley

terraces. Surficial valley fill, up to 200 m thick, consists of multiple sequences of glacial diamictons (tills), silt-clay glaciolacustrine sediments, and gravel-rich glaciofluvial outwash (**Figure 2b, e**).

At Kamloops, the CN tracks follow the North Thompson valley through the Monashee Mountains, connecting with the CN line from Prince George at Valemont. From there, the primary CN corridor follows the upper reach of Fraser River, through the Rocky Mountains, crossing the continental divide west of Jasper, and then heads southeast to the Assiniboine River valley. Deformed igneous, metamorphic and sedimentary sequences and coarse-grained colluvium are the dominant earth materials exposed on transportation corridor steep slopes (>30º) with high relief (>1000 m) through the Monashee Mountains (Fulton 1995; **Figure 2a, e**). West-facing slopes receive at least 2700 mm yr^{-1} as orographic rainfall and snowfall. South-facing slopes in tributary watersheds receive most insolation through the year, and experience the greatest seasonal snowmelt and glacial ice melt. Glacial sediments mantle lower valley slopes, forming fans and terraces. These low to moderate relief glacial landforms (<500 m), with slopes from 2º to 18º, are incised and draped by alluvial and lake lag deposits along the modern valley floor **Figure 2b, e**).

3.3 Landslide susceptibility along the CP railway corridor

The primary CP railway corridor approximately follows the CN routing from Vancouver through the Fraser Lowland to Hope, crossing low to moderate relief terrain (<200 m) and slopes <2º to 18º converted to croplands and urban development (**Figure 2a, f**). Similarly, the corridor runs north through Coast Mountains to Ashcroft and Kamloops in the Interior Plateaus along the lower, but usually opposite, slopes of the Fraser and Thompson valleys (**Figure 2f**). The CP corridor also cuts across moderate to steep high relief (500 m to >1000 m) exposures of deformed igneous, metamorphic and sedimentary rocks, fine-grained glaciolacustrine sediments, coarse-grained colluvium, tills and glaciofluvial outwash (Monger and McMillan 1989; Ryder 1976; Johnsen and Brennand 2004; **Figure 2b**). Between Hope and Lytton, annual precipitation falls below 2700 mm yr^{-1} in the rain shadow of the leeward Coast Mountains, and sparse mixed forest and grassland replaces dense coniferous forests along the CP corridor.

From Spences Bridge to east of Kamloops, the CP transportation corridor crosses the Interior Plateaus, with moderate to low relief (<500 m), and slopes between 18º and 30º (**Figure 2f**). Grassland and cropland in the Thompson River canyon replaces sparse forest cover on corridor slopes in the rain shadow of the leeward Coast Mountains. Deformed igneous, metamorphic and sedimentary rocks and coarse-grained colluvium are the dominant earth materials on steep slopes in the Thompson River canyon. Confined to mountain toe slopes and <1 km from Thompson River, the CP corridor cuts across bedrock, outwash fans and valley terraces. Surficial valley fill, up to 200 m thick, consists of multiple sequences of tills, silt-clay glaciolacustrine sediments, and gravel-rich glaciofluvial outwash (Ryder 1976; Clague and Evans 2003; Johnsen and Brennand 2004; (**Figure 2b**).

East of Kamloops, the CP corridor follows the interior lakeshores in the Monashee Mountains to Revelstoke. Secondary, but currently decommissioned, rail corridors for CP (and CN) run through the

Okanagan Highlands and Okanagan Valley, terminating in Kelowna. From Revelstoke, the primary CP route crosses the glacierized Selkirk and Rocky Mountains before exiting into the Interior Plains west of Calgary and tracking eastward (**Figure 2a, f**). Montane terrain has moderate to high relief (>500 m to >1000 m) with bedrock and colluvial slopes from 18° to >30°. West-facing slopes receive at least 2700 mm yr^{-1} as orographic rainfall and snowfall. South-facing slopes in tributary watersheds receive most insolation through the year, and experience the greatest seasonal snowmelt and glacial ice melt. Isolated permafrost terrain extends to lower elevations on north-facing mountain slopes receiving minimal insolation through the year. Faulted and folded igneous, metamorphic and sedimentary sequences and coarse-grained colluvium are the dominant earth materials exposed on transportation corridor steep slopes. Glacial sediments mantle lower valley slopes, forming fans and terraces with low to moderate relief (<500 m) and slopes from 2° to 18° (**Figure 2f**). Along modern valley floors, lake and alluvial lag deposits drape these landforms (**Figure 2b**).

Between Ashcroft and Spences Bridge (**Figure 2a, f**), the primary CN and CP railway corridors traverse terrain highly susceptible to slow-moving deep-seated, large volume rotational-translational debris and earth slides (**Figure 3**). In the late 19th Century, prehistoric mass movements failed as reactivated, sudden onset, rapid retrogressive flow-slides during, and after the summer months, at a time when terraces were intensively irrigated for agricultural land use, and toe slopes were incised and over-steepened during railway construction (Stanton 1898; Evans 1984; Clague and Evans 2003). Recent InSAR monitoring (Journault et al. 2018; Huntley et al. 2021) indicate that at least five translational slides remain active and have potential to adversely impact railway infrastructure and services. The economic importance of this transportation corridor, along with the need to understand and manage the safety risk related to the landslides that threaten the route, mandate the Thompson River valley a research priority for NRCAN and the GSC (**Figure 3**).

4. Targeted Landslide Research Methods, Results, and Analyses

IMOU-5170 aims to gain a better understanding of how extreme weather events and climate change influence landslide activity in the Thompson River valley, British Columbia, and the Assiniboine River valley, Saskatchewan-Manitoba. This fundamental geoscience information will contribute to more robust landslide hazard management to maintain the resilience and accessibility of critical transportation infrastructure along strategically important sections of the national railway network, while also protecting the natural environment, community stakeholders, and Canadian economy. This report builds upon foundational work presented in GSC Open Files 7531, 8548, 8735, 8736, 8742, 8745 and 8838 (Huntley and Bobrowsky 2014; Huntley et al. 2019c; Huntley et al. 2020b-e; Huntley et al. 2021a, b). Anticipating scenarios of future extreme weather events and climate change in the Thompson and Assiniboine river valleys, geological hazard management solutions will require a clearer understanding of the form and function of landslides. Research and monitoring efforts contribute to: 1) Understanding the composition and internal structure of the landslide, including the range of earth materials and nature of failing rupture surfaces. 2) Delimiting the spatial extent of unstable slopes and slide bodies. 3) Establishing the timing,

amount, direction, and rates of surface displacement from year to year. 4) Defining the interactions between climate-driven triggering mechanisms (e.g., groundwater pressure) and landslide activity.

4.1 ICL-IPL Project landslide laboratory

Landslides along a ten-kilometre stretch of the Thompson River valley between Ashcroft and Spences Bridge (**Figure 2a**; **Figure 3a**) have negatively impacted critical railway infrastructure, arable land, fisheries, and other natural resources since the 1880s (**Figure 3b**). In the late 19th Century, prehistoric mass movements reactivated as sudden onset, rapid retrogressive flow-slides during the fall and winter months at a time when terraces were intensively irrigated for agricultural land use, and toe slopes were incised and over-steepened during railway construction (Stanton 1898; Clague and Evans 2003).

As part of the International Consortium on Landslides (ICL) International Programme on Landslides (IPL) Project 202, landslides in the Thompson and Assiniboine valleys serve as field laboratories to test and compare the reliability and effectiveness of different static, dynamic, and real-time monitoring technologies (e.g., Huntley et al. 2017; Huntley et al. 2019a, b). The three primary research and development objectives include: 1) Better understand controls on landslide movement, and in particular, the impacts of extreme weather events and climate change. 2) Compare, evaluate, and identify the monitoring technologies which provide the most accurate information on why, how, and when landslides move. 3) Help identify reliable real-time monitoring solutions for critical railway infrastructure (e.g., ballast, tracks, retaining walls, tunnels and bridges) able to withstand the harsh environmental conditions of Canada.

For the Thompson River valley, field-based geological and geophysical mapping, combined with InSAR analyses (**Figure 3c**), and *in situ* semi-continuous monitoring, provide insight into landslide activity, deformation mechanisms, and potential acceleration triggers along this critical section of the national railway transportation corridor (Bunce and Chadwick 2012; Journault et al. 2018; Huntley et al. 2019a, b; Holmes et al. 2020). Each of these techniques record increased landslide activity in winter, when river and groundwater levels are lowest (Macciotta et al. 2014; Hendry et al. 2015; Schafer et al. 2015; Journault et al. 2018). Permanent global navigation satellite system (GNSS) monuments on Ripley Landslide record cumulative annual displacement on the order of 10 cm yr^{-1} to 20 cm yr^{-1}, peaking in winter (Bunce and Chadwick 2012; Macciotta et al. 2014; Hendry et al. 2015; Huntley et al. 2021a). RADARSAT-2 (RS-2) and SENTINEL-1 (S1) synthetic aperture radar interferometry (InSAR) results from 2013 to 2020 indicate similar magnitudes and spatial-temporal patterns of displacement (Journault et al. 2018; Huntley et al. 2021b, c). From south to north along the railway transportation corridor, these include the following landslides of concern with an average 1D line-of-sight (LoS) displacement greater than 3 cm yr^{-1}: Ripley Landslide, Red Hill Slide, South Slide, North Slide, and Goddard Slide (**Figure 3c**). Regions of highest landslide activity intersecting with railway infrastructure correlate with cutbank erosion and channel bed scour on the outside bends of the river.

4.1.1 Research objectives: understanding landslide form and function through monitoring

Although some landslides in the Thompson River valley failed and moved rapidly in the past, today all are slow-moving compound features within Pleistocene valley fill (Porter et al. 2002; Eshraghian et al. 2007; Eshraghian et al. 2008; Bunce and Chadwick 2012; Huntley et al. 2020). Descriptions of local topographic, bathymetric, surficial and bedrock geological conditions, including earth materials and landforms, and their hydrological properties are essential for understanding landslide compositions, structures, and behaviours. Geospatial relationships between landslide distribution and specific terrain features, and the environmental conditions triggering instability, are determined from field-based, on-site geological and geophysical studies, combined with geotechnical, petrophysical, and geochemical laboratory analysis, which are then codified and quantified in geographic information systems (GIS). Temporal relationships between landslides and the environmental conditions triggering instability are determined from time-series monitoring and GIS analyses of satellite InSAR, UAV photograms, and ground-based real-time kinematic ground-based RTK-GNSS surveys. In this section, we describe field-based landslide mapping in the Thompson valley railway corridor and supporting desktop geospatial analyses undertaken in 2021 and 2022 (**Figure 2a, b**).

4.2 Landslide form: remote sensing, field mapping and geophysical surveys

Understanding form and function begins with terrain analysis and landslide inventory. Descriptions of local bathymetric, surficial and bedrock geological conditions, including earth materials, landforms and structures, and their hydrological properties are essential for understanding landslide composition, structures, and behaviours. Digital layers were compiled in a GIS using Global Mapper ™ following the methodology of Bobrowsky and Dominguez (2012). A base topographic layer of Canada merges WORDVIEW Imagery with a digital elevation model (DEM) generated from ASTER GDEM v2 worldwide elevation data (1 arc-second resolution). The topographic base map (**Figure 2a**) and cross-sections (**Figure 2d-f**) derived from this geographic information system (GIS) show the contrasting landscapes, sculpted by ice sheets, glaciers, rivers and oceans, representative of large areas of the country (**Figure 1**).

For the Thompson River valley railway corridor, terrain polygons and features characteristic of landslide activity are delimited on optical satellite imagery (e.g., LANDSAT, WORDVIEW), conventional air photographs, and unoccupied aerial vehicle (UAV) photogrammetry. At ground control points (GCP), geo-referenced observations were made of slope gradient, surficial materials, material texture, material thickness, slope morphology, moisture conditions, ongoing geomorphic processes, land cover, and nearby anthropogenic activities. These onsite descriptions corroborated terrain and landslide classifications determined from optical satellite imagery and UAV photogrammetry. Hydrogeological units were distinguished in surficial deposits and fractured bedrock through field mapping, exploratory drilling, and geophysical surveys (Huntley and Bobrowsky 2014; Huntley et al. 2017a; Huntley et al. 2019a-c; Holmes et al. 2020; Huntley et al. 2020a). Terrain and landslide classifications (**Figure 4**) were benchmarked with ground observations of slope gradient, surficial materials, material texture, material thickness, slope morphology, moisture conditions, ongoing geomorphic processes, and land cover (Huntley and Bobrowsky 2014; Huntley et al. 2017a; Holmes et al. 2018; Huntley et al. 2019a-c; Holmes et al. 2020; Huntley et al.

2020a). Coding of surficial geological units and landforms followed BC and GSC mapping standards (Fulton 1995; Howes and Kenk 1997; Deblonde et al. 2018).

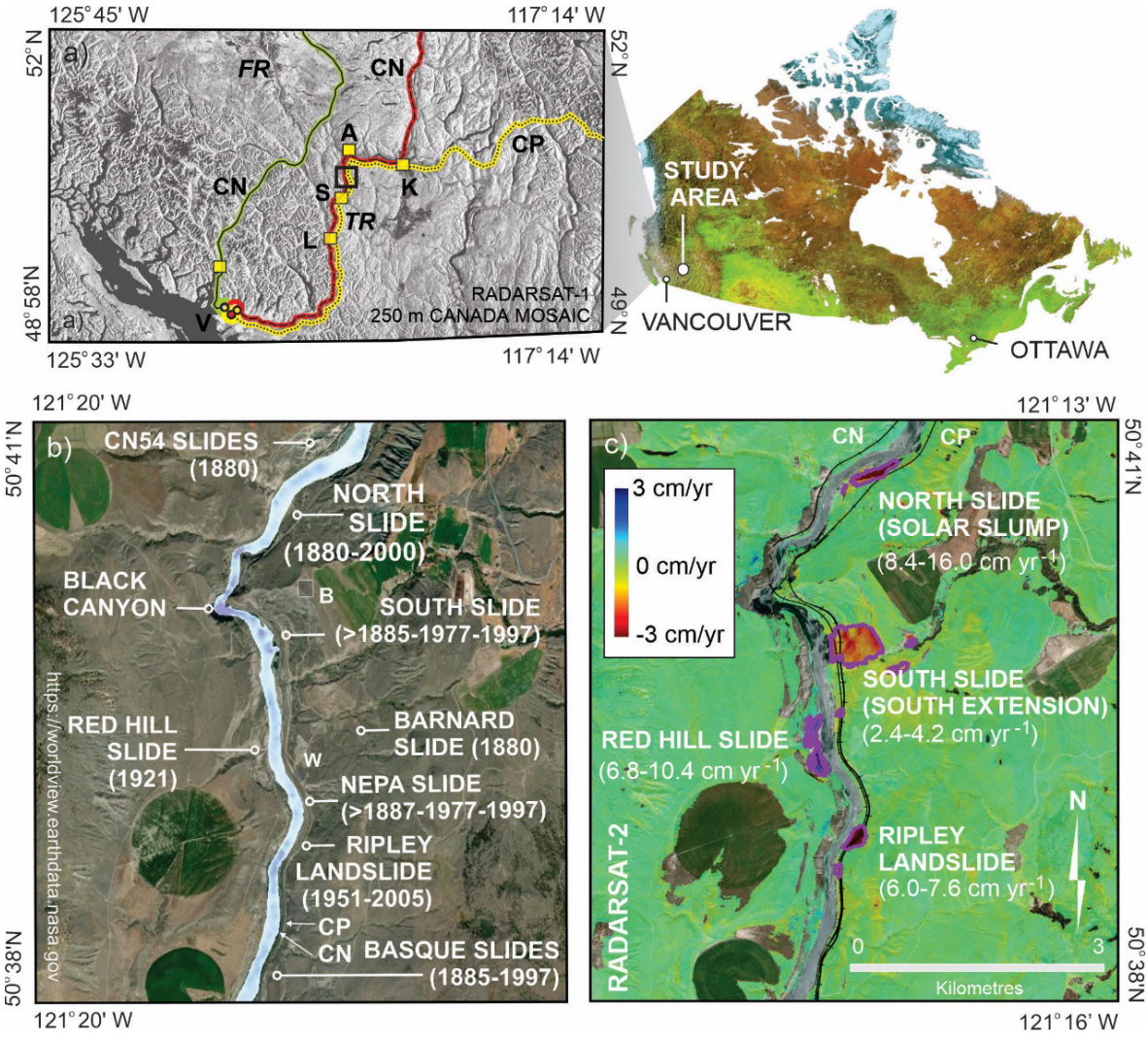

Figure 3. Study area, showing landslides in relation to national railway infrastructure: **a)** southwestern British Columbia showing major transportation corridors. **b)** Historical activity of slow-moving landslides of the Thompson with potential to negatively impact national railway infrastructure, operational services, the environment, local communities, and national economy (after Clague and Evans 2003). **c)** Landslides of concern determined from InSAR results for the Thompson River valley, showing CN and CP tracks (solid black lines); RADARSAT-2 average linear displacement rate rastered at 3 cm yr^{-1}, with purple polygons delimiting 4-sigma confidence levels (modified from Huntley et al. 2021c). **CN** – Canadian National Railways; **CP** – Canadian Pacific Railways; ***TR*** – Thompson River; ***FR*** – Fraser River.

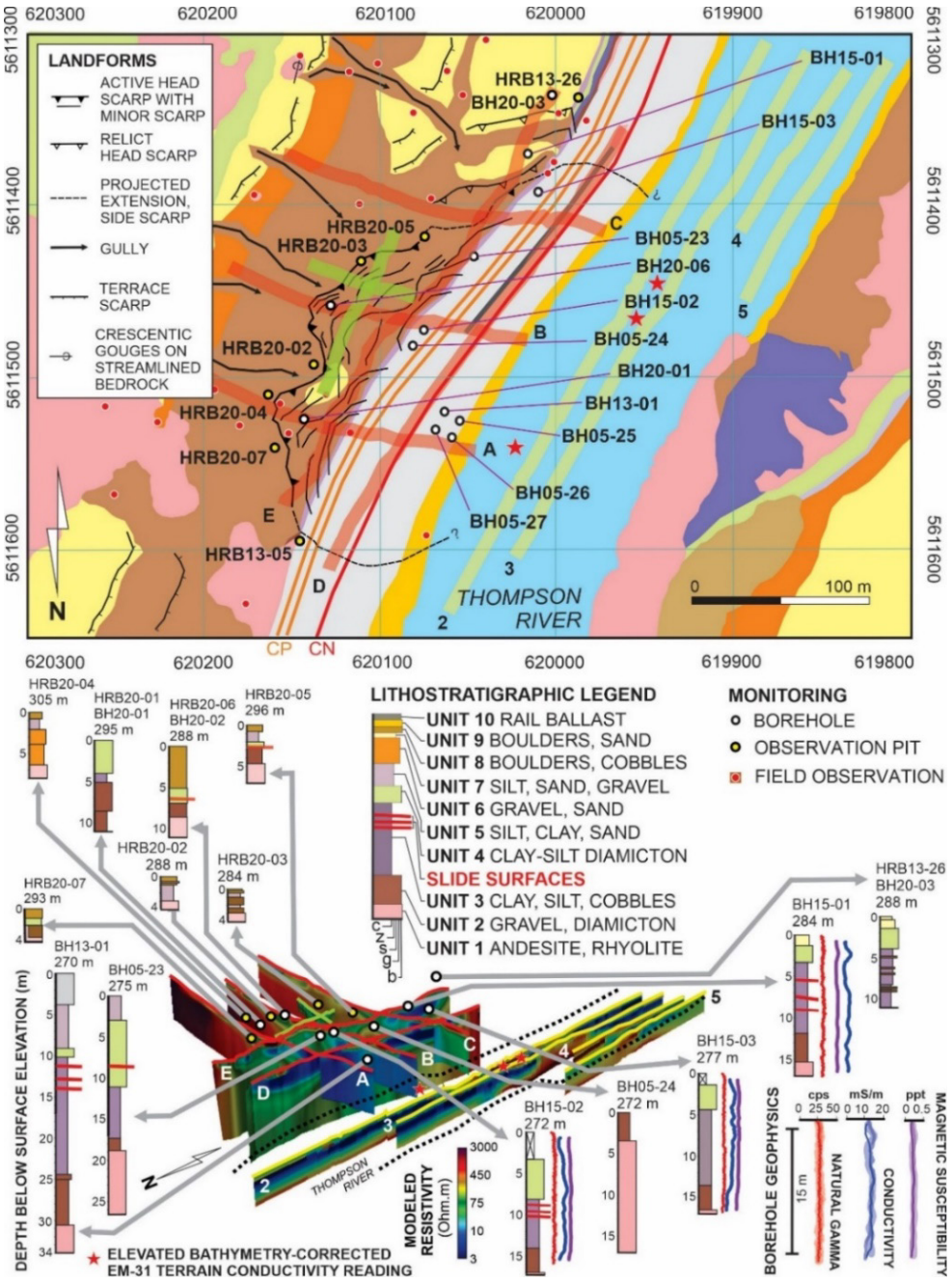

Figure 4. GIS output generated from field studies and laboratory results. Surficial hydrogeological units and landforms of Ripley Landslide, in the Thompson River valley, southwestern BC, as revealed by field-based mapping and geophysical surveys (after Huntley and Bobrowsky 2014; Huntley et al. 2019c; Huntley et al. 2020a). Locations of logged and monitored boreholes, observation pits, field observations, and ERT survey lines indicated on surficial geology map. ERT pseudosections produced by the British Geological Survey (© UK Research and Innovation 2020). Terrestrial ERT survey – red lines (A-E); waterborne ERT and EM-31 survey – yellow lines (2-5); PRIME installation - green lines (oriented N-S and E-W).

The ten earth material classes recognized at Ripley Landslide (**Figure 4**) also outcrop and underlie the railway corridor in this portion of the Thompson River valley. Bedrock influences slope hazards where surficial cover is thin especially on terrain with slopes >35°. Elsewhere, drift cover is thicker and surficial materials have a greater influence on slope instability. Large retrogressive rotational-translational earth-debris slides were initially triggered by deep incision of Pleistocene fill in the Thompson River valley during the early Holocene (Clague and Evans 2003). Subsequently, the river influenced slope stability and landslide susceptibility by changing: a) the pore water pressure in the slope mass, and along rupture surfaces; b) the supporting force on landslide toes; and c) through cutbank erosion, thereby affecting the geometry of the landslide. Back-tilted blocks and rapid debris slumps move over weak, curvilinear rupture zones in glaciolacustrine clay-silt units confined between overlying till and underlying bedrock (Porter et al. 2002; Eshraghian et al. 2007; Eshraghian et al. 2008; Huntley et al. 2020a). Single-beam and multi-beam river surveys (Huntley et al. 2021a) reveal variations in channel bed composition south of Ashcroft and north of Spences Bridge range from sand and silt draping bedrock, to coarse gravel and boulders overlying clay-rich valley fill. Shallow waters (riffles) with rapids lie adjacent to stable terrain, separated by deep scour pools (up to 5 m below river level) adjacent active slide toes.

Geophysical surveys, borehole logging, and laboratory analysis of geotechnical and geochemical properties of earth materials, including stratigraphic layers and structures (e.g., joints, faults, shear planes and tension cracks) provide additional information on internal geological structures and failure mechanisms, as well as how and where groundwater flows through landslide bodies and surrounding bedrock (**Figure 4**; cf. Whiteley et al. 2018). Electrical resistivity tomography (ERT), frequency modulated electromagnetic conductivity (FEM), ground-penetrating radar (GPR), seismic primary wave refraction (PWR), and multichannel analysis of shear waves (MASW) surveys provide the most useful information on the distribution earth materials, in addition to the distribution and quantity of groundwater (Huntley et al. 2017a; Huntley et al. 2019a). Geophysical methods adopted for hydrogeological logging of observation wells include down-hole measurement of natural gamma radiation (GR), induction conductivity (IC) and magnetic susceptibility (MS). Subsurface borehole monitoring, combining ShapeAccelArray inclinometers with piezometer head levels, indicate that the landslides studied in the Thompson River valley are failing along sub-horizontal, weak, basal shear surfaces in highly plastic clay beds that extend under the river, and are exposed at the valley bottom in some cases (Porter et al. 2002; Eshraghian et al. 2007; Eshraghian et al. 2008). At Ripley Landslide, detailed borehole logging shows that the central and northern parts are translating sub-horizontally (2.1° to 2.5°), whereas the southern portion near a lock-block retaining wall has a steeper (28°) slide surface (Macciotta et al. 2014; Hendry et al. 2015; Schafer et al. 2015).

For the Thompson River valley, slow-moving landslides are influenced by the distribution of forests, shrublands, grasslands, wetlands, water, croplands, and railway infrastructure. Vegetation cover generally contributes to increased slope stability through the action of binding roots and water absorption in soils. However, extensive, deep-penetrating roots on steep slopes also contributes to the mechanical and chemical weathering of soils and parent materials by providing additional materials for remobilization if triggered by other factors (e.g., seismic shaking and precipitation events). Lying leeward of the Coast Mountains, the

valley experiences semi-arid conditions with annual precipitation as rainfall and snow <2,700 mm (Dominguez-Cuesta and Bobrowsky 2011). Greater cyclic and seasonal ground moisture changes due to evapotranspiration varying strongly between winter and summer will also drive deterioration of slope stability.

4.3 Landslide form: UAV and bathymetric surveys

UAVs allow flexible, inexpensive acquisition of low-altitude aerial images, while various off-the-shelf photogrammetric Structure from Motion (SfM) software packages enable production of high-resolution DEMs, digital surface models (DSM), and orthophoto mosaics from such images. These UAV surveys help characterize landslide surface morphology and the spatial extent of displacement. DSMs and corresponding orthophoto mosaics provide very high spatial resolution datasets enabling detailed topographical and textural information (cf. Huntley et al. 2020a; Huntley et al. 2021a). UAVs, when equipped with a LiDAR sensor, penetrate the vegetation cover and provide elevation data in areas where the photogrammetry based SfM method is likely not to produce a representative ground surface. Merged mosaics and DSMs capture the surface condition of landslides, and the extent of bare earth and vegetation growth (e.g., grasses, shrubs, and trees). Metre-scale anthropogenic features (e.g., train tracks, lock-block retaining walls, culverts) are resolvable in high-resolution raster imagery.

In 2021, the GSC began operating a DJI Phantom 4 Pro V2 with a 48-megapixel optical payload, and a DJI Matrice 300 with 35 mm lens; both with real-time kinetic positioning (RTK) capabilities. These upgrades allowed flight altitudes >70 m above ground level, shorter flight times and fewer battery changes, and a smaller number of images and file sizes per flight plan. Flight plans for Ripley Landslide, South Slide, North Slide and Nepa Slide (**Figure 5**) were set up using Spexi Geospatial and DJI platforms prior to fieldwork. Flight and photogrammetry variables included: altitude above ground level (72 m = 2 cm per pixel resolution); front and side overlaps for photograms (80% and 70%, respectively); flight direction (0º to 180º); speed (8 m s^{-1}); and gimbal pitch (-90º for planform photograms). High-resolution photogrammetry and change-detection monitoring (cf. Huntley et al. 2021a, b) requires a UAV with an optical sensor payload in excess of 250 grams, subscription-based commercial software for flight plans and data acquisition, along with trained and certified operators and observers following strict Transport Canada (TC) rules for operating remote piloted aircraft systems (RPAS). The number of UAVs and appropriately trained field operatives available limits the duration and spatial coverage of surveys, and generic utility as a geohazard monitoring tool. In the fall of 2021 and spring of 2022, we tested a scalable RPAS platform developed by Spexi Geospatial Inc. (www.fly.spexigeo.com [URL 2022]), and its abilities as a tool for landslide inventory mapping and change-detection monitoring in western Canada. This RPAS streamlined UAV flight operations for data capture, cloud processing and image rendering to aid in the inventory and monitoring of slow-moving landslides of the Thompson River valley railway corridor.

Multiple landslides were surveyed each day, depending on areal extent of the flight plans, weather conditions, and time of day (**Figure 5**). Flights were undertaken on October 20 (Nepa Slide, Ripley Landslide, South Slide), November 01 2021 (Red Hill Slide, North Slide), and March 20 2022 (Ripley

Landslide, Nepa Slide, South Slide, North Slide). For each survey, UAV RTK base stations were established over stable GCPs (e.g., NP-02, **Figure 6**). Geo-referenced image files captured during flights were stored on UAV memory cards, and then downloaded to cloud storage for later desktop processing. Contour maps (50 cm intervals), DEMs, DSMs, and orthomosaic photograms were readily generated from selected imagery and point clouds using the Spexi Geospatial platform, and exported into Global Mapper and ArcGIS software for further processing and change-detection monitoring. Useful platform review products included metadata reports on survey parameters, UAV and camera properties, camera locations with X, Y, and Z error estimates, point cloud parameters, and coordinate systems.

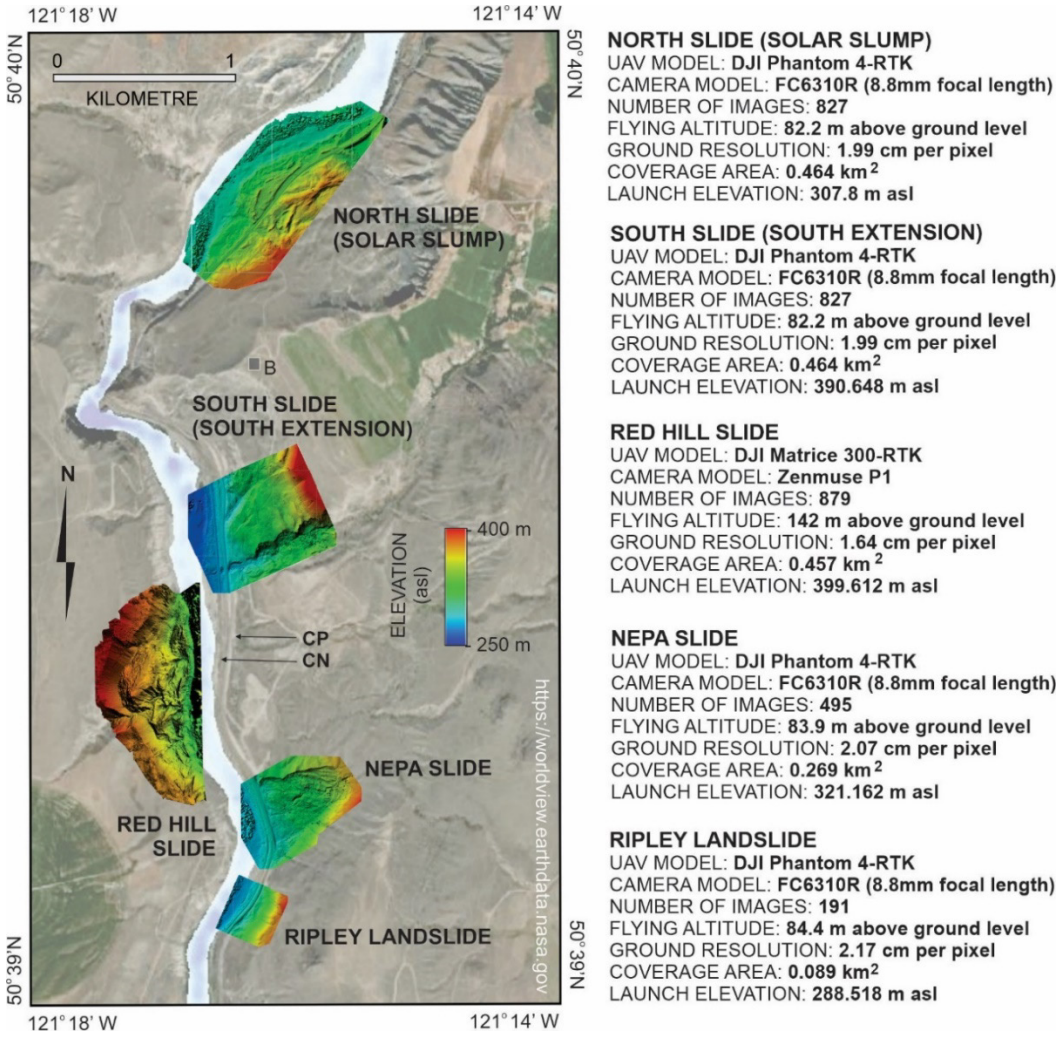

Figure 5. Landslide of concern along the Thompson River valley railway corridor: flight plan footprints and DEMs generated from point clouds for the 2021 UAV surveys. Flight statistics generated using the Spexi Geospatial platform. Orthomosaic DSMs are shown in **Figure 6**.

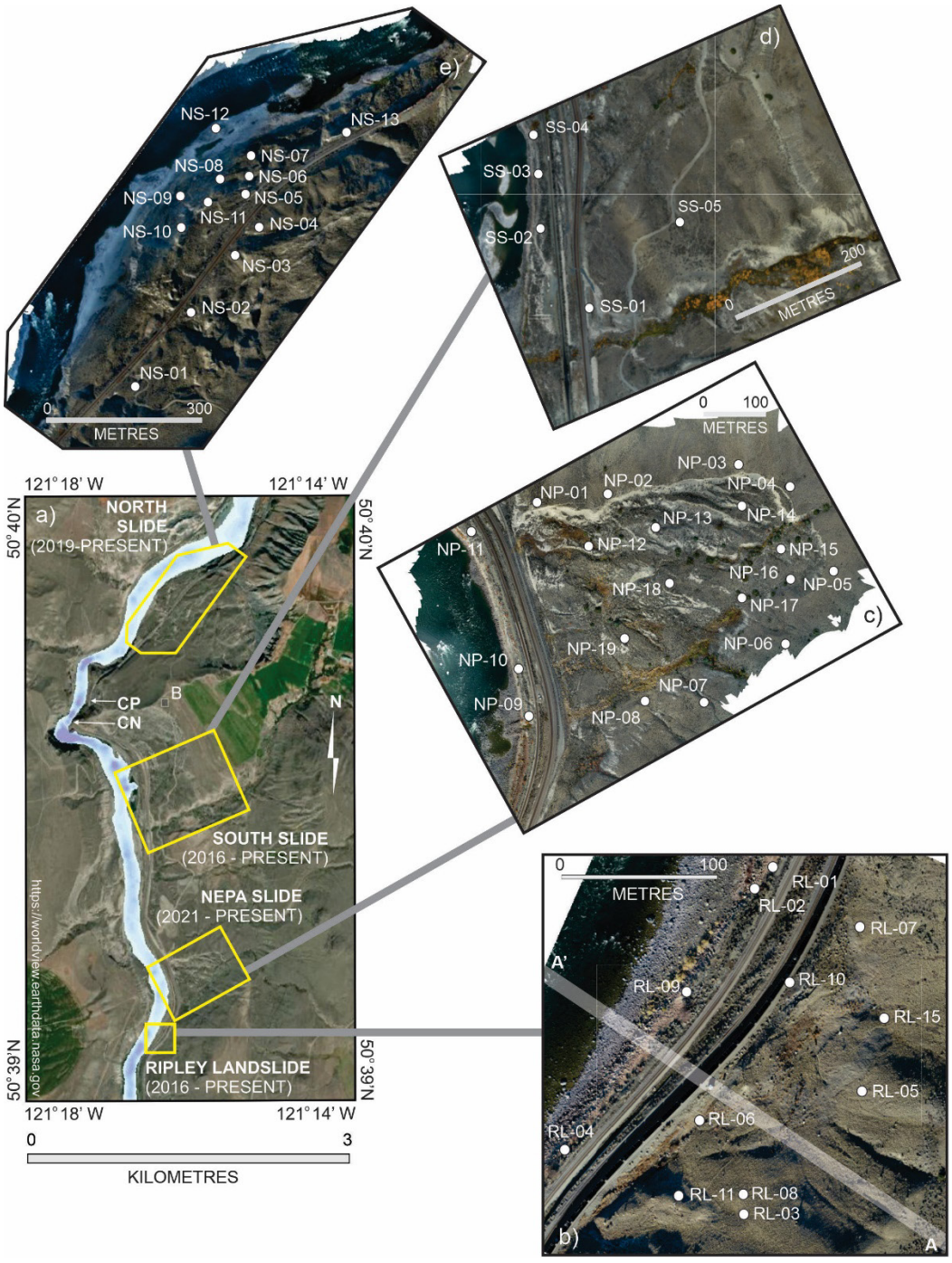

Figure 6. Landslides of concern in the Thompson River valley with GCPs and UAV digital surface mosaics. **a)** Location of RTK-GNSS surveyed landslides along the railway corridor. **b)** Ripley Landslide, 15 GCPs established in 2016 (GCP-06 and GCP-12 are beyond the southern limit of landslide captured in photogram). **c)** Nepa Slide, 19 GCPs established in 2021. **d)** South Slide, 11 GCPs established in 2016 (GCP-06 to GCP-11 are beyond the northern limit of landslide captured in photogram); **e)** North Slide, 13 GCPs established in 2019-2021.

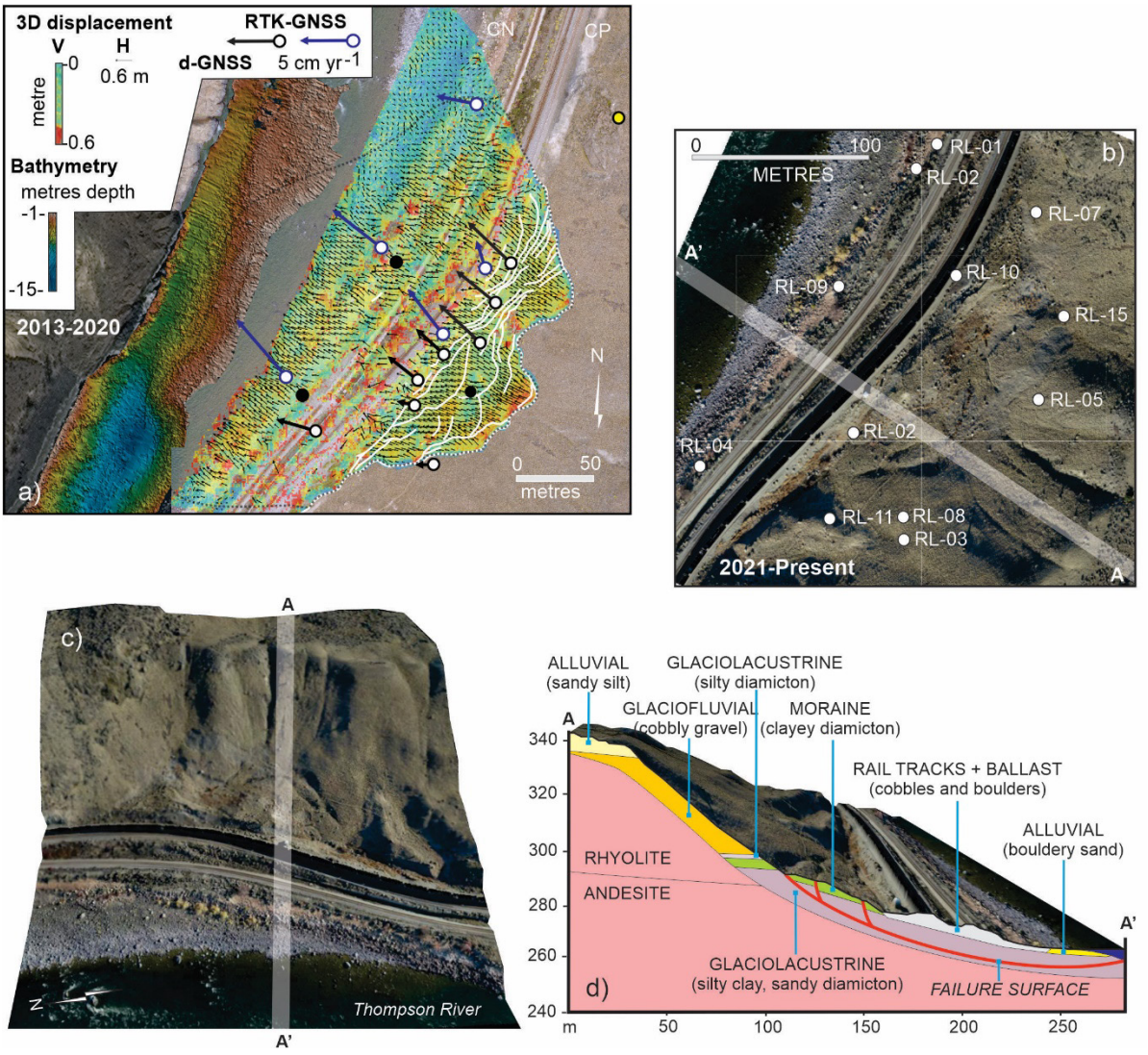

Figure 7. Ripley Landslide: **a)** surface displacement data derived from UAV overflights in 2016 and 2018 and multi-beam bathymetry data collected in 2018; plotted with RTK-GNSS (average annual rate for 2017, 2018 and 2019) and d-GNSS displacement data (November 2018 to June 2019, expressed as cm yr^{-1}). Stable d-GNSS unit – yellow dot; active d-GNSS unit – black and white dot; inactive d-GNSS – black dot. Active GCP - blue dot (modified from Huntley et al. 2021a). **b)** Orthomosaic showing location of GCPs and cross-section A-A'. **c)** DSM (2.5 X vertical exaggeration), showing location of cross-section A-A'. **d)** Cross-section A-A' showing surficial hydrogeological units and inferred failure surfaces comprising landslide.

Bathymetric surveys better characterized the geometry of submerged landslide toe slopes and identified reaches with channel incision and erosion. Acoustic single-beam and multi-beam river surveys combined with GPR and ERT reveal variations in channel bed composition ranging from sand and silt draping bedrock to coarse gravel and boulders overlying clay-rich valley fill (Huntley et al. 2019a-c; Huntley et al. 2021a).

Significantly, shallow waters (riffles) with rapids lie adjacent to stable terrain, while deep scour pools (up to 50 m below river level) are found adjacent active slide toes and unstable river canyon walls.

4.3.1 Ripley Landslide

At 0.089 km^2, Ripley Landslide has the smallest flight plan footprint and areal extent (0.026 km^2) (**Figure 7a**). Orthomosaic images and DSMs from 2016 to 2021 capture the active floodplain of Thompson River at *ca.* 260 m asl, and railway infrastructure crossing a gentle to steep slope (<12° to >35°) with subdued translational-rotational slide blocks, tension cracks, closed depressions, and prominent head and side scarps. A glacial outwash terrace, with a surface elevation of 360 m asl, lies upslope and east of the active landslide. Fifteen permanent GCPs were established on stable boulders and anthropogenic features in 2016 (**Figure 6b**; **Figure 7a, b**). Nine earth material units are recognized from ground observations in the vicinity of GCPs, and on UAV imagery from 2016 to 2021 (**Figure 7a**; Huntley et al. 2020). GCPs along the CN and CP tracks (RL-01, -04, -09 and -10) are established on cobble and boulder ballast up to 3 m thick. This anthropogenic layer overlies up to 25 m of glaciolacustrine clay and silt, and glacial boulder-rich diamicton (basal till) with shear surfaces 10-15 m below surface, resting on fractured andesite (Huntley et al. 2019; Huntley et al. 2020). Upslope of the tracks, unconsolidated sediment thickness decreases in the main slide body, with GCPs established on silt and sand-rich alluvial outwash, colluviated till and glaciofluvial gravels. Beneath RL-02, -08 and -11, this veneer covers up to 5 m of glaciolacustrine clay and silt draped on fractured andesite and rhyolite. Above the head scarp, GCPs are established shallow deposits (< 2 m thick) of colluvium and glaciofluvial outwash resting on igneous bedrock (RL-03, -05, -07, -15).

4.3.2 Red Hill Slide

The Red Hill Slide flight plan footprint is 0.457 km^2, with the 2021 orthomosaic image and DSM capturing a 0.298 km^2 rotational-translational landslide with moderate to steep slopes between >12° and <37° and 145 m of relief (**Figure 5**). Vegetation-free slide blocks with back scarps 5-20 m high are incised by a steep-sided ephemeral gully channelling irrigation seepage and hillslope runoff. The stratigraphy exposed above the active river floodplain (ca. 265 m asl) comprises glaciolacustrine silt and clays, truncated and overlain till diamicton, sand and gravel outwash, and wind-reworked silt-rich alluvial terrace formed at 410 m asl.

4.3.3 Nepa Slide

The flight plan footprint for Nepa Slide is 0.254 km^2, with the disturbed land covering 0.136 km^2. The 2021 orthomosaic image and DSM capturing the active floodplain of Thompson River at ca. 265 m asl, and railway infrastructure crossing a gentle toe slope (<12°). The main translational slide body consists of sparsely vegetated hummocky blocks and closed depressions, flanked by prominent head and side scarps. A dendritic network of ephemeral channels, infilled with saturated silt and sand-rich alluvial outwash and organic sediments, and fed by springs and irrigation runoff, incises these blocks. Nineteen GCPs were installed on Nepa Slide in 2021 (**Figure 6c**; **Figure 8a**) to establish whether portions of the main body are reactivating. Below the CN and CP tracks, NP-09, -10 and -11 rest on cobble and boulder ballast up to 3 m thick. Like Ripley Landslide, this anthropogenic layer overlies >10 m of fine-grained glaciolacustrine deposits and boulder-rich till with shear surfaces extending under Thompson River (**Figure 8b**). GCPs on

stable terrain north of the slide body (NP-01, -02, -03 and -04) sit on a wind-reworked alluvial silt and sand veneer draping boulder-rich till (< 3 m thick). These coarser surface units overlie glaciolacustrine silt and clay >20 m in thickness (**Figure 8c**). Along the southern flank, boulder-rich till (2-5 m thick), resting on fractured andesite and rhyolite, underlies NP-05, -06, -07 and -08. Across the main slide body and upslope of the tracks, GCPs (NP-12 to NP-19) sit on slide blocks comprising colluviated till and glaciofluvial sand and gravel (<5 m thick), overlying glaciolacustrine clay and silt beds (>10-15 m thick).

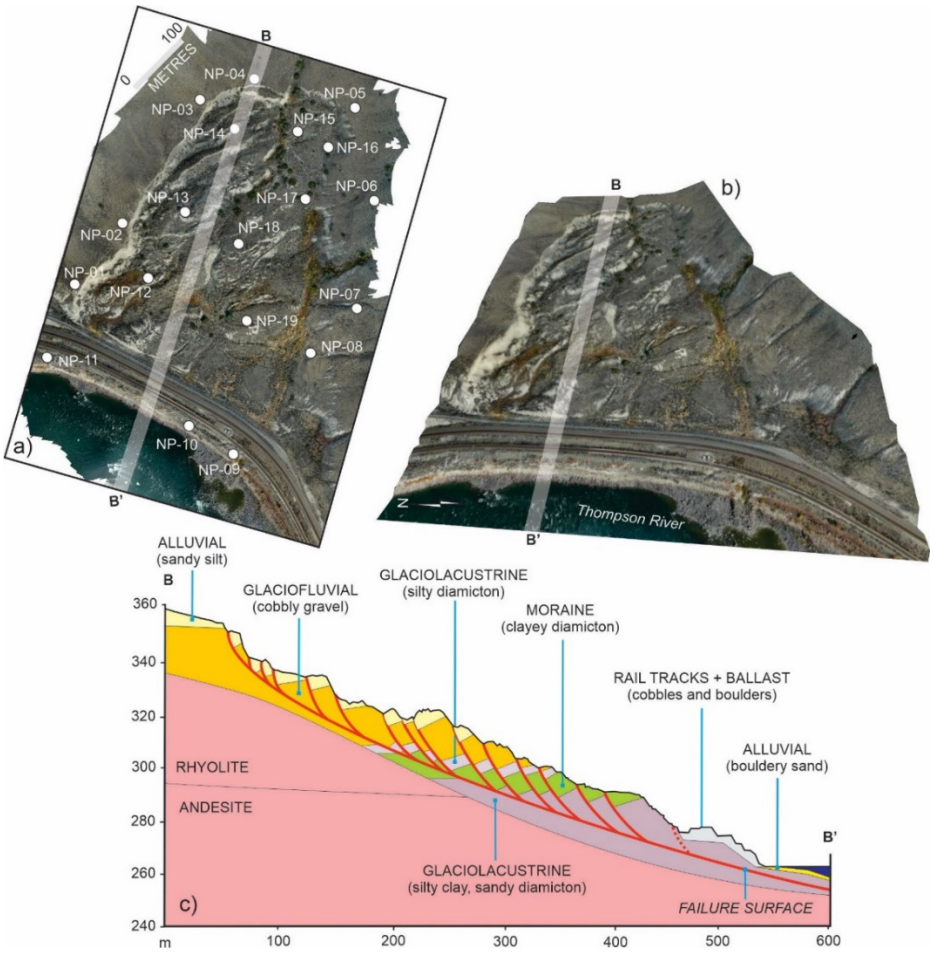

Figure 8. Nepa Slide: **a)** Orthomosaic showing location of GCPs and cross-section B-B'. **b)** DSM (2.5 X vertical exaggeration), showing location of cross-section B-B'. **c)** Cross-section B-B' showing surficial hydrogeological units and inferred failure surfaces comprising landslide.

4.3.4 South Slide (South Extension)

At 0.464 km^2, the South Slide (South Extension) shares the largest flight plan footprint with the North Slide (Solar Slump) (**Figure 5**). The "South Extension" has an approximate area of 0.144 km^2. The October 2021 orthomosaic image and DSMs captures the active floodplain of Thompson River and tributary alluvial fan

at ca. 265 m asl. Railway infrastructure crosses the slide toe with slopes ranging from >12º to <27º. The slide body consists of a northern portion with eroded slide blocks and closed depressions, relatively free of vegetation cover; and a southern extension showing no surficial evidence of movement (e.g., tension cracks, slide scarps). Eleven GCPs were positioned across the headwall, toe slope and south extension of South Slide in 2016 (**Figure 6d**). GCPs along the CN and CP tracks (SS-01, -02, -03 and -04, -09) are established on thick (>15 m) glaciolacustrine clay, silt and glacial boulder-rich diamicton (basal till). The toe slope is excavated to accommodate the CN and CP tracks, and draped in a cobble and boulder ballast up to 5 m thick. Upslope of the tracks, unconsolidated sediment thickness increases in the main slide body, with SS-05 to SS-11 established on silt and sand-rich alluvial outwash, overlying glaciolacustrine and till units >25 m in thickness.

4.3.5 North Slide (Solar Slump)

At 0.464 km^2, the North Slide (Solar Slump) shares the largest flight plan footprint with the South Slide (South Extension) (**Figure 5**; **Figure 9a-d**). The "Solar Slump" has an approximate area of 0.044 km^2. The merged mosaics and DSMs (**Figure 5**; **Figure 9c**) capture the baseline surface condition of the North Slide, long with the extent of bare earth and vegetation growth (e.g., grasses, shrubs, and trees). Metre-scale anthropogenic features (e.g., train tracks, signals bungalow, solar panel array) are resolvable in the orthophoto mosaic and DSM. Geomorphic features visible include: terraces graded to 340 m and 300 m asl, with steep river-cut scarps; ephemeral gullies draining the inactive 19th Century slide surface; active slide blocks, scarps and tension cracks across the "Solar Slump"; several grabens, and an interpreted toe bulge in the active floodplain of Thompson River (**Figure 9c, d**). In 2019, eleven permanent GCPs were installed across the North Slide toe slope; another station was added in 2020 on the floodplain toe slope bulge; and a thirteenth installed at the NW limit of the active toe slope in 2021 (**Figure 9c**). On the Thompson River floodplain (*ca.* 270 m asl), a boulder veneer drapes back-tilted clay and silt beds beneath NS-12. Bedrock does not outcrop in the survey area. Inactive and active slide blocks with GCPs are incised by ephemeral gullies and by cut-bank erosion during high river stages (during summer months). Over the slide toe, GCPs are established boulders resting on boulder-rich diamicton (basal till) and glaciofluvial sand and gravel outwash (5-10 m thick) overlying >20 m of glaciolacustrine clay and silt. Landslide scarps across the "Solar Slump" form subparallel to the orientation of the river channel. In the northwest, cutbank erosion along a 200 m section of Thompson River has exposed and triggered a series of slumps in terraced glaciolacustrine and till deposits below 280 m asl. These small slumps ($\leq$ 50 m^2) are directly impacting railway infrastructure as slope down dropping is observed immediately beneath the track at the interpreted solar slump headscarp (**Figure 7b, e**). Landslide scarps follow the arc of relict back-rotated slide blocks (GCPs NS-05, -06, -10 and -11), and increase in size and activity toward the river (GCPs NS-07, -08 and -09). Tension cracks are extrapolated beneath railway ballast close to the solar panel array and signals bungalow (between GCPs NS-04, -05 and -13).

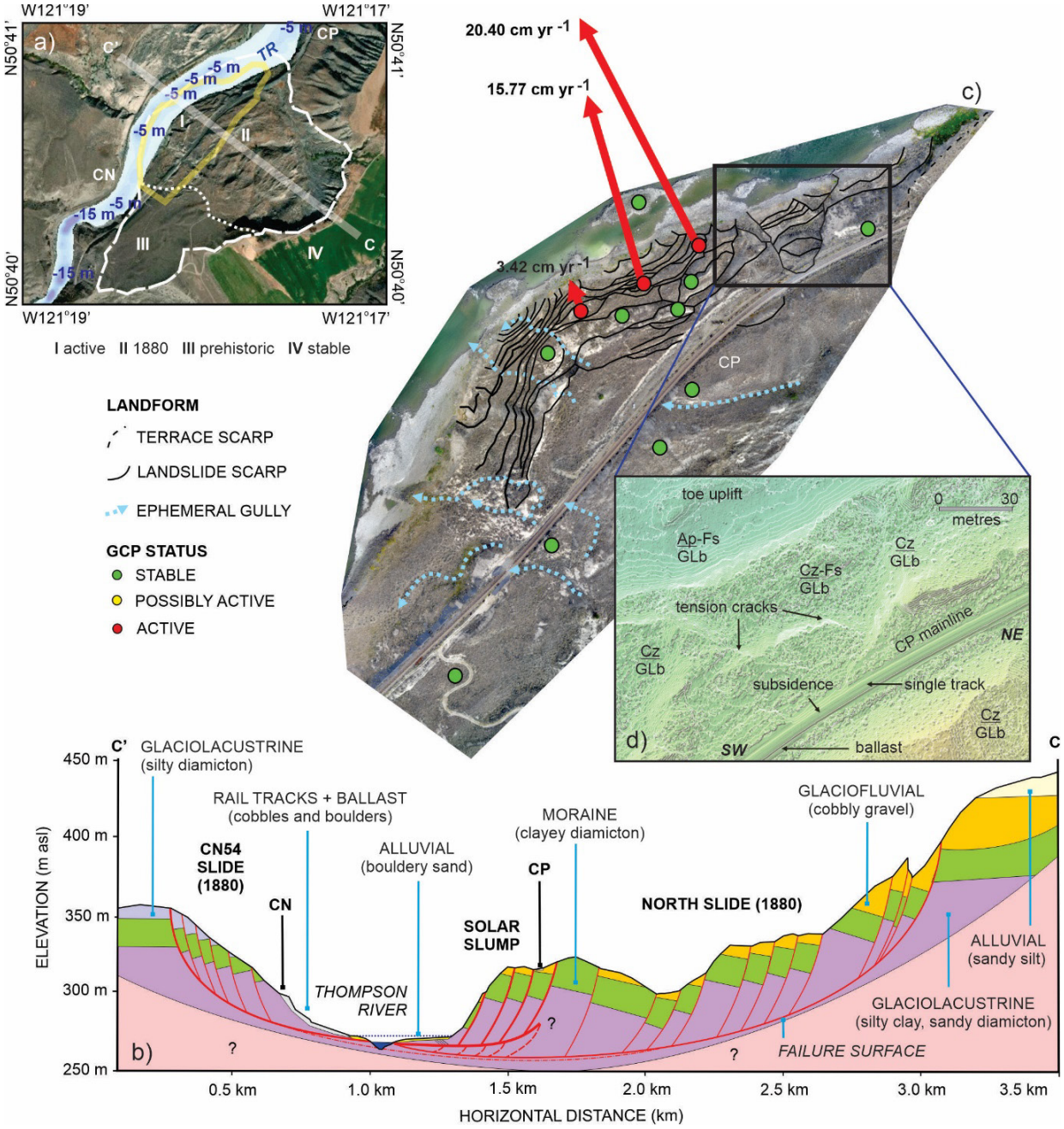

Figure 9. North Slide: **a)** WORLDVIEW image capturing extent of active "Solar Slump" (I), historical (II) and prehistoric movement (III) movement, stable terrain (IV) and location of cross-section C-C'. **b)** Cross-section C-C' showing surficial hydrogeological units and inferred failure surfaces comprising landslide **c)** Orthomosaic showing location of GCPs and landforms. d) DEM showing terrain units and key landslide features in relation to railway infrastructure.

Southeast and upslope of the CP tracks, retrogressive translational back-rotated slide blocks and scarps from the 1880 landslide are now subdued features due to 140 years of wind deflation, soil creep, and surface

runoff. Slopes ≥12° are draped in a veneer of colluviated till, glaciofluvial outwash and glaciolacustrine sediments. The historical landslide and active "Solar Slump" are gullied by ephemeral streams that drain to a coarse alluvial fan prograding into Thompson River flanking the western margin of the toe slope (**Figure 9c**).

4.4 Landslide function: satellite InSAR change-detection monitoring

Satellite remote sensing is an effective first approach for determining the risks posed from ground hazards and whether further site investigation is required. InSAR provides the best opportunity to determine the extent of landslide activity in the Thompson River valley (Journault et al. 2016; Huntley et al. 2017b; Journault et al. 2018). Slope deformation is monitored using persistent scatterer InSAR techniques, with landslide mapping, modelling, back-analysis of deformation velocities, and long-term deformation trends derived from datasets (e.g., Macciotta et al. 2014; Journault et al. 2016; Huntley et al. 2017c; Journault et al. 2018). Trihedral aluminium corner reflectors, permanent coherent artificial InSAR targets, improves the precision and accuracy of subsequent image processing of images. Different LoS viewing geometries allow for the projection of vertical and horizontal displacement. Ground movement measured by space-borne InSAR produces results with precision comparable to RTK-GNSS measurements, but with the advantage of monitoring displacement over large areas (Huntley et al. 2017c; Journault et al. 2018).

Satellite InSAR monitoring indicates at least five large volume rotational-translational landslides remain active and have potential to adversely impact CN and CP railway infrastructure and services (Journault et al. 2016; Huntley et al. 2017b; Journault et al. 2018; Huntley et al. 2021a-c). From south to north along the railway transportation corridor, these include the following landslides of concern with an average 1D line-of-sight (LoS) displacement greater than 3 cm yr^{-1}: Ripley Landslide, Red Hill Slide, South Slide, North Slide, and Goddard Slide (**Figure 3c**). SAR platforms with repeat visit times of weeks (e.g., RADARSAT-2 [RS2] and SENTINEL-1 [S1]) to days (e.g., RADARSAT Constellation Mission [RCM]) provide rapid monitoring capability with cm-scale precision and accuracy when periodically benchmarked with ground-based RTK-GNSS measurements and UAV photogrammetry. RS-2 and S1 InSAR results from 2013 to 2020 indicate similar magnitudes and spatial-temporal patterns of displacement. Regions of highest landslide activity intersecting with railway infrastructure correlate with cutbank erosion and channel bed scour on the outside bends of the river. Ground movement is shown to be generally concentrated within the main body of most sliding masses. Rates of displacement detected by InSAR vary seasonally, with slower displacement rates occurring during the May to August interval, and higher values from September to April each year.

4.4.1 North Slide (Solar Slump)

RCM SAR datasets were examined to further refine the spatial and temporal distribution of landslide activity at the North Slide (**Figure 10a**). The combination of relatively high spatial and temporal resolution offered by RCM resolves rapid movement over small areas that would otherwise be aliased by the coarser spatial and temporal resolution of RS2 and S1 (Huntley et al. 2021b-d). Twelve RCM scenes from the end of August to early December, 2020, and twenty scenes from January to September 2021 were acquired

during descending orbit passes (west-ranging) at a nominal ground resolution of 3 m, with an ideal revisit frequency of 4 days (Huntley et al. 2021b, c). RCM data was processed using GAMMA software (Wegmüller et al. 2019) following the methodology of Samsonov et al. (2017) and Dudley et al. (2020). SAR images were precisely aligned with a chosen master using normalized cross-correlation to yield SAR data cubes that could be analyzed spatially, or in time (**Figure 10b,** step 1).

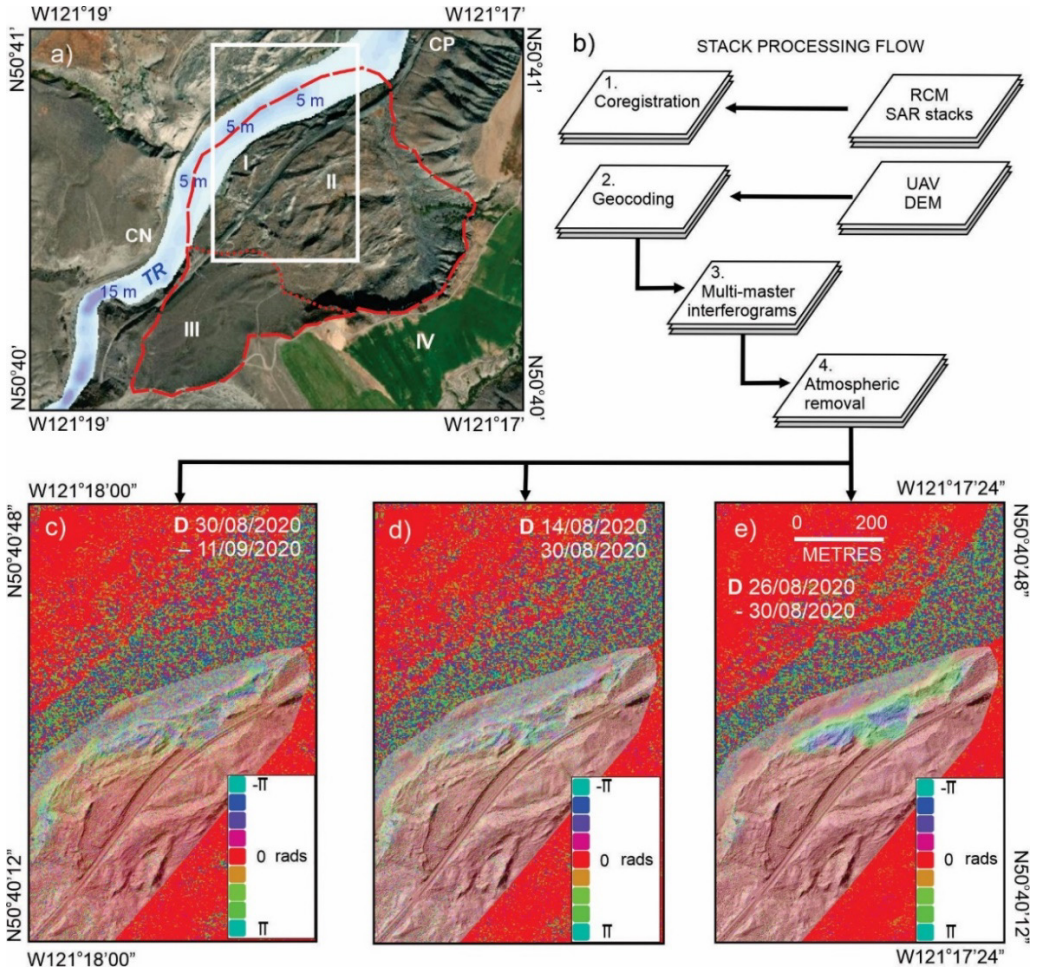

Figure 10. Differential InSAR analysis of RCM time-series results. **a)** Extent of North Slide. I) Active slide toe (0.08 km^2) with tension cracks, sparse vegetation and steep scarp faces (post 2000). II) Inactive slide main body and head scarp (0.55 km^2) with sparse vegetation, and subdued scarp faces and slide blocks (ca. 1880). III) Inactive slide body (0.37 km^2) with established vegetation ground cover, and subdued surface morphology (ancient, i.e., >300 years before present). IV) Stable postglacial slopes and terraces supporting irrigated crops and cattle pasture. **b)** Generalized InSAR processing steps followed in this paper (modified from Huntley et al. 2021b). **c)** RCM interferogram, 2020/08/30 – 2020/09/11 (28 days). **d)** RCM interferogram, 2020/08/14 – 2020/08/30 (16 days). **e)** RCM interferogram, 2020/08/26 – 2020/08/30 (4 days). UAV-derived SFM-DSM overlain at 50% transparency for topographic context (modified from Huntley et al. 2021b, c).

InSAR processing and landslide change-detection benefited from an accurate high-resolution DEM to simulate and remove the topographic effects from the interferograms (Barret et al. 2012; Hu et al. 2019).

Co-registered RCM stacks were benchmark geocoded with a 1 m-pixel resolution airborne LiDAR dataset, 1 arc-second resolution Advanced Land Observation Satellite (ALOS) World DEM data, UAV photogrammetry (2 cm pixel-resolution), and ground-based RTK-GNSS measurements (x, y, z ± 3 cm) (**Figure 7**; **Figure 10b**, step 2). DEMs were resampled and aligned with the multi-master interferograms to provide a height value for each SAR pixel. This helped to remove topographic signals in interferograms (**Figure 6b**, steps 3 and 4; **Figure 10a**), corrected orbit information as needed, and provided the relationship between SAR and map data used later for projecting results back into map space (Huntley et al. 2021b, c). Additional RCM processing created a robust time-series for LoS displacement of GCPs in 2021 (**Figure 10a**). RTK-GNSS measurement from 2019-2020 are shown for comparison (**Figure 7a**).

The 2020 RCM InSAR results reveal slope deformation from the end of August to middle September (**Figure 10c-e**). Several fringes indicate movement of approximately 2 cm to 5 cm over 28-day (**Figure 5c**) and 16-day periods (**Figure 5d**), indicating a rapid and complex deformation pattern in the most affected zones. The 4-day interferogram (**Figure 5e**) shows nearly a full fringe cycle, indicating a rapid and complex deformation pattern on shorter time scales. Maximum deformation over this 4-day period is estimated to be ~2 cm. For the January to May 2021 interval (**Figure 11a**) The spatial extent captured by RCM showing the cumulative deformation from January 5, 2021 to May 9, 2021 is very similar to that seen with the UAV imagery (**Figure 11b**). The colour stretch is +/-5cm, indicating measurement of approximately 5-6 cm of line-of sight deformation at NS-07 and NS-08. There is also uplift between NS-07 and NS-12, which is where back-tilted clay-silt beds are exposed in the active floodplain (Huntley et al. 2021b). Research efforts are now directed at comparing the two time-series and converting satellite LoS displacements to correspond with movement vectors derived from UAV and RTK-GNSS datasets.

4.5 Landslide function: UAV change-detection monitoring

In many parts of the world, unoccupied aerial vehicle (UAV) photogrammetry is increasingly incorporated into local, regional and national geohazard monitoring protocols for vulnerable economic infrastructure and communities (Casagli et al. 2017; Turner et al. 2015; Rossi et al. 2018; Sestras et al. 2021). From environmental, economic, logistical and transportation safety perspectives, rapidly deployable UAVs offer a low-carbon footprint alternative to geological mapping using fixed-wing aircraft and helicopters, particularly along linear transportation routes and around remote northern communities. Rigorous change detection requires accurate and precise elevation models to serve as reference base topographic maps. Optical UAV imagery and light detection and ranging (LiDAR) data captured during field surveys can be desktop-processed to generate point cloud digital surface models (DSMs) and digital elevation models (DEMs). UAV photogrammetry, when benchmarked with satellite synthetic aperture radar interferometry (InSAR) and ground-based real-time kinematic (RTK) global navigation satellite system (GNSS) measurements, provides cm-scale resolution geospatial data for geohazard mapping and landscape change-detection monitoring (Booth et al. 2013; Handwerger et al. 2021; Huntley et al. 2021 a, b).

Repeat UAV surveys have aimed to better characterize the spatial extent, magnitude and direction of landslide movement over time in the Thompson River valley (Huntley et al. 2021a, d). Change-detection

monitoring focused on the most active landslides identified during inventory: Ripley Landslide (2016-2018) and North Slide (2019-2021), and results are reported on here. As part of the new UAV and RTK-GNSS change-detection program initiated in 2022, the orthophoto mosaic, DEMs and DSMs of Ripley, Nepa, Red Hill, South and North slides captured in October and November 2021 (**Figure 4**) will serve as the baseline for further RPAS and InSAR change-detection monitoring.

The GSC RPAS allows trained UAV pilots to quickly and easily capture imagery, and transfer processed data to stakeholders (e.g., government agencies, railway industry, remote communities) in a timely manner. The time elapsed from flight request to data delivery is comparable to commercial SfM applications. The RPAS is capable of simultaneous deployment on multiple landslides > 3 km^2 allowing for more productive fieldwork. Geospatial datasets (orthophoto mosaics, DEMs and DSMs) derived from UAV surveys have processed X, Y, Z accuracies of 3 to 5 cm: comparable to RTK-GNSS and InSAR measurements. Resulting datasets from the collected and processed imagery with a pixel resolution of 2.5 cm can easily resolve small surface features (e.g., GCPs, railway ties, bedrock fractures and tension cracks). Orthophoto mosaics, DEMs and DSMs captured in 2021 (**Figure 5**; **Figure 6**) will serve as the baseline for further RPAS landslide change-detection monitoring along the national railway corridor in the Thompson River valley.

4.5.1 Ripley Landslide

Repeat UAV surveys of Ripley Landslide in 2016 and 2018 characterized the spatial extent, magnitude and direction of landslide movement (**Figure 7a**). Planimetric displacement was first mapped using co-relation processing (cf. Lucieer et al. 2014; Turner et al. 2015; Türk 2018) on hill-shaded UAV DSMs with 1.5 times exaggeration, and the sun at azimuth 310° and 45° altitude. Areas of vegetation and recent track ballast work on hill-shaded images were masked prior to processing to reduce the areas with substantial change not related to slide movement. Two images were created for E/W (x) and N/S (y) displacement, while elevation changes (z) were derived from the 2016 and 2018 DSMs. These values were added and squared to produce a single raster containing positive 3D displacement values and line of-sight directions, with larger values representing more displacement (**Figure 7a**; Huntley et al. 2021a). Co-relation results from 2016-2018 show >50 cm NW displacement of blocks along steep-dipping, retrogressive backscarps to the main slide body (**Figure 7a**). Over much of the slide body, movement is to the NW, except along the northern and southern flanks, where displacement is W. In contrast, channel scour along the slide toe and submerged bedrock bounding the landslide drives the body mass generally to the W. This high value is consistent with the InSAR and GNSS monument data that captured significant displacement in 2017 (Bunce and Chadwick 2012; Huntley et al. 2021a). Displacement along the tracks reflects subsidence of the slide body (also expressed in deformation of the lock-block retaining wall), and the addition of ballast during routine safety maintenance. A zone of high displacement at the south flank of the slide foot is likely the consequence of toe-slope erosion as evidenced by the 15 m-deep scour pool mapped by the bathymetric surveys (**Figure 7a**). Across much of the foot slope however, 3D displacement values are lower, reflecting translational movement of the slide mass over sub-horizontal failure planes beneath the tracks and river.

A new UAV and RTK-GNSS change-detection program was initiated in 2022 following significant slope modification during a stakeholder geotechnical investigation in 2020-2021 (Huntley et al. 2021c). The DEM and DSM captured in October 2021 (**Figure 5**; **Figure 6b**; **Figure 7b, c**) will serve as the baseline for further RPAS change-detection monitoring at Ripley Landslide.

4.5.2 North Slide (Solar Slump)

For the North Slide, a more sophisticated, but less personnel time-consuming approach was possible with recent advances in cloud-based data storage and processing. Following the methodology of Gojcic et al. (2021), we employed a fully automated deformation analysis workflow that estimated 3D displacement vectors from point cloud data. Dense 3D displacement vector fields were estimated by searching for corresponding cloud points across DSM epochs at September 2019 and September 2021. Aligning the GCPs and manually picking tie points to improve point cloud registration between the two surveys significantly enhanced the quality of the M3C2 point-cloud comparison results (**Figure 11b, c**). An area of 436 m^2 with displacement values > 5 cm between September 2019 and September 2021 lies NW of the CP track (NS-07, -08 and -13), extending onto the Thompson River floodplain (NS-12). Significantly, UAV change-detection photogrammetry shows landslide activity immediately beneath railway infrastructure (ballast and tracks; **Figure 9d**). Localized displacement SW of NS-10 records the formation of colluvial cones by a small debris fall along the river embankment.

4.6 Landslide function: RTK-GNSS change-detection monitoring

GNSS techniques have been successfully employed to determine the three-dimensional coordinates of moving points on landslides (Macciotta et al. 2017; Rodriguez et al. 2018). Repeat RTK-GNSS ground surveys aim to better characterize the magnitude and direction of landslide movement over time. A prime ground control point (GCP) was established on a stable post-glacial terrace near Black Canyon (**Figure 3b**). The absolute position of this base station (WGS84 + NAD83 UTM Zone 10 E5614082.268 N619963.25, 390.648 m asl) was determined from a post-processed RINEX file using the Canadian Spatial Reference System Precise Point Positioning tool after a nine-hour occupation. The reported absolute positional accuracy was 0.8 cm horizontally and 1.3 cm vertically (95% Σ). Ground control points (GCP) were then established across landslides of interest, using stable boulders and anthropogenic features on, and adjacent to railway infrastructure (**Figure 6b-e**). RTK-GNSS rover measurements at GCPs occupied for a minimum of two minutes at 1 Hz were reported with horizontal precisions of better than 2 cm and vertical precisions of 3 cm. All RTK-GNSS positioning data have been reviewed, corrected for antenna laybacks, heights and edited for erroneous data points (Huntley et al. 2017a; Huntley et al. 2021a). RTK-GNSS change-detection monitoring focused on the most active landslides identified during inventory: Ripley Landslide (2016-2018) and North Slide (2019-2021).

4.6.1 Ripley Landslide

A total of 15 GCPs are positioned on stable boulders and anthropogenic features at Ripley Landslide (**Figure 6b**). Between 2017 and 2019, five GCPs recorded horizontal displacement on the landslide. GCPs showing 3 cm or less movement are discounted from discussion as they are below the measurement

precision and accuracy of the RTK-GNSS. Immediately upslope of the train tracks (within a few metres), on the main slide body, RL-10 recorded 8.7 cm of movement to the NNW. Disturbance during track maintenance accounted for the anomalous vector for RL-10 and slower displacement rate. Downslope of the tracks, across the slide toe, 11.3 cm of WNW displacement was measured at RL-02; RL-04 displaced 16.4 cm NW; and RL-09 moved 18.3 cm NW over the three-year observation period. The remaining GCPs were on stable portions of the slope, and adjacent to the landslide (Huntley et al. 2021a).

Periodic monitoring of GCPs and railway infrastructure provides limited information on the seasonal variation in displacement rates and amounts. GNSS provide continuous, near real-time monitoring of surface displacement, but only at three trackside locations monuments (Bunce and Chadwick 2012; Macciotta et al. 2014). A Geocube (GeoKylia) ^{TM} continuous differential (d-) GNSS network was installed to address both issues of spatial and temporal coverage (Huntley et al. 2021a). Displacement results from November 2018 to June 2019 are discussed here. Immediately apparent is the generally NW displacement trend of relative location data (X, Y, Z) averaged every 15 days over the eight month-long observation trial (**Figure 6a**). The NW displacement trends are consistent with the displacement vectors derived from change detection analysis of the RTK-GNSS survey, and UAV imagery using the SfM and Cosi-Corr software (**Figure 7a**). In the northern sector of the landslide, d-GNSS units capture movement at varying rates from November 2018 to June 2019, suggesting displacement of multiple slide blocks. The unit on the most northerly block moved horizontally NW 5.5 cm, while dropping 1.8 cm in elevation. A second unit, in a graben block, moved NW 4.5 cm with a 1.7 cm drop in elevation. The third unit, on the central block, moved horizontally NW 5.0 cm, dropping 1.5 cm over the trial. In the southern sector, generally slower horizontal, but greater vertical displacements are recorded over the eight month observation period. The unit on the slide block near the CP tracks and signals bungalow captured 3.2 cm horizontal movement to the NW, with a drop of 3.0 cm. Units located in a graben toward the southern margin of the slide moved horizontally NW 0.1 and 3.4 cm, while dropping up to 1.8 cm prior to power failure during the winter. The unit on the lock-block retaining wall recorded 3.9 cm of horizontal movement NW, and experienced 3.2 cm vertical downward displacement - the greatest vertical downward displacement across the slide body – before power failure in early May 2019. A unit above the southern head scarp, captured 1.2 cm of horizontal movement to W, while dropping in height by 0.08 cm. These small displacement values may be an indication of developing (i.e. retrogressive) instability upslope of the active headscarp. The two areas of maximum displacement recorded by the d-GNSS network coincide with maximum displacement indicated by InSAR and UAV analysis. The larger northern zone spans the CN and CP tracks, while a smaller zone at the south end of the landslide near the lock-block retaining wall (Macciotta et al. 2014; Rodriguez et al. 2018; Huntley et al. 2020b; Huntley et al. 2021a).

4.6.2 North Slide (Solar Slump)

Similar to Ripley Landslide, displacement patterns and magnitudes derived from UAV photogrammetry (**Figure 9c**; **Figure 11c**) were evaluated with RTK-GNSS measurements of GCPs collected at the same time as UAV surveys (**Figure 11**). Limits on RTK-GNSS measurement precision and accuracy discounts points showing 3 cm or less movement (**Figure 9c**; **Figure 11b**; NS-01, -02, -03, -04, -05, -06, -10 and -

11). Those GCPs with annual differences of >3 cm were considered robust measurements. Individual slide blocks are resolved with RTK-GNSS measurements. Between 2019 and 2020, NS-07, -08 and -09 all showed displacement vectors to the NNW (**Figure 9c**). Maximum annual displacement values of 15.77 cm yr^{-1} (NS-08) and 20.40 cm yr^{-1} (NS-07). Between March and September 2021 (**Figure 11b**), NS-07 records 10 cm of NW displacement, corroborating UAV and dInSAR change-detection results (**Figure 11 a, c**). Significantly, the displacement vectors indicate movement toward the scour pools lying adjacent to the "Solar Slump" (**Figure 6a**; **Figure 9a**).

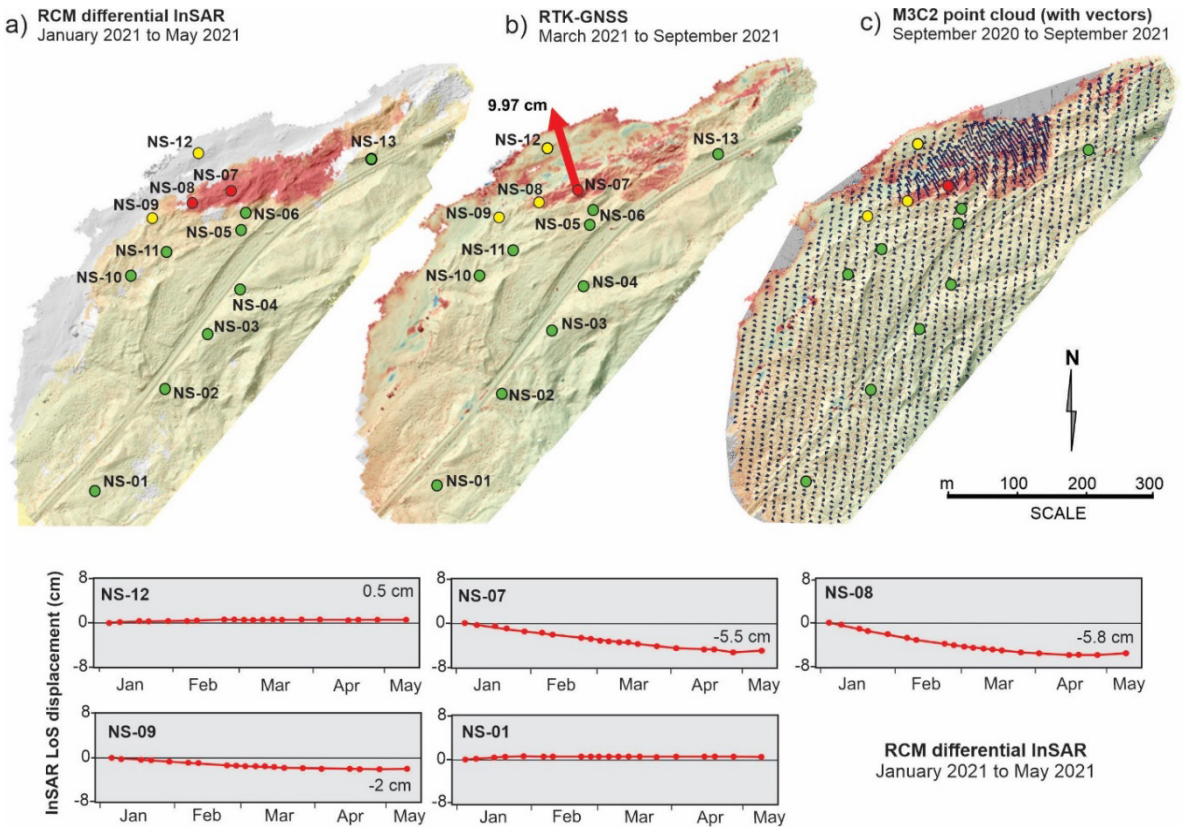

Figure 11. North Slide 2019 DSM and change-detection time-series: **a**) RCM dInSAR results (August 2020 to September 2021) indicating approximately 5-6 cm of LoS deformation at NS-07 and NS-08 (+/-5cm colour stretch, green to red). **b**) RTK-GNSS measurements of GCPs showing almost 10 cm of NW displacement at NS-07 between survey epochs (September 2019 and September 2021). **c**) Dense 3D displacement vector fields estimated across DSM epochs (September 2019 and September 2021).

4.7 Landslide function: *in situ* instrumental change-detection monitoring

Elevated soil moisture was recognized as a driver of slope failure in the Thompson River valley since the first slope stability study in the area (Stanton 1898). Regional and local groundwater conditions contribute to high pore pressures and slope instability along the transportation corridor. Since clay impedes groundwater flow, pore pressure increases along the surface of clay layers, resulting in reduced material strength and decreased slope stability (Porter et al. 2002; Clague and Evans 2003). On active landslides,

Piezometers terminating in fractured glaciolacustrine deposits at depths greater than 5 m record upward hydraulic gradients and elevated pore pressures on active landslides, confirming toe slopes are in a discharge zone of a regional groundwater flow system (Eshraghian et al. 2008; Hendry et al. 2015). In addition to upslope irrigation and surface rainfall, a strong correlation between river stage and pore pressures suggests Thompson River partly controls the distribution of groundwater in the slide mass. This it achieves by acting as a lower hydraulic boundary for the regional groundwater regime within the fractured bedrock; and by allowing horizontal connectivity through higher conductivity layers of fluvial cobbles, gravels and sands (Hendry et al. 2015; Schafer et al. 2015).

Proactive infrastructure monitoring and evaluation (PRIME) with continuous ERT and soil moisture acquisitions capture subsurface responses in interannual and seasonal variations in precipitation, in addition to temperature, surface runoff, and snowmelt (Sattler et al. 2018; Holmes et al. 2018; Huntley et al. 2019b, c; Holmes et al. 2020; Sattler et al. 2020; **Figure 12a, b**). Noticeable increases in rate of movement occur when high, prolonged flows of Thompson River sustained by snowmelt are followed by low groundwater flow through the autumn and winter months (Macciotta et al. 2014; Schafer et al. 2015; Tappenden 2016). The greatest displacement rates occur from November to March when transitional ground conditions allow snowmelt and rainfall to penetrate deep into the still frozen (or thawing) slide body by way of tension cracks, planar fractures, and bedding surfaces (**Figure 12c, e, g**). Resistivity and soil suction show similar seasonal trends, responding cyclically to changing weather conditions from December to March (**Figure 12d, f, h**). Fibre Bragg grating (FBG) and Brillouin optical time domain reflectometry (BOTDR) indicate peak strain rates in the lock-block retaining wall at the south end of Ripley Landslide also occur in the fall and winter months (Huntley et al. 2017c).

To understand climatic controls, local weather conditions, including wind speed and direction, rainfall and snow depth, air temperature, ground temperature, and soil matric suction are monitored (W, Fig. 3; Fig. 4m). Weather station data confirm that major precipitation events occur mostly between fall and spring when landslide activity increases (Fig. 6b). Fluctuations in temperature over the winter months also contribute to intervals of landslide activity with thawing soil moisture recharging groundwater (Holmes et al. 2018; Huntley et al. 2019 b, c; Holmes et al. 2020; Sattler et al. 2020; Sattler et al. 2021).

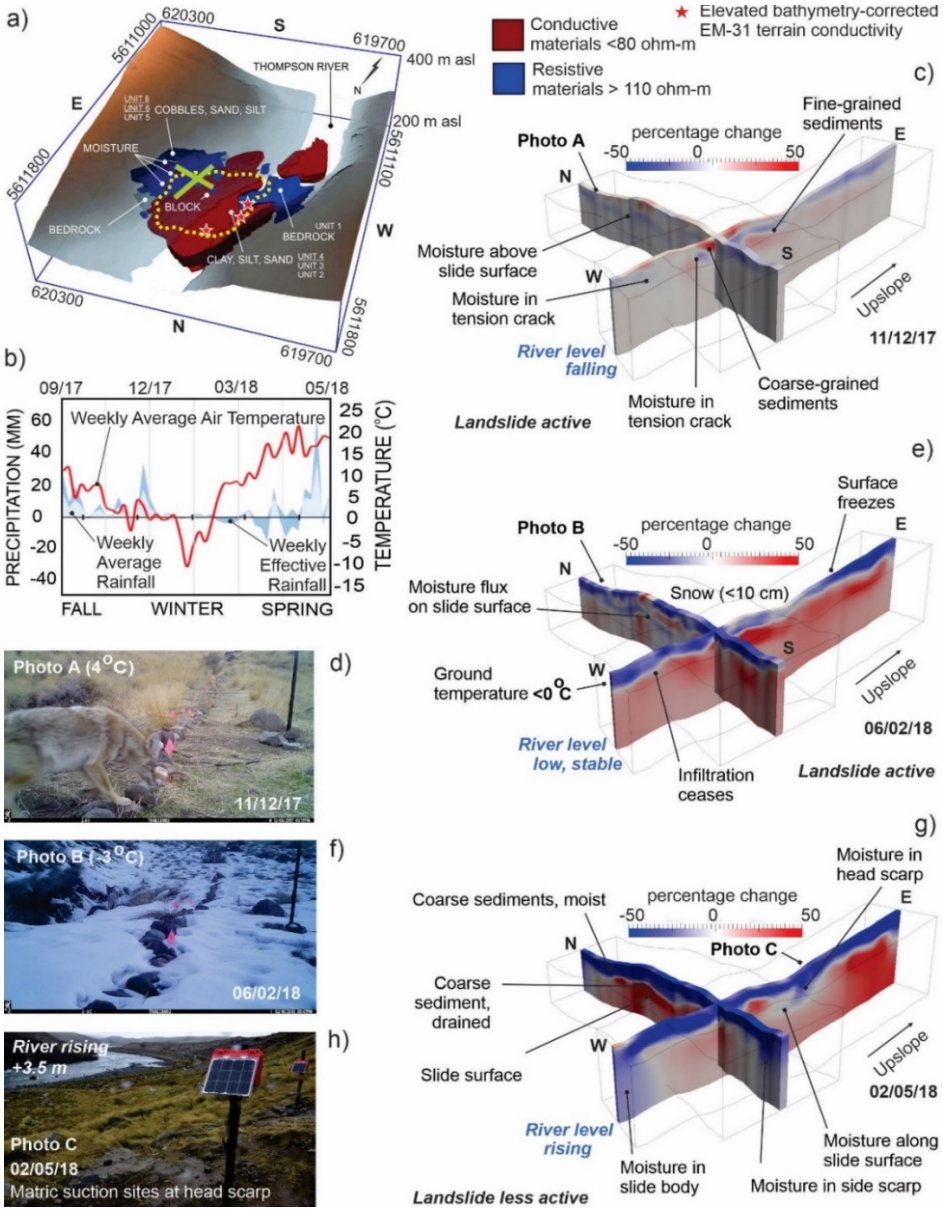

Figure 12. *In situ* ERT time-series monitoring observations, results and interpretation for Ripley Landslide, in the Thompson River valley, southwestern BC. a) 3D block diagram of merged ERT data captures a static proxy image of subsurface resistive and conductive earth materials (see **Figure 3**). b) Precipitation, expressed as a weekly average rainfall and effective rainfall; and temperature expressed as a weekly average from September 2017 to May 2018 (Holmes et al. 2020; Sattler et al. 2020). c) and d) Resistivity profile of PRIME cross-sections (north-south, east-west) with observations of ground conditions and changes in resistivity (Ωm) from December 5, 2017. e) and f) Ground and resistivity conditions February 6, 2018. g) and h) Ground and resistivity conditions for May 2, 2018 (after Holmes et al. 2018; Sattler et al. 2018; Huntley et al. 2019c; British Geological Survey © UK Research and Innovation 2020).

5. Summary Discussion and Research Directions for 2022 to 2025

5.1 Climate-driven landslides and consequences in the national railway corridor

Across Canada, relief, slope, aspect, distance from hydrological features, environmental conditions, surficial geology, and land cover conspire to produce a wide range of rapid and slow-moving landslides (**Table 1**) with the potential to impact railway infrastructure and operations. Landslides have been responsible for numerous casualties, injuries and deaths, costly damage to transportation infrastructure and property, socioeconomic losses, and environmental degradation since the late 18th Century (Blais-Stevens 2020). Since the late 1800s, the operational and economic consequences of slope failure along the national railway transportation corridors have depended on the scale and rate of movement, and temporal relationship between landslide activity and train timetables.

In the Thompson River valley transportation corridor (**Figure 3**), small amounts of cumulative displacement (<10 cm yr^{-1}) between 2008 and 2022 have been detected by InSAR, UAVs and periodic RTK-GNSS surveys (e.g., **Figure 7**; **Figure 9**; **Figure 10**; **Figure 11**) at the Ripley Landslide and North Slide. Incremental surface displacements contribute to minor track misalignment, requiring short-term (seasonal) reorganization of train schedules to allow the safe addition of ballast and realignment of tracks, and to avoid significant time-tabling impacts (i.e., intrinsic consequences). Greater surface displacement will damage bridges, culverts, retaining walls and access roads, and cause major track misalignment with potential for train derailments and service disruption. Potential accompanying negative environmental impacts (i.e., extrinsic consequences) include the loss of natural resources, including fish, wildfowl, game animals, cattle and crops, and potable water for communities.

Global climate change is anticipated to lead to more extreme regional weather events across Canada, along with an increase in the frequency and magnitude of landslides, floods, wildfires and other geological hazards in all provinces and territories (Sauchyn and Nelson 1999; Couture and Evans 2006; St. George 2007). For example, increasing precipitation and higher sustained river flows will change groundwater pressures on slide rupture surfaces extending below rivers and lakes, contributing to increased instability of slopes along the national railway transportation corridors. Climate-driven geological hazards can potentially compromise the safe and secure transport of rural resources and intermodal goods across the continent. A cascade of resulting negative intrinsic and extrinsic consequences for transportation and energy infrastructure, supply chains for goods and services, as well as the environment, will challenge the integrity and resilience of national transportation infrastructure and local communities (Evans and Clague 1997; Geertsema et al. 2006a, b; Blais-Stevens 2020).

The extreme storm system of November 14, 2021, in southwestern BC and its aftermath illustrates such a cascade of events. Following a dryer-than-normal summer and wetter-than-normal fall along all major transportation corridors through the Cascades and Coast Mountains (**Figure 2**), wildfire-disturbed slopes received >100 mm of rain in 24 hours (and up to 300 mm over 48 hours) during an extreme "atmospheric river event" (https://weather.gc.ca/ [URL 2021]). Along with the loss of life (human and livestock),

railways, highways, pipelines, power transmission networks, light industrial, and rural-urban infrastructure (e.g., potable water conduits and sewage treatment plants) sustained significant damage because of widespread storm-driven landslides and flooding. The costly relocation of whole communities and reorganization of transportation and shipping schedules led to national socioeconomic losses through service disruption and broken supply chains extending well beyond the winter of 2021-2022. Long-term negative environmental consequences include widespread contamination of agricultural lands and damage to natural fish and wildlife habitats.

5.2 Landslide laboratories along the national railway corridor

Testing of landslide monitoring technologies as part of IMOU 5170 began in 2013 along the Thompson River valley, BC; and expanded to the Assiniboine River valley, MN in 2019. Since 2020, three primary research and development objectives have been to: 1) Understand controls on landslide movement, and in particular, the impacts of extreme weather events and climate change. 2) Compare, evaluate, and identify the monitoring technologies that provide the most useful information on why, how, and when landslides move. 3) Identify reliable real-time monitoring solutions for railway infrastructure able to withstand the harsh environmental conditions of Canada. GSC Open File 8931 presents a comprehensive landslide change-detection mapping protocol combining fundamental geoscience with monitoring results. Terrain inventories, landslide susceptibility, and risk assessments are informed by: 1) RS2, S1 and RCM InSAR analyses; 2) Uninhabited aerial vehicle (UAV) change-detection photogrammetry; 3) Field-based monitoring of slope displacement using a real-time kinematic global navigation satellite system (RTK-GNSS); and 4) Instrumental measurement of climate and hydrological variables (precipitation, temperature, seasonal changes in river discharge).

COVID-19 significantly influenced research plans, equipment procurement, and geoscientific outreach in 2021-2022 outlined in **Appendix 1** and **Appendix 2**. Continual changes in operational processes challenged and realigned productivity goals for team members and stakeholders. Travel prohibitions limited access to conferences and field sites. Consequently, team members continued to develop in-house (or at-home) functionality and capability using cloud storage and processing services. Similar to 2020-2021, stakeholder collaboration consisted of a blend of virtual meetings with more traditional modes of communication. In 2021-2022, new information on slow-moving landslide hazards was published in national and international journals, as textbook chapters, presented at virtual national and international conferences, and summarized in this open file report (**Appendix 3**). These publications provide fundamental geoscience knowledge to help key industry stakeholders (e.g., CN and CP) and university partners (e.g., UA and USASK) measure, manage, and mitigate landslide geohazards and their consequences. **Appendix 4** lists the acronyms used in GSC Open File 8931.

5.3 Developing geohazard mapping protocols for slow-moving landslide research

Proactive landslide disaster-risk management requires knowledge of the timing and magnitude of ground displacement events. Observations of geological, geophysical, and geotechnical properties of landslides at national, regional and local scales are incorporated with site-specific benchmark monitoring acquired using

an array of remote sensing platforms, and *in situ* change-detection monitoring technologies and methodologies. Temporal relationships between landslides and the environmental conditions triggering instability are determined from time-series monitoring and GIS analyses of satellite InSAR, UAV orthophotos, and ground-based RTK-GNSS surveys. Although each change-detection method has limitations, our multi-sensor approach provides supplementary information to close data gaps and corroborate results. From 2022 to 2025, research in the Thompson River valley, BC and Assiniboine River valley MN-SK will combine field-based landslide investigations with multi-year geospatial and *in-situ* time-series monitoring (**Appendix 1**; **Appendix 2**). Research activities will contribute to a more resilient national railway transportation network able to meet Canada's future socioeconomic needs, and ensures protection of the environment and resource-based communities from landslides related to extreme weather events and climate change.

Mapping efforts in the Thompson River valley in 2022-2023 (and until 2025) will focus on benchmarking field observations where needed, and desktop compilation of geographic and temporal datasets (e.g., GCPs, DSMs, InSAR, GNSS stations and Geocubes ™), the production of a Canadian Geoscience Map for Ripley Landslide, South Slide, and other landslides in the transportation corridor. These GSC map products, incorporating remote predictive mapping of hyperspectral satellite imagery and landslide susceptibility, will be useful working tools for industry and academic partners, contractors, and risk managers (**Appendix 1**; **Appendix 2**). In addition to the continuing mapping efforts in the Thompson River valley, beginning in the summer of 2022, fieldwork undertaken in the Assiniboine River valley will ground-truth terrain interpretations, and describe sedimentological characteristics that cannot be determined by remote mapping. The PRIME system refined picture of moisture-driven processes for landslides in this semi-arid terrain (e.g., Holmes et al. 2020; Huntley et al. 2020a; Sattler et al. 2021). Evaluated in the context of other monitoring results (e.g., Geocubes ™, InSAR and UAV change detection), these data are helping researchers understand the mechanisms involved in landslide movement (e.g., precipitation and groundwater recharge), and to reduce the costs of maintenance and improve the effectiveness of mitigation plans in the Thompson River valley.

Collaboration with the British Geological Survey (BGS), provincial and university partners, colleagues at Newcastle University in the UK, and University College, Dublin, Ireland, and contractors (e.g., Spexi Geospatial Inc., Symroc, Frontier Geosciences Inc.) will continue through 2022 to 2025. Geophysical research objectives are to: 1) understand the impact of extreme precipitation events (monitored by the weather station) on slope stability in the Thompson River valley by comparing climate data with the results of the Geocube ™ and InSAR installations. 2) Establish how surface water infiltration contributes to groundwater conditions on the slope by installing piezometers, soil moisture meters, and extensometers across the slide body (monitoring sites selected from UAV orthophotos and optical satellite images). 3) Determine whether slope stability can be monitored by combining ultra-wide broadband seismic/vibration sensing technology, soil moisture, climate data, and benchmarked InSAR change-detection analysis. Transmission of these data in real-time (or every 4-12 days for SAR satellites) will allow stakeholders and government agencies.

5.4 Developing satellite InSAR analyses protocols for slow-moving landslide research

Proactive risk management requires knowledge of the timing and magnitude of ground displacement events. The active North Slide is currently the test site for applications of RCM and other SAR satellite platforms and development of change-detection software. RS2, S1, and RCM InSAR databases provide spatially expansive and temporal records of motion, but are restricted to one- and two-dimensional line-of-sight components. The higher spatial resolution of RCM resolves earlier RS2 and S1 sampling issues (e.g., due to rapid motion or snow cover). Our studies show that satellite InSAR platforms with repeat visit times of weeks (e.g., RS2 and S1) to days (e.g. RCM) provide rapid monitoring capability with cm-scale precision and accuracy when periodically "ground-truthed" with UAV photogrammetry and ground-based RTK-GNSS measurements. Benchmarked InSAR datasets clearly demonstrate that the North Slide toe slope is active (> 20 mm yr^{-1}), with peak movement occurring between the months of September and November when river discharge is falling. The RS2, S1, and RCM InSAR time-series show an apparent relationship between the amounts of cumulative annual displacement of persistent and temporary target pixels, peak LoS displacement velocities, and river discharge.

RCM with optimal 3-4 day return times for scene acquisition (**Figure 10**), when combined with automated image processing (cf. Huntley et al. 2021a, b) is a powerful tool for change-detection monitoring in the Thompson River valley; and will become so elsewhere along national railway transportation corridors (e.g., Assiniboine River valley, Manitoba). The spatial and temporal overlap of RS2, S1 and RCM allows greater coverage and monitoring redundancy. In 2022, the installation of aluminum trihedral corner reflectors across North Slide will enable submillimeter accuracy of InSAR change-detection time-series (cf. Ferretti et al. 2007). InSAR corner reflectors will be identified in the growing stack of SAR imagery by examining the degree of phase stability over time for every resolution cell within the study area. By considering only targets with persistent scatterer characteristics and correcting for phase change contributions caused by orbital position errors, topography and atmospheric effects, a time-series of deformation for each target corner reflector will be recovered, with measurement accuracies of several mm (cf. Henschel et al. 2015).

Satellite InSAR analysis, when combined and other geospatial and temporal datasets, will help stakeholders develop a more resilient railway national transportation network able to meet Canada's future socioeconomic needs, while ensuring protection of the environment and resource-based communities from natural disasters related to extreme weather events and climate change.

5.5 Developing remote piloted aircraft system protocols for slow-moving landslide research

GSC Open File 8931 demonstrates the investigative capacity of a RPAS for landslide monitoring along the Canada's national railway transportation corridor. When benchmarked with RTK-GNSS measurements, UAV photogrammetric techniques allow the representation of large surfaces with dense spatial sampling of cm-scale resolution geospatial data for geohazard mapping and landscape change-detection monitoring, providing three-dimensional coordinates of moving points on landslides. The RPAS presented, generating high spatial resolution epochal imagery, offers clear advantages with respect to InSAR time-series analysis

providing LoS displacement measurements over large areas, and RTK-GNSS surveys of GCPs which provide data that are spatially accurate, but necessarily limited to a small number of control points. UAV photogrammetry and RTK-GNSS surveys show landslides have a significant motion that is only partly captured by satellite InSAR monitoring. This is a clear demonstration of a limitation in east-west-up-down sensitive InSAR, since failing slopes are largely moving NW or SE, so a significant amount of movement is likely not recognized by satellite monitoring alone. UAV photogrammetry, when benchmarked with RTK-GNSS, satellite InSAR, and other geospatial and temporal datasets will help stakeholders develop a more resilient railway national transportation network able to meet Canada's future socioeconomic needs, while ensuring protection of the environment and resource-based communities from natural disasters related to extreme weather events and climate change.

In 2022-2023, the GSC aims to develop an RPAS landslide-monitoring program using Spexi Geospatial Platform that allows the quick and easy capture imagery by trained UAV pilots, and transfer processed data to stakeholders in a timely manner (e.g., government agencies, railway industry, and remote communities). The RPAS aims to be capable of simultaneous deployment on multiple landslides > 3 km^2, allowing for more productive fieldwork. Geospatial datasets (orthophoto mosaics, DEMs and DSMs) will have processed X, Y, Z accuracies of 3 to 5 cm: comparable to RTK-GNSS and InSAR measurements. Resulting datasets from the collected and processed imagery with a pixel resolution of 2.5 cm or less can easily resolve small surface features (e.g., GCPs, railway ties, bedrock fractures and tension cracks). Orthophoto mosaics, DEMs and DSMs captured in 2021-2022 (**Figure 5**; **Figure 6**) will serve as the baseline for further UAV landslide change-detection monitoring along the national railway corridor in the Thompson River valley, and elsewhere across Canada.

5.6 Developing RTK-GNSS survey protocols for slow-moving landslide research

GNSS spatial data help understand the behaviour and drivers of slope instabilities affecting rail transport in the Thompson and Assiniboine river valleys. In the Thompson River valley transportation corridor, permanent GNSS monuments (Bunce and Chadwick 2012) and epochal measurement of GCPs (Huntley et al. 2021a) provide baseline measures of landslide activity for the assessment of other monitoring techniques. For both Ripley Landslide and South Slide, GNSS displacement records capture full (i.e., three-dimensional) displacement vectors with high temporal resolution (Macciotta et al. 2014; Hendry et al. 2015). These localized high-resolution spatial data are complementary to remote sensing techniques that provide spatially expansive records of motion with generally lower accuracy (e.g., UAV surveys) or are restricted to line-of-sight components (e.g., InSAR analyses).

An objective for 2022-2025, will be to develop a GNSS monitoring protocol that captures patterns and rates of movement, and changes in landslide activity. For the Thompson Valley, Geocube ™ networks on Ripley Landslide and South Slide will be joined by installation of units across the North Slide "Solar Slump" in 2022. RTK-GNSS and Geocubes ™ will help to understand the spatial and temporal distribution of movement and displacement across the Assiniboine landslides, beginning with installation in 2022 by UA and USASK collaborators. At the CN 184.4, a Geocube ™ network will help to improve characterization

of slope activity by combining three-dimensional displacement measurements with more spatially detailed line-on-sight displacements measured by, for example InSAR or UAV photogrammetry.

As these networks stabilize, data collected (remotely and on-site) will be processed and presented to show graphically: 1) Displacement trends (grey-scaled or colour-graded by month, ArcGIS shapefiles). 2) 3D displacement (mm) -vs- Date (month, year). 3) Surface angle of movement (angle, degrees) -vs- Date (month, year). 4) Precipitation (mm) and 3D displacement (mm) -vs- Date (month, year). 5) Temperature (º C) and 3D displacement (mm) -vs- Date (day, month, year). Key questions to be addressed starting in 2022 are: 1) whether the pattern of landslide activity captured by the Geocube ™ system compares with other monitoring data (e.g., InSAR, UAV, UBVS); and, 2) are changes in river level, soil moisture and groundwater levels monitored in boreholes and test pits across the landslides related to changes in movement detected by the Geocube ™ system?

Detailed examination of Geocube ™ records will provide insight on the rates and spatial pattern of creep as well as the timing, and possibly precursors of changes in creep behaviour. The resulting knowledge will help to characterize landslide hazard, and ultimately reduce landslide risk. The locations of highest creep rates as indicted by the Geocube ™ networks will help identify where track damage can be expected if creep is continuous. Spatial variability in landslide motion will help inform the mechanism of the monitored landslides, such as whether failure involves complex interactions between structurally separate blocks, thus improving landslide characterization and mitigation efforts. Comparing displacement trends with proxy records of possible landslide drivers – including temperature, precipitation, river level and irrigation will help establish landslide-warning thresholds based on environmental conditions. Such comparisons will include detailed analysis of Geocube ™ displacement histories spanning acceleration periods indicated by the CPR GNSS markers (at Ripley Landslide) in an effort to identify possible environmental triggers. If gradual acceleration is found to precede failure events, future Geocube-measured accelerated creep can be used to forecast impending failures.

5.7 Developing *in situ* geoclimatic monitoring to slow-moving landslide research

The magnitude and frequency of landslides and other geohazards are expected to increase as a response to rising precipitation amount (as rain and snow), temperature ranges, and wildfires. The climate monitoring station in the Thompson River valley collected valuable data on precipitation, snowfall, air temperature between 2016 and 2019. This installation was vandalized in 2020 and remained offline for the duration of the COVID-19 pandemic. With the acquisition of two new total weather stations in 2021 (with tipping-bucket rain gauges, air temperature sensors, snow-depth gauges, anemometers and wind vanes), NRCAN-GSC, TC-IC, and collaborators will begin to address outstanding questions on the impact of past and future extreme weather and climate change on landslide activity in the Thompson River valley, BC and Assiniboine River valley MN-SK.

Beginning in 2022, multi-year climate-series will be compared with borehole monitoring results of groundwater levels and subsurface displacement, GNSS, UAV, and InSAR to investigate inter-annual

variation in seasonal displacement rates. A research goal for landslide research in the Thompson River valley will be to establish the degree to which the amount and duration of precipitation (as snow and rain) events, and air temperature are important controls on ground displacement at the start of melt season in late winter-early spring (cf. Holmes et al. 2020). For the Assiniboine River valley, an important test will be to determine the degree to which climate variables influence groundwater conditions and landslide activity (cf. Schafer et al. 2015; Holmes et al 2018; Holmes et al. 2020; Sattler et al. 2018; Sattler et al. 2020). Fluctuations in temperature over the winter months may also contribute to intervals of ground thaw, changes in pore-water pressures and landslide activity. These relationships will be tested over the coming years through validation of landslide deformation records (e.g., Geocube, UAV, and InSAR change detection monitoring) correlated to climate variables.

6.1 Acknowledgements

Annually, research funding is secured with the help of Brooke Jones (Innovation Centre, Transport Canada). Field studies are made possible through the support of Danny Wong (Canadian Pacific Railways, Calgary, Alberta) and Trevor Evans (Canadian National Railways, Kamloops, BC), and Bill Lakeland and Alec Wilson (Spexi Geospatial Inc.). Philip LeSueur (M.Sc., P. Eng., P. Geo.) provided an internal Geological Survey of Canada critical peer review of the draft manuscript.

7. REFERENCES

Aylsworth, J.M., Duk-Rodkin, A., Robertson, T. and Traynor, J.A. 2000. Landslides of the Mackenzie valley and adjacent mountainous and coastal regions. In: The Physical Environment of the Mackenzie Valley, Northwest Territories: A Base Line for the Assessment of Environmental Change. Geological Survey of Canada, Bulletin 547: pp. 167-176

Ballantyne, C.K. 2002. Paraglacial geomorphology. Quaternary Science Reviews, Vol. 21: pp. 1935-2017

Baum, R., McKenna, J., Godt, J., Harp, E. and McMullen, S. 2005. Hydrologic monitoring of landslide-prone coastal bluffs near Edmonds and Everett, Washington, 2001-2004. USGS Open-File Report 1063: 42 p.

Behnia, P., Harris, J., Rainbird, R., Williamson, M. and Sheshpari, M. 2012. Remote predictive mapping of bedrock using image classification of Landsat and SPOT data, western Minto Inlier, Victoria Island, Northwest Territories, Canada, International Journal of Remote Sensing, Vol 33 (21): pp. 6876-6903, https://doi.org/10.1080/01431161.2012.693219

Berg, N., Smith, A., Russell, S., Dixon, N., Proudfoot D. and Take, W.A. 2018. Correlation of acoustic emissions with patterns of movement in an extremely slow-moving landslide at Peace River, Alberta, Canada. Canadian Geotechnical Journal, Vol. 55: pp. 1475-1488

Blais-Stevens, A. 2020. Historical landslides that have resulted in fatalities in Canada (1771-2019). Geological Survey of Canada, Open File 8392: 1 sheet, https://doi.org/10.4095/326167

Blais-Stevens, A., Couture, R., Page, A., Koch, J., Clague, J.J. and Lipovsky, P. 2010. Landslide susceptibility, hazard and risk assessments along pipeline corridors in Canada. Proceedings of the 63rd Canadian Geotechnical Conference and 6th Canadian Permafrost Conference: pp. 878-885

Blais-Stevens, A., Behnia, P. Kremer, M., Page, A., Kung, R. and Bonham-Carter, G. 2012. Landslide susceptibility mapping of the Sea to Sky transportation corridor, British Columbia, Canada: comparison of two methods. Bulletin of Engineering Geology and Environment, Vol. 71: pp. 447-466

Blais-Stevens, A., Maynard, D., Weiland, I., Geertsema, M. and Behnia, P. 2016. Surficial geology and landslide inventory in Douglas Channel fjord, northwest British Columbia', GeoVancouver, Canadian Geotechnical Society, 7 p.

Blatz, J. A., Ferreira, N.J. and Graham, J. 2004. Effects of near-surface environmental conditions on instability of an unsaturated soil slope. Canadian Geotechnical Journal, Vol. 41: pp. 1111-1126

Bobrowsky, P.T. and Dominguez, M.J. 2012. Landslide Susceptibility Map of Canada. Geological Survey of Canada, Open File 7228: 1 sheet

Bobrowsky, P. 2013. Recent advances in landslide monitoring. Paper presented at CIRiDe-International Congress on Disaster Risk and Sustainable Development, Catamarca, Argentina, 1 p.

Bobrowsky, P. 2016. Ripley Landslide: a Canadian test site for landslide investigation and monitoring. International Consortium on Landslides, Technical Presentation, ICL Board Meeting, Paris, 1 page

Bobrowsky, P. 2018. IPL-202 Ripley Landslide Monitoring Project (Ashcroft, B.C., Canada). International Programme on Landslides, Unpublished Annual Report, 1 p.

Bobrowsky, P. and Sladen, W. 2013. Installing Fibre Optics with the China Geological Survey. NRCAN-ESS S&T Newsletter, Issue #21 (NRCan Wiki online digital version only)

Bobrowsky, P., MacLeod, R., Huntley, D., Niemann, O., Hendry, M., Macciotta, R. 2018. Ensuring Resource Safety: Monitoring Critical Infrastructure with UAV Technology. Resources for Future Generations, Conference Abstracts Volume, Vancouver, Canada, 1 p.

Bostock, H.S. 2014. Geology, Physiographic Regions of Canada. Geological Survey of Canada, Map 1254A (2nd edition), scale 1:5 million-scale map: 3 sheets, https://doi.org/10.4095/293408

Bovis, M.J. 1985. Earthflows in the Interior Plateau, southwest British Columbia. Canadian Journal of Earth Sciences, Vol. 22: pp. 313– 334

Bovis M.J. and Jones, P. 1992. Holocene history of earthflow mass movements in south-central British Columbia: the influence of hydroclimatic changes. Canadian Journal of Earth Sciences, Vol. 29: pp. 1746-1755

Brideau, M-A., Stead, D. and Couture, R. 2006. Structural and engineering geology of the East Gate Landslide, Purcell Mountains, British Columbia, Canada. Engineering Geology, Vol. 84: pp. 183-206

Bruce, J.P. and Cohen, S.J. 2004. Impacts of climate change in Canada (Chapter 4). In Coward, H. and Weaver, A.J. (editors); Hard Choices: climate change in Canada; Wilfred Laurier Press, 273 p., ISBN 0-88920-442-X

Bunce C. and Chadwick, I. 2012. GPS monitoring of a landslide for railways. In Landslides and Engineered Slopes - Protecting Society through Improved Understanding, pp. 1373-1379

Campbell, J.E., Harris, J.R., Huntley, D.H., McMartin, I., Wityk, U., Dredge, L.A., and Eagles, S., 2013. Remote Predictive Mapping of Surficial Earth Materials: Wager Bay North Area, Nunavut - NTS 46-E (N), 46-K (SW), 46-L, 46-M (SW), 56-H (N), 56-I and 56-J (S); Geological Survey of Canada, Open File 7118 https://doi:10.4095/293158

Cervi, F., Berti, M., Borgatti L., Ronchetti, F., Manenti, F. and Corsini, A. 2010. Comparing predictive capability of statistical and deterministic methods for landslide susceptibility mapping: a case study in the northern Apennines (Reggio Emilia Province, Italy). Landslides, Vol. 7: pp. 433-444

Charbonneau, A.A. and Smith, D.J. 2018. An inventory of rock glaciers in the central British Columbia Coast Mountains, Canada, from high resolution Google Earth imagery. Arctic, Antarctic, and Alpine Research, Vol. 50: 24 p.

Chen, Z. and Grasby, S.E. 2009. Detection of decadal and interdecadal oscillations and temporal trend analysis of climate and hydrological time-series, Canadian Prairies. Geological Survey of Canada Open File 5782: 13 p.

Chen, Z, Grasby, S. E., Osadetz, K.G., Fesko, P. 2006. Historical climate and stream flow trends and future water demand analysis in the Calgary region, Canada. Water Science and Technology, Vol. 53: no. 10, pp. 1-11

Ciurleo, M., Cascini, L. and Calvello, M. 2017. A comparison of statistical and deterministic methods for shallow landslide susceptibility zoning in clayey soils. Engineering Geology, Vol. 223: pp. 71-81

Clague, J.J. 2002. The earthquake threat in southwestern British Columbia. Natural Hazards, Vol. 26: pp. 7-34

Clague, J.J. and Evans, S.G. 2003. Geologic framework of large historic landslides in Thompson River valley, British Columbia. Environmental & Engineering Geoscience, Vol. 9: pp. 201–212

Conway, K.W. and Vaughn Barrie, J. 2018. Large bedrock slope failures in a British Columbia, Canada fjord: first documented submarine sackungen. Geo-Marine Letters, Vol. 38: pp. 195-209

Couture, R. and Evans, S.G. 2002. A rock topple–rock avalanche, near Goat Mountain, Caribou Mountains, British Columbia, Canada. Proceedings of the 9th Congress International Association of Engineering Geology and the Environment: 1 p.

Couture, R. and Evans, S. 2006. Slow-moving disintegrating rockslides on mountain slopes. In Landslides from massive rock slope failure: proceedings of the NATO Advanced Research Workshop on Massive Rock Slope Failure: New Models for Hazard Assessment. In Evans, S.G., Scarascia Mugnozza, G., Strom, A and Hermanns, R.L. (editors); NATO Science Series, Sub-Series IV: Earth and Environmental Sciences, Vol. 49: pp. 377-393

Couture, R. and Riopel, S. 2008. Regional landslide susceptibility mapping and inventorying in the Mackenzie Valley, Northwest Territories. Proceedings of the 4th Canadian Conference on Geohazards: From Causes to Management: 8 p.

Couture, R., Blais-Stevens, A., Page, A., Koch, J., Clague, J.J. and Lipovsky, P. 2010. Landslide susceptibility, hazard and risk assessments along pipeline corridors in Canada. Congress Proceedings of the 11th International Association for Engineering Geology and Environment: pp. 1023-1031

Cruden, D.M. 1985. Rock slope movements in the Canadian Cordillera. Canadian Geotechnical Journal, Vol. 22: pp. 528-540

Cruden, D.M., Thomson, S., Bornhold, B.D., Chagnon, J.-Y., Locat, J., Evans, S.G., Heginbottom, J.A., Moran, K., Piper, D.J.W., Powell, R., Prior, D. and Quigley, R.M. 1989. Landslides extent and economic significance in Canada. In: Landslides: Extent and Economic Significance: 23 p.

Cruden, D.M. and Varnes, D.J. 1996. Landslide types and processes. In: Landslides: Investigation and mitigation. National Research Council Transportation Research Board, Special Report 247: pp. 36-75

Cruden, D. and VanDine, D.F. 2013. Classification, description, causes, and indirect effects – Canadian Geotechnical Guidelines and Best Practices related to Landslides: a national initiative for loss reduction. Geological Survey of Canada, Open File 7359: 22 p.

Deblonde, C. Cocking, R.B., Kerr, D.E., Campbell, J.E., Eagles, S., Everett, D., Huntley, D. H., Inglis, E., Parent, M., Plouffe, A., Robertson, L., Smith, I.R. and Weatherston, A. 2018. Science Language for an Integrated Geological Survey of Canada Data Model for Surficial Geology Maps (Version 2.3.14), Geological Survey of Canada, Open File 8236: 50 pages (2 sheets)

Doll, C., Trinks, C., Sedlacek, N., Pelikan, V., Comes, T. and Schultmann, F. 2014. Adapting rail and road networks to weather extremes: case studies for southern Germany and Austria. Natural Hazards, Vol. 72: 63-85.

Dominguez-Cuesta, M. and Bobrowsky, P.T. 2011. Proposed landslide susceptibility map of Canada based on GIS. Proceedings of the Second World Landslide Forum: 8 p.

Dudley J.P. and Samsonov S.V. 2020. The Government of Canada automated processing system for change detection and ground deformation analysis from RADARSAT-2 and RADARSAT Constellation Mission Synthetic Aperture Radar data: description and user guide; Geomatics Canada, Open File 63: 65 p. https://doi.org/10.4095/327790

Dufrense, A. and Geertsema, M. 2020. Rock slide-debris avalanches: flow transformation and hummock formation, examples from British Columbia. Landslides, Vol. 17: pp. 15-32

Eshraghian, A., Martin, C. and Cruden, D. 2007. Complex earth slides in the Thompson River Valley, Ashcroft, British Columbia. Environmental and Engineering Geoscience, Vol. XIII: pp. 161-181

Eshraghian, A., Martin, C. and Morgenstern, N. 2008. Movement triggers and mechanisms of two earth slides in the Thompson River Valley, British Columbia, Canada. Canadian Geotechnical Journal, Vol. 45: pp. 1189-1209

Evans, S.G. 1982. Landslides and surficial deposits in urban areas of British Columbia. Canadian Geotechnical Journal, Vol. 19: pp. 269-288

Evans, S.G. 1984. The 1880 landslide dam on Thompson River, near Ashcroft, British Columbia. In: Current Research, Part A: Geological Survey of Canada Paper 84-1A: pp. 655–658

Evans, S.G. and Clague, J.J. 1997. The impact of climate change on catastrophic geomorphic processes in the mountains of British Columbia, Yukon, and Alberta. In: Responding to global climate change in British Columbia and Yukon, Vol I of the Canada Country Study: Climate Impacts and Adaptation, edited by E. Taylor and B. Taylor, Chapter 7: 16 p.

Eyles, N. and Miall, A. 2007. Canada rocks: a geologic journey. Fitzhenry and Whiteside: 512 p. ISBN-13:978-155041-860-6

Fell, R. 1994. Landslide risk assessment and acceptable risk. Canadian Geotechnical Journal, Vol. 31: pp. 261–272

Fulton, R.J. 1995. Surficial Earth Materials of Canada. Geological Survey of Canada Map 1880A, 1:5,000,000

Geertsema, M., Cruden, D.M. and Schwab, J.W. 2005. A large rapid landslide in sensitive glaciomarine sediments at Mink Creek, northwestern British Columbia, Canada. Engineering Geology, Vol. 83: pp. 36-63

Geertsema, M., Schwab, J.W. and Blais-Stevens, A. 2006a. Landslides impacting linear infrastructure in west-central British Columbia. In Proceedings of the 1st Specialty Conference on Disaster Mitigation, pp. DM 1- 10

Geertsema, M., Schwab, J.W. and Blais-Stevens, A. 2006b. Landslides impacting linear infrastructure in west-central British Columbia. In Proceedings of the 1st Specialty Conference on Disaster Mitigation, pp. DM 1- 10

Geertsema, M., Highland, L. and Vaugeouis, L. 2009a. Environmental impact of landslides. In: Landslides – Disaster Risk Reduction: pp. 589-607

Geertsema, M., Schwab, J., Blais-Stevens, A. and Sakals, M. 2009b. Landslides impacting linear infrastructure in west central British Columbia. Natural Hazards, Vol. 48: pp. 59-72

Gendzwill, D.J. and Hajnal, Z. 1971. Seismic investigation of the Crater Lake Collapse Structure in southeastern Saskatchewan. Canadian Journal of Earth Sciences, Vol. 8: pp. 1514-1524

Gerath, R.F. and Hungr, O. 1982. Landslide terrain, Scatter River valley, northeastern British Columbia. Geoscience Canada, Vol. 10: pp. 30-32

Germain, D., Dagenais-Du-Fort, É., Lajeunesse, P. and Simard, M. 2018. Dendrogeomorphic reconstruction of the seasonal timing and rainfall threshold for debris slide occurrence in eastern Canada. Dendrochronologia, Vol. 52: pp. 57-66

Gibson, A., Culshaw, M., Dashwood, C. and Pennington, C. 2013. Landslide management in the UK – the problem of managing hazards in a 'low-risk' environment. Landslides, Vol. 10: pp. 599-610

Glastonbury, J. and Fell, R. 2010. Geotechnical characteristics of large rapid rock slides. Canadian Geotechnical Journal, Vol. 47: pp. 116-132

Harris, S.A. 1973. Studies of soil creep, western Alberta, 1970-1972. Arctic and Alpine Research, Vol. 5: pp. 171-180

Harris, J., and Grunsky, E. 2015. Predictive lithological mapping of Canada's North using Random Forest classification applied to geophysical and geochemical data. Computers and Geosciences, Vol. 80: pp. 9-25

Haque, U., Blum, P., da Silva, P., Andersen, P., Pilz, J., Chalov, S., Malet, J-P., Auflič, M., Andres, N., Poyiadji, P., Lamas, P., Zhang, W., Peshevski, I., Pétursson, H., Kurt, T., Dobrev, N., García-Davalillo, J., Halkia, M., Ferri, S., Gaprindashvili, G., Engström, J. and Keellings, D. 2016. Fatal landslides in Europe. Landslides, Vol. 13: pp. 1545-1554

Heginbottom, J.A., Dubreuil, M.A., Harker, P.T., Caron, A. Paul, P. and Rose, I. 1995. Canada Permafrost; National Atlas of Canada, 5th Edition, Scale 1:7 500 000

Hendry, M., Macciotta, R. and Martin, D. 2015. Effect of Thompson River elevation on velocity and instability of Ripley Slide. Canadian Geotechnical Journal, Vol. 52(3), pp. 257-267

Hermanns, R., Oppikofer, T., Böhme, M., Dehls, J., Yugsi Molina, F. and Penna, I. 2016. Rock slope instabilities in Norway: first systematic hazard and risk classification of 22 unstable rock slopes from northern, western and southern Norway. Landslides and Engineered Slopes. Experience, Theory and Practice, pp. 1107–1114

Hervás J. and Bobrowsky P. 2009. Mapping: Inventories, Susceptibility, Hazard and Risk. In: Landslides – Disaster Risk Reduction: pp. 321-349

Highland, L.M. and Bobrowsky, P. 2008. The landslide handbook – a guide to understanding landslides. U.S. Geological Survey Circular 1325: 129 p.

Holmes, J., Chambers, J., Donohue, S., Huntley, D., Bobrowsky, P., Meldrum, P. Uhlemann, S., Wilkinson, P. and Swift, R. 2018. The Use of Near Surface Geophysical Methods for Assessing the Condition of Transport Infrastructure. Civil Engineering Research Association, Special Issue on Structural Integrity of Civil Engineering Infrastructure, Journal of Structural Integrity and Maintenance, 6 p.

Holmes, J., Chambers, J., Meldrum, P., Wilkinson, B., Williamson, P., Huntley, D., Sattler, K., Elwood., D., Sivakumar, V., Reeves, H. and Donohue, S. 2020. 4-Dimensional electrical resistivity tomography for continuous, near-real time monitoring of a landslide affecting transport infrastructure in British Columbia, Canada. Near Surface Geophysics, 15 p. https://doi.org/10.1002/nsg.12102

Howes, D.E. and Kenk, E. 1997. Terrain classification system for British Columbia (revised edition): a system for the classification of surficial materials, landforms and geological processes of British Columbia. B.C. Ministry of Environment Manual 10: 90 p.

Huntley, D.H. 2008. Landslide geohazard mapping in complex terrains. Geological Survey of Canada, Open File 5747: 16 p.

Huntley, D.H. and Duk-Rodkin, A. 2008. Field recognition, inventory, and analysis of landslides in the Camsell Bend map area, southern Mackenzie River watershed, Northwest Territories. Geological Survey of Canada, Current Research 2008-10: 14 p.

Huntley, D. and Bobrowsky, P. 2014. Surficial geology and monitoring of the Ripley Slide, near Ashcroft, British Columbia, Canada; Geological Survey of Canada, Open File 7531: 21 p.

Huntley, D., Bobrowsky, P., Parry, N., Bauman, P., Candy, C. and Best, M. 2017a. Ripley Landslide: the geophysical structure of a slow-moving landslide near Ashcroft, British Columbia, Canada. Geological Survey of Canada, Open File 8062: 59 p.

Huntley, D., Bobrowsky, P., Charbonneau, F., Journault, J. and Hendry, M. 2017b. Innovative landslide change detection monitoring: application of spaceborne InSAR techniques in the Thompson River valley, British Columbia, Canada. In: Landslide Research and Risk Reduction for Advancing Culture and Living with Natural Hazards, Volume 3, 4th World Landslide Forum (ICL-IPL), Ljubljana, Slovenia 29- May – 2 June 2017, Springer Nature, 13 p.

Huntley, D., Bobrowsky, P., Hendry, M., Macciotta, R., Elwood, D., Sattler, K., Reeves, H., Chambers, J., Meldrum, P. Holmes, J. and Wilkinson, P. 2018a. Using multi-dimensional ERT modelling to provide new insight into the hydrogeological structure of a very slow-moving landslide in glacial sediments, Thompson River valley, British Columbia, Canada. Geological Society of America Annual Meeting, Session T65, Abstract Volume, 1 p.

Huntley, D., Bobrowsky, P., MacLeod, R. and Roberts, N. 2018b. New insights into form and function of very slow-moving landslides from bathymetric surveys of Thompson River, British Columbia Geological Society of America Annual Meeting, Session T53, Abstract Volume, 1 p.

Huntley, D., Bobrowsky, P., Hendry, M., Macciotta, R. and Best, M. 2019a. Multi-technique geophysical investigation of a very slow-moving landslide near Ashcroft, British Columbia, Canada. Journal of Environmental and Engineering Geophysics, Volume 24 (1): pp. 85-108

Huntley, D., Bobrowsky, P., Sattler, K., Elwood, D., Holmes, J., Chambers, J., Meldrum, P. Holmes, J. and Wilkinson, P. Hendry, M. and Macciotta, R. 2019b. PRIME installation in Canada: protecting national railway infrastructure by monitoring moisture in an active landslide near Ashcroft, British Columbia. 32nd SAGEEP, Environmental and Engineering Geophysical Society. Proceedings Volume of the Annual Meeting, Portland, Oregon, USA, 1 p.

Huntley, D., Bobrowsky, P., MacLeod, R., Cocking, R., Joseph, J., Sattler, K., Elwood, D., Holmes, J., Chambers, J., Meldrum, P., Wilkinson, P., Hendry, M., Macciotta, R. 2019c. Geological Survey of Canada, Open File 8548: 1 sheet, https://doi.org/10.4095/314548

Huntley, D., Bobrowsky, P., Hendry, M., Macciotta, R., Elwood, D., Sattler, K., Chambers, J., and Meldrum, P. 2019d. Application of multi-dimensional electrical resistivity tomography datasets to investigate a very slow-moving landslide near Ashcroft, British Columbia, Canada. Landslides, Vol. 16: pp. 1033-1042, https://doi.org/10.1007/s10346-019-01147-1

Huntley, D., Holmes, J., Bobrowsky, Chambers, J., Meldrum, P., Wilkinson, P., Elwood, D., Sattler, K., Hendry, M. and Macciotta, R. 2020a. Hydrogeological and geophysical properties of the very slow-moving Ripley Landslide, Thompson River valley, British Columbia. Canadian Journal of Earth Sciences, Vol 57 (12): 21 p. https://doi.org/10.1139/cjes-2019-0187

Huntley, D., Bobrowsky, P., Cocking, R., Joseph, P., Neelands, N., MacLeod, R., Rotheram-Clarke, D., Usquin, R. and Verluise, F. 2020b. Installation, operation and evaluation of an innovative global navigation satellite system monitoring technology at Ripley Landslide and South Slide, near Ashcroft, British Columbia; Geological Survey of Canada, Open File 8742, 36 p.

Huntley, D., Bobrowsky, P., Rotheram-Clarke, D., MacLeod, R., Cocking, R., and Joseph, J. 2020c. Understanding Plateau landslides: current research in the Thompson River valley, Interior Plateau, British Columbia (2013-2020); Geological Survey of Canada, Open File 8736: 60 p. https://doi:10.4095/326830

Huntley, D., Bobrowsky, P., Rotheram-Clarke, D., Cocking, R., and Joseph, J. 2020d. Understanding Prairie landslides: current research in the Assiniboine River valley, Manitoba-Saskatchewan (2019-2020). Geological Survey of Canada, Open File 8735: 26 p. https://doi:10.4095/326821

Huntley, D., Rotheram-Clarke, D., Cocking, R., Joseph, J. and Bobrowsky, P. 2020e. Understanding Plateau and Prairie Landslides: research plans for the Thompson River valley, British Columbia, and the Assiniboine River valley, Manitoba-Saskatchewan (2020-2025); Geological Survey of Canada, Open File 8743: 25 p.

Huntley, D., Rotheram-Clarke, D., Bobrowsky, P., MacLeod, R., and Brillon, C. 2020f. InSAR investigation of sackung-like features and debris flows in the vicinity of Hawkesbury Island and Hartley Bay, British Columbia, Canada: reducing landslide and tsunami risks for coastal communities and vulnerable infrastructure. Slope Stability 2020, Symposium Special Volume, 10 p. https://doi.org/10.36487/ACG_repo/2025_09

Huntley, D., Rotheram-Clarke, D., Cocking, R., and Joseph, J. 2021a. Landslide change detection monitoring with a benchmarked RADARSAT CONSTELLATION MISSION high temporal resolution dataset. Institute of Electrical and Electronic Engineers, International Geoscience and Remote Sensing Symposium, Special Volume, 4 p.

Huntley, D., Rotheram-Clarke, D., Pon, A., Tomaszewicz, A., Leighton, J., Cocking, R. and Joseph, J. 2021b. Benchmarked RADARSAT-2, SENTINEL-1 and RADARSAT CONSTELLATION MISSION change detection monitoring at North Slide, Thompson River valley, British Columbia: implications for a landslide-resilient national railway network. Canadian Journal of Remote Sensing. https://doi.org/10.1080/07038992.2021.1937968

Huntley, D., Bobrowsky, Rotheram-Clarke, D., MacLeod, R., Cocking, R., Joseph, J., Holmes, J., Donohue, S., Chambers, J., Meldrum, P., Wilkinson, P., Hendry, M. and Macciotta, R. 2021c. Protecting Canada's railway network using remote sensing technologies. Advances in Remote Sensing for Infrastructure, 26 p., Springer International Publishing, https://doi:10.36487/AGC_repo/2025_09

Huntley, D., Bobrowsky, P., MacLeod, R., Cocking, R., Joseph, J. and Rotheram-Clarke, D. 2021d. Ensuring resilient socio-economic infrastructure: field testing innovative differential GNSS-InSAR-UAV monitoring technologies in mountainous terrain near Ashcroft, British Columbia, Canada. *Journal of Mountain Science*, Vol. 18 (1): pp. 1-20; https://doi.org/10.1007/s11629-020-6552-y

Intergovernmental Panel on Climate Change 2014. Working Group II Report: Climate Change 2014 Impacts, Adaptation and Vulnerability. IPCC 5th Assessment Report; https://www.archive.ipcc.ch/

Intergovernmental Panel on Climate Change, 2022. Working Group II Report: Climate Change 2022 Impacts, Adaptation and Vulnerability. IPCC 6th Assessment Report; https://www.ipcc.ch/report/ar6/

Jackson, L.E. 2002. Landslides and landscape evolution in the Rock Mountains and adjacent Foothills area, southwestern Alberta, Canada. In: Catastrophic Landslides: effects, occurrence, and mechanisms. Geological Society of America Reviews; Engineering Geology, Vol. 15: pp. 325-344

Jespersen-Groth, Potthoff, D., Clausen, J., Huisman, D., Kroon, L., Marotí, G. and Nielsen, M. 2009. Disruption management in passenger railway transportation. In: Robust and Online Large-Scale Optimization, Springer-Verlag: pp. 399-421

Johnsen, T. and Brennand, T. 2004. Late-glacial lakes in the Thompson Basin, British Columbia: paleogeography and evolution. Canadian Journal of Earth Sciences, Vol. 41: pp. 1367-1383

Johnson, P.G. and Lacasse, D. 1988. Rock glaciers of the Dalton Range, Kluane Ranges, south-west Yukon Territory, Canada. Journal of Glaciology, Vol. 34: pp. 327-332

Journault, J., Macciotta, R., Hendry, M., Charbonneau, F., Bobrowsky, P., Huntley, D., Bunce, C., and Edwards, T. 2016. Identification and quantification of concentrated movement zones within the Thompson River valley using satellite borne InSAR. Canadian Geotechnical Society, Proceedings Volume of GeoVancouver2016 Annual Meeting, 13 p.

Journault, J. Macciotta, R., Hendry, M., Charbonneau, F., Huntley, D. and Bobrowsky, P. 2018. Measuring displacements of the Thompson River valley landslides, south of Ashcroft, B.C., Canada, using satellite InSAR. Landslides. Vol. 15 (4): pp. 621-636, DOI 10.1007/s10346-017-0900-1

Journeay, M.J., Williams, S.P., and Wheeler, J.O. 2000. Tectonic assemblage map, Vancouver, British Columbia-USA. Geological Survey of Canada, Open File 2948, scale 1:1,000,000

Klassen, R. 1972. Wisconsin events and the Assiniboine and Qu'Appelle valleys of Manitoba and Saskatchewan. Canadian Journal of Earth Sciences, Vol. 9 (5): pp. 544-560

Knox, J.C. 2000. Sensitivity of modern and Holocene floods to climate change. Quaternary Science Reviews, Vol. 19: pp. 439-457

Laimer, H. 2017. Anthropogenically-induced landslides – a challenge for railway infrastructure in mountainous regions. Engineering Geology, Vol. 222: pp. 92-101.

Lévy, S., Jaboyedoff, M., Locat, J. and Demers, D. 2012. Erosion and channel changes as factors of landslides and valley formation in Champlain Sea Clays: the Chacoura River, Quebec, Canada. Geomorphology, Vol 145: pp. 12-18

Lindgren, J., Jonsson, D., Carlsson-Kanyama, A. 2009. Climate adaptation of railways: lessons from Sweden. European Journal of Transportation Infrastructure Research, Vol. 9 (2): pp. 164-181

Locat, A., Leroueil, S., Bemander, S., Demers, D., Jostad, H.P. and Ouehb, L. 2011. Progressive failures in eastern Canadian and Scandinavian sensitive clays. Canadian Geotechnical Journal, Vol. 48: pp. 1696-1712

Lonergan, S. 2004. The human challenges of climate change (Chapter 3). In Coward, H. and Weaver, A.J. (editors); Hard Choices: climate change in Canada; Wilfred Laurier Press, 273 pages, ISBN 0-88920-442-X

Luckman, B.H. and Crockett, K.J. 1977. Distribution and characteristics of rock glaciers in the southern part of Jasper National Park, Alberta. Canadian Journal of Earth Sciences, Vol. 15: pp. 540-550

Macciotta, R., Hendry, M., Martin, D., Elwood, D, Lan, H., Huntley, D., Bobrowsky, P., Sladen, W, Bunce C., Choi, E and Edwards, T. 2014. Monitoring of the Ripley Slide in the Thompson River Valley, B.C. Geohazards 6 Symposium, Proceedings Volume, Kingston, Ontario, Canada

Martinović, K., Gavin, K. and Reale, C. 2016. Development of a landslide susceptibility assessment for a rail network. Engineering Geology, Vol. 215: pp. 1-9.

Mathews, W. and Monger, J. 2010. Roadside geology of southern British Columbia. ISBN 978-1-926613-34-5: 404 p

Maynard, D., Weiland, I., Blais-Stevens, A. and Geertsema, M. 2017. Surficial geology, Hartley Bay, Douglas Channel area, British Columbia, parts of NTS 103-H/6 and 11. Geological Survey of Canada, Natural Resources Canada, https://doi.org/10.4095/299824

Min, D-H. and Yoon, H-K. 2021. Suggestion for a new deterministic model coupled with machine learning techniques for landslide susceptibility mapping. Scientific Reports, Vol. 11:6594, 24 p.

Mollard, J.D. 1977. Regional landslide types in Canada. Reviews in Engineering Geology, Vol. III: pp. 29-41

Mugridge, S-J. and Young, R. 1983. Disintegration of shale by cyclic wetting and drying and frost action. Canadian Journal of Earth Sciences, Vol. 20 (4): pp. 568-576

Nastev, M. 2014. Adapting HAZUS for seismic risk assessment in Canada. Canadian Geotechnical Journal, Vol. 51: pp. 217-222

Petrova, E. 2011. Critical infrastructure in Russia: geographical analysis of accidents triggered by natural hazards. Environmental Engineering Management Journal, Vol. 10 (1): pp. 53-38

Pon, A., Tomaszewicz, A., and Leighton, J. 2020. Monitoring of Thompson River Valley, BC, Canada. Geological Survey of Canada, Unpublished Technical Report and Supplementary Database, 61 p.

Porter, M., Savigny, K., Keegan, T., Bunce, C. and MacKay, C. 2002. Controls on stability of the Thompson River landslides. In: Proceedings of the 55th Canadian Geotechnical Conference: Ground and Water – Theory to Practice, Canadian Geotechnical Society, pp. 1393-1400

Price, L. W. 1991. Subsurface movement on solifluction slopes in the Ruby Range, Yukon Territory, Canada – a 20-year study. Arctic and Alpine Research, Vol. 23: pp. 200-205

Quinn, P.E., Hutchinson, D.J., Diederichs, M.S. and Rowe, R.K. 2010. Regional-scale landslide susceptibility mapping using the weight of evidence method: an example applied to linear infrastructure. Canadian Geotechnical Journal, Vol. 47: pp. 905-927

Quinn, P.E., Hutchinson, D.J., Diederichs, M.S. and Rowe, R.K. 2011. Characteristics of large landslides in sensitive clay in relation to susceptibility, hazard, and risk. Canadian Geotechnical Journal, Vol. 48: pp. 1212-1232

Resource Inventory Committee 1996. Terrain stability mapping in British Columbia: a review and suggested methods for landslide hazard and risk mapping. Resource Inventory Committee Publications, www.publications.gov.bc.ca (URL 2011)

Rodriguez, J., Hendry, M., Macciotta, R., and Evans, T. 2018. Cost-effective Landslide Monitoring GPS: Characteristics, Implementation and Results. Geohazards, Vol. 7: 8 p.

Ronchetti, F., Borgatti, L., Cervi., F., Gorgoni, C., Piccinini, L., Vincenzi, V. and Corsini, A. 2009. Groundwater processes in a complex landslide, northern Apennines, Italy. Natural Hazards and Earth System Science, Vol. 9: pp. 895-904.

Ryder, J.M. 1976. Terrain inventory and Quaternary geology, Ashcroft, British Columbia. Geological Survey of Canada, Paper 74-79: 17 p.

Ryder, J.M., Fulton, R.J. and Clague, J.J. 1991. The Cordilleran Ice Sheet and the Glacial Geomorphology of Southern and Central British Colombia. Géographie physique et Quaternaire 45: pp. 365–377, doi:10.7202/032882ar

Sa'adin, S., Kaewunruen, S. and Jaroszweski, D. 2016. Risks of climate change with respect to the Singapore-Malaysia high-speed rail system. Climate, Vol. 4 (65): 21 p.

Samsonov, S.V., Feng, W. and Short, N. 2017. DInSAR products and applications for the RADARSAT Constellation Mission. Geomatics Canada, Open File 37, 19 p.

Sattler, K., Elwood, D., Hendry, M, Macciotta, R., Huntley, D., Bobrowsky, P. and Meldrum, P. 2018. Real-time monitoring of soil water content and suction in slow-moving landslide. GeoEdmonton 2018, Proceedings Paper, 8 p.

Sattler, K., Elwood, D., Hendry, M., Huntley, D., Holmes, J., and Wilkinson, P. 2020. Effect of pore-pressure dynamics on progressive failure in clay shale landslides. Landslides, 17 p. https://doi.org/10.1007/978-3-030-60706-7_45

Sattler, K., Elwood, D., Hendry, M., Berscheid, B., Marcotte, B., Abdulrazagh, P. and Huntley, D. 2021. Field collection of geotechnical measurements for remote or low-cost data-logging requirements. Geotechnical Testing Journal, Vol. 45 (1) https://doi.org/10.1520/GTJ20200323

Sauchyn, D.J. and Nelson, H.L. 1999. Origin and erosion of the Police Point landslide, Cypress Hills, Alberta. In Holocene climate and environmental change in the Palliser Triangle: a geoscientific context for evaluation the impacts of climate change on the southern Canadian prairies; Lemmen, D.S. and Vance, R.E. (editors); Geological Survey of Canada, Bulletin 534: pp. 257-265

Sauer, K. 1978. The engineering significance of glacier ice-thrusting. Canadian Geotechnical Journal, Vol. 15 (4): pp. 457-472

Schafer, M., Macciotta, R., Hendry, M., Martin, D., Bobrowsky, P., Huntley, D., Bunce, C. and Edwards, T. 2015. Instrumenting and Monitoring a Slow Moving Landslide. GeoQuebec 2015 Paper, 7 p.

Schetselaar, E., Harris, J., Lynds, T. and de Kemp, E. 2007. Remote Predictive Mapping 1. Remote Predictive Mapping (RPM): A Strategy for Geological Mapping of Canada's North. Geoscience Canada, Vol. 34 (3/4): pp 93-111

Short, N., LeBlanc, A-M., Sladen, W., Oldenborger, G., Mathon-Dufour, V. and Brisco, B. 2014. RADARSAT-2 D-InSAR for ground displacement in permafrost terrain, validation from Iqaluit Airport, Baffin Island, Canada. Remote Sensing of Environment, Vol. 141:pp. 40-51

Shugar, D. and Clague, J.J. 2011. The sedimentology and geomorphology of rock avalanche deposits on glaciers. Sedimentology, Vol. 58: pp. 1762-1783

Schuster, R. and Fleming, R. 1986. Economic losses and fatalities due to landslides. Bulletin of the Association of Engineering Geology, Vol. XXIII (1): pp. 11-28.

Smith, S.L. and Burgess, M.M. 2011. Permafrost and Climate Interactions. In Singh, V. P. and Singh, P. and Haritashya, U.K. (editors); Encyclopedia of Earth Sciences, Vol. 46, Pt. 15: pp. 852-857

Soeters, R. and van Westen, C.J. 1996. Slope instability recognition, analysis and zonation. In: Landslides, investigation and mitigation. Transportation Research Board, National Research Council, Special Report 247: pp. 129-177

Stacey, C.D., Lintern, D.G., Shaw, J. and Conway, K.M. 2020. Slope stability hazard in a fjord environment: Douglas Channel. Geological Society, London, Special Publications 500 (1): pp. 427-451

Stanton, R.B. 1898. The great land-slides on the Canadian Pacific Railway in British Columbia. Proceedings of Civil Engineers, Vol. 132 (2), pp. 1–48

St. George., S. 2007. Stream flow in the Winnipeg River basin, Canada: trends, extremes and climate linkages. Journal of Hydrology, Vol. 332: pp. 396-411

Sun, S., Wang, J. and Zheng, J. 2013. Analysis of a railway embankment landslide induced by the Wenchuan Earthquake, China Soil Mechanics Foundation, Vol. 15 (2): pp. 56-60

Tappenden, K.M. 2016. Impact of Climate Variability on Landslide Activity in the Thompson River Valley Near Ashcroft, B.C. In: Proceedings of the 69th Canadian Geotechnical Conference, October 2-5, 2016, Vancouver, Canada

Tavenas, F. and Leroueil, S. 1981. Creep and failure of slopes in clays. Canadian Geotechnical Journal, Vol. 18: pp. 106-120

Thompson, S.C., Clague, J.J. and Evans, S.G. 1997. Holocene activity of the Mt. Currie Scarp, Coast Mountains, British Columbia, and implications for its origin. Environmental and Engineering Geoscience, Vol. III: pp. 329-348

Urgeles, R., Locat, J., Lee, H.J. and Martin, F. 2002. The Saguenay Fjord, Quebec, Canada: integrating marine geotechnical and geophysical data for spatial seismic slope stability and hazard assessment. Marine Geology, Vol. 185: pp. 319-340

Valentin, C., Poesen, J. and Li, Y. 2005. Gully erosion: impacts, factors and control. Cantena, Vol. 63: pp. 132-153

VanDine, D. 1983. Drynoch landslide, British Columbia – a history. Canadian Geotechnical Journal, Vol. 20: pp. 82-103

VanDine, D.F. 1985. Debris flows and debris torrents in the southern Cordillera. Canadian Geotechnical Journal, Vol. 22: pp. 44-68

VanDine, D.F. and Bovis, M. 2002. History and goals of Canadian debris flow research, a review. Natural Hazards, Vol. 26: pp. 69-82

Wang, B. and Lesage, K. 2007. Impact of climate change on slope stability in permafrost regions. Proceedings of the 8th International Symposium on Cold Region Development,11 p.

Weaver, A.J. 2004. The Science of Climate Change (Chapter 2). In Coward, H. and Weaver, A.J. (editors); Hard Choices: climate change in Canada; Wilfred Laurier Press, 273 pages, ISBN 0-88920-442-X

Wegmüller, U., Werner, C., Wiesmann, A. and Frey O. 2019. GAMMA, Version 1.6, computer software, Gamma Remote Sensing, Gumligen, http://www.gamma-rs.ch [URL 2020]

Wieczorek, G.F., Eaton, L.S., Morgan, B.A., Wooten, R.M. and Morrissey, M. 2009. An examination of selected historical rainfall-induced debris-flow evens within the central and southern Appalachian Mountains of the Eastern United States. U.S. Geological Survey Open File Report 2009-1155: 25 p.

Wolfe, S.A. 1997. Impact of increased aridity on sand dune activity in the Canadian Prairies. Journal of Arid Environments, Vol. 36: pp. 421-432

Wolfe, S.A. 2001. Eolian activity. In A synthesis of geological hazards in Canada; Brooks, G R (ed.); Geological Survey of Canada, Bulletin 548: pp. 231-240, 1 sheet

Yang, H., Dijst, M., Witte, P., van Ginkel, H. and Wang, J. 2019. Comparing passenger flow and time schedule data to analyse high-speed railways and urban networks in China. Urban Studies, Vol. 56 (6): pp. 1267-1287.

Young, H. and Moore, P. 1994. Composition and depositional environment of the silicaceous Odanah Member (Campanian) of the Pierre Shale in Manitoba. Geological Society of America, Special Papers, Vol. 287: pp. 175-196

APPENDIX 1
Overview Timetable for Field Investigations (2020-2025)

Project activity (collaborators)	2020-2021 COMPLETED	2021-2022 COMPLETED	2022-2023 IN PROGRESS	2023-2024	2024-2025
Terrain mapping [A, B, C] surficial geology, geophysics (GSC, BGS, MGS)	Image acquisition; Cloud storage and processing Maintenance	Image acquisition; Desktop mapping; ERT; Benchmarking	Image acquisition; Desktop mapping; ERT; Seismic; Bathymetry; Benchmarking	Image acquisition; Desktop mapping; ERT; Seismic; Bathymetry; Benchmarking	Decommissioning; Image acquisition; Desktop mapping
GNSS [A, B, C] fixed and mobile (GSC, UA, USASK, MGS)	Data acquisition; Cloud storage and processing; Maintenance	Data acquisition; Cloud storage and processing; Interpretation; Maintenance	Data acquisition; Cloud storage and processing; Interpretation; Maintenance	Data acquisition; Cloud storage and processing; Interpretation; Maintenance	Decommissioning; Cloud storage and processing; Interpretation
UAV overflights [A, B, C] (GSC, UA, USASK)	Data and software acquisition; Cloud storage and processing	Data acquisition; Cloud storage and processing; Interpretation	Data acquisition; Cloud storage and processing; Interpretation	Data acquisition; Cloud storage and processing; Interpretation	Decommissioning; Cloud storage and processing; Interpretation
InSAR* [A, B, C] data, scenes (CN, CPR, 3v Geomatics, CCMEO)	Corner reflectors acquisition; Data acquisition; Cloud storage and processing	Corner reflector installation; Data acquisition; Cloud storage and processing; Interpretation	Data acquisition; Cloud storage and processing; Interpretation	Data acquisition; Cloud storage and processing; Interpretation	Decommissioning; Cloud storage and processing; Interpretation
Climate station data [A, B, C] climate variables (GSC, MGS, USASK)	Data acquisition Cloud storage and processing Maintenance	Component acquisitions; Climate station installation; Data acquisition; Cloud storage and processing; Interpretation; Maintenance	Climate station installation; Data acquisition; Cloud storage and processing; Interpretation; Maintenance	Data acquisition; Cloud storage and processing; Interpretation; Maintenance	Decommissioning; Cloud storage and processing; Interpretation
Boreholes and soils* [A, B, C] Matric suction, piezometers, SSI, SAA (GSC, UA, USASK, MGS)	Soil monitoring acquisitions; Interpretation; Maintenance	Borehole drilling*; Borehole installations; Downhole geophysics Data acquisition; Cloud storage and processing; Interpretation; Maintenance	Borehole installations; Data acquisition; Cloud storage and processing; Interpretation Maintenance	Borehole installations; Data acquisition; Cloud storage and processing; Maintenance	Decommissioning; Cloud storage and processing; Interpretation
Publications geoscience outreach (GSC, UA, USASK, MGS)	Conference abstracts Open file / Annual report Workshop Presentation Proceedings paper Book chapters Journal papers	Conference abstracts Proceedings paper Open file / Annual report Workshop Presentation	Conference abstracts Proceedings paper Open file / Annual report Workshop Presentation	Conference abstracts Journal paper Open file / Annual report Workshop Presentation	Conference abstracts Journal paper Geoscience Map Open file / Annual report Workshop Presentation

*Expected that partners will contribute in-kind funding in support for selected activities. Superscript [A] – project activities in the Thompson River valley. Superscript [B] – project activities in the Assiniboine-Qu'Appelle river valleys. Beyond 2022, other research sites may be included in the study. Superscript [C] – project activities elsewhere (e.g., Kelowna, Kitimat-Terrace-Prince Rupert).

APPENDIX 2

Work Plan (2020-2025)

COMPLETED Fiscal Year 2020/21 Research Activities (IMOU-5170)

Project outputs: Conference abstracts, Open file / Annual report, Workshop presentation, Book chapters, Proceedings papers, Journal papers

ACTIVITY GROUP 1: Geohazard Mapping and Borehole Studies

Terrain mapping and fieldwork: Logistical support for ground-truth fieldwork in Thompson River Valley (TRV) and Assiniboine River Valley (ARV); GNSS surveys; PRIME; Desktop mapping; Benchmarking DSMs (in-kind support by British Geological Survey - BGS, Manitoba Geological Survey - MGS)

Borehole and soil studies: Procurement of soil sampling equipment and moisture sensors; Logistical support for fieldwork, workshops and conferences (in-kind support by CN, CP, University of Alberta - UA, University of Saskatchewan - USASK)

ACTIVITY GROUP 2:
Change detection with InSAR, GNSS, UAVs and Weather Stations

InSAR monitoring: Procurement of InSAR corner reflectors and supporting equipment for installation; Acquisition of (multispectral/hyperspectral) satellite imagery in TRV, processing, analyses and archiving; Logistical support for ground-truthing in TRV, workshops and conferences (in-kind support by 3vGEOMATICS - 3vG, Canada Centre for Mapping and Earth Observation - CCMEO)

GNSS monitoring: Procurement of Geocube components from Ophelia (France) and GNSS components and software for in-house system; Logistical support for systems maintenance, fieldwork (TRV and ARV), workshops and conferences (in-kind support by CN, CP, UA, USASK, MGS)

UAV change detection: Procurement of UAVs, software, components enabling high-resolution RGB, LiDAR and multispectral inventories; GigaPAN photogrammetry; Logistical supporting for fieldwork (TRV and ARV), workshops, conferences (in-kind support by CN, CP, UA, USASK, MGS)

Monitoring climate change variables: Logistical support for routine maintenance of equipment, replacement and new units, replacing and augmentation of power sources, data storage enhancements with remote access to data transfer (TRV and ARV); logistical support for workshops and conferences (in-kind support by CN, CP, UA, USASK)

COMPLETED Fiscal Year 2021/22 Research Activities (IMOU-5170)

Project outputs: Conference abstracts, Open file / Annual report, Workshop presentation, Book chapters, Proceedings papers, Journal papers

ACTIVITY GROUP 1: Geohazard Mapping and Borehole Studies

Terrain mapping and fieldwork: Logistical support for ground-truth fieldwork in TRV; GNSS and UAV surveys; Desktop mapping of ARV, Okanagan valley (OKV) and Kitimat-Terrace-Prince Rupert (KTP); Cloud storage and processing (in-kind support by SPEXI Geospatial) Logistical support for workshops and conferences (in-kind support by CN, CP, UA, USASK)

ACTIVITY GROUP 2:
Change detection with InSAR, GNSS, UAVs and Weather Stations

InSAR monitoring: Processing, analyses, archiving and interpretation of satellite imagery in TRV, ARV, OKV and KTP; procurement of satellite InSAR corner reflectors; Logistical support for ground-truthing in TRV; Cloud storage and processing; Logistical support for workshops and conferences (in-kind support by CCMEO)

GNSS monitoring: Data acquisition; Cloud storage and processing; Logistical support for systems maintenance, fieldwork (TRV); Logistical support for workshops and conferences (in-kind support by CN, CP, UA, USASK)

UAV change detection and RPAS testing: Procurement of UAV software, components enabling high-resolution optical imagery; Logistical supporting for fieldwork (TRV); Cloud storage and processing; Interpretation; logistical support for workshops and conferences (in-kind support by CN, CP, UA, USASK)

Monitoring climate change variables: Procurement of climate monitoring station (air pressure, temperature, rain gauge, snow sensor, anemometer and wind vane, insolation), moisture meters, piezometers, supporting hardware, software, data loggers, batteries, solar panels and data communication components; Logistical support for routine maintenance of equipment, replacement and new units, replacing and augmentation of power sources, data storage enhancements with remote access to data transfer (TRV and OKV); logistical support for workshops and conferences (in-kind support by CN, CP, UA, USASK)

IN PROGRESS Fiscal Year 2022/23 Research Activities (IMOU-5170)

Project outputs: Conference abstracts, Open file / Annual report, Workshop presentation, Book chapters, Proceedings papers, Journal papers

ACTIVITY GROUP 1: Geohazard Mapping and Borehole Studies

Terrain mapping and fieldwork: Logistical support for ground-truth fieldwork in TRV, ARV, OKV and KTP; GNSS surveys; sample analyses, desktop mapping; ERT, Seismic; Bathymetry; Benchmarking; Cloud storage and processing (in-kind support by BGS, SPEXI Geospatial)

Geophysical, borehole and soil studies: Procurement of borehole inclinometers and piezometers for test pits and observation wells at CN and CP sites in TRV and ARV; Installation of Ultrawide Broadband Seismic Vibration Monitoring System on North Slide; Maintenance or borehole inclinometers and piezometers, installation, data acquisition, downhole geophysics, sample analyses, and monitoring of observation wells at CN and CP sites in TRV, ARV, OKV and KTP; Cloud storage and processing; Interpretation; Logistical support for workshops and conferences (in-kind support by CN, CP, UA, USASK)

ACTIVITY GROUP 2:
Change detection with InSAR, GNSS, UAVs and Weather Stations

InSAR monitoring: Processing, analyses, archiving and interpretation of satellite imagery in TRV and ARV; Logistical support for ground-truthing in TRV, ARV, OKV and KTP; cloud storage and processing; Logistical support for workshops and conferences (in-kind support by CCMEO)

GNSS monitoring: Data acquisition; Cloud storage and processing; Logistical support for systems maintenance, fieldwork (TRV, ARV, OKV and KTP); Logistical support for workshops and conferences (in-kind support by CN, CP, UA, USASK, MGS)

UAV change detection: RGB, NIR, LiDAR and multispectral data acquisition; Logistical supporting for fieldwork (TRV, ARV, OKV and KTP); Cloud storage and processing; Interpretation; Logistical support for workshops and conferences (in-kind support by CN, CP, UA, USASK, MGS)

Monitoring climate change variables: Installation of weather station (air pressure, temperature, rain gauge, snow sensor, anemometer and wind vane; insolation), moisture meters, piezometers, supporting hardware, software, data loggers, batteries, solar panels and data communication components; Logistical support for routine maintenance of equipment, replacement and new units, replacing and augmentation of power sources, data storage enhancements with remote access to data transfer (TRV, ARV, OKV and KTP); Cloud storage and processing; Interpretation; Logistical support for workshops and conferences (in-kind support by CN, CP, UA, USASK)

Fiscal Year 2023/24 Research Activities (IMOU-5170)

Project outputs: Conference abstracts, Open file / Annual report, Workshop presentation, Book chapters, Proceedings papers, Journal papers

ACTIVITY GROUP 1: Geohazard Mapping and Borehole Studies

Terrain mapping and fieldwork: Logistical support for ground-truth fieldwork in TRV, ARV, OKV and KTP; GNSS surveys; sample analyses, desktop mapping; ERT, Seismic; Bathymetry; Benchmarking; Cloud storage and processing (in-kind support by BGS, MGS)

Geophysical, borehole and soil studies: Maintenance of UBSV sensors, borehole inclinometers and piezometers, data acquisition at CN and CP sites in TRV, ARV, OKV and KTP; Cloud storage and processing, Interpretation; Logistical support for workshops and conferences (in-kind support by CN, CP, UA, USASK)

ACTIVITY GROUP 2:
Change detection with InSAR, GNSS, UAVs and Weather Stations

InSAR monitoring: Processing, analyses, archiving and interpretation of satellite imagery in TRV and ARV; Logistical support for ground-truthing in TRV, ARV, OKV and KTP; Cloud storage and processing; Logistical support for workshops and conferences (in-kind support by 3vG, CCMEO)

GNSS monitoring: Data acquisition; cloud storage and processing; Logistical support for systems maintenance, fieldwork (TRV, ARV, OKV and KTP); Logistical support for workshops and conferences (in-kind support by CN, CP, UA, USASK, MGS)

UAV change detection: RGB, NIR, LiDAR and multispectral data acquisition; Logistical supporting for fieldwork (TRV, ARV, OKV and KTP); Cloud storage and processing; Interpretation; logistical support for workshops and conferences (in-kind support by CN, CP, UA, USASK, MGS)

Monitoring climate change variables: Data acquisition (air pressure, temperature, rain gauge, snow sensor, anemometer and wind vane, insolation, moisture meters, piezometers); logistical support for routine maintenance of equipment (TRV, ARV, OKV and KTP); Cloud storage and processing; Interpretation; Logistical support for workshops and conferences (in-kind support by CN, CP, UA, USASK, MGS)

Fiscal Year 2024/25 Research Activities (IMOU-5170)

Project outputs: Conference abstracts, Open file / Annual report, Workshop presentation, Book chapters, Proceedings papers, Journal papers

ACTIVITY GROUP 1: Geohazard Mapping and Borehole Studies

Terrain mapping and fieldwork: Logistical support for decommissioning installations; Desktop mapping; Cloud storage and processing (in-kind support by BGS, MGS)

Geophysical, borehole and soil studies: Maintenance and decommissioning of UBSV sensors, borehole inclinometers and piezometers, data acquisition at CN and CP sites in TRV, ARV, OKV and KTP; Cloud storage and processing; Interpretation; logistical support for workshops and conferences (in-kind support by CN, CP, UA, USASK)

ACTIVITY GROUP 2:
Change detection with InSAR, GNSS, UAVs and Weather Stations

InSAR monitoring: Archiving and interpretation of satellite imagery in TRV and ARV; cloud storage and processing; logistical support for workshops and conferences (in-kind support by 3vG, CCMEO)

GNSS monitoring: Logistical support for decommissioning GNSS installations (TRV, ARV, OKV and KTP); Cloud storage and processing; Logistical support for systems maintenance and decommissioning fieldwork (TRV, ARV, OKV and KTP); Logistical support for workshops and conferences (in-kind support by CN, CP, UA, USASK, MGS)

UAV change detection: RGB, NIR, LiDAR and multispectral data acquisition; Logistical supporting for fieldwork (TRV, ARV, OKV and KTP); Cloud storage and processing; Interpretation; Logistical support for workshops and conferences (in-kind support by CN, CP, UA, USASK, MGS)

Monitoring climate change variables: Logistical support for decommissioning weather stations, moisture meters, piezometers (TRV, ARV, OKV and KTP); Cloud storage and processing; Interpretation; Logistical support for workshops and conferences (in-kind support by CN, CP, UA, USASK, MGS)

APPENDIX 3

Publications Released in 2021-2022

1. Huntley, D., Rotheram-Clarke, D., Cocking, R., and Joseph, J. 2021a. Landslide change detection monitoring with a benchmarked RADARSAT CONSTELLATION MISSION high temporal resolution dataset. Institute of Electrical and Electronic Engineers, International Geoscience and Remote Sensing Symposium, Special Volume, 4 p.

2. Huntley, D., Rotheram-Clarke, D., Pon, A., Tomaszewicz, A., Leighton, J., Cocking, R. and Joseph, J. 2021b. Benchmarked RADARSAT-2, SENTINEL-1 and RADARSAT CONSTELLATION MISSION change detection monitoring at North Slide, Thompson River valley, British Columbia: implications for a landslide-resilient national railway network. Canadian Journal of Remote Sensing. https://doi.org/10.1080/07038992.2021.1937968

3. Huntley, D., Bobrowsky, Rotheram-Clarke, D., MacLeod, R., Cocking, R., Joseph, J., Holmes, J., Donohu S., Chambers, J., Meldrum, P., Wilkinson, P., Hendry, M. and Macciotta, R. 2021c. Protecting Canada's railway network using remote sensing technologies. Advances in Remote Sensing for Infrastructure, 26 p., Springer International Publishing, https://doi:10.36487/AGC_repo/2025_09

4. Huntley, D., Bobrowsky, P., MacLeod, R., Cocking, R., Joseph, J. and Rotheram-Clarke, D. 2021d. Ensuring resilient socio-economic infrastructure: field testing innovative differential GNSS-InSAR-UAV monitoring technologies in mountainous terrain near Ashcroft, British Columbia, Canada. *Journal of Mountain Science*, Vol. 18 (1): pp. 1-20; https://doi.org/10.1007/s11629-020-6552-y

5. Sattler, K., Elwood, D., Hendry, M., Berscheid, B., Marcotte, B., Abdulrazagh, P. and Huntley, D. 2021. Field collection of geotechnical measurements for remote or low-cost data-logging requirements. Geotechnical Testing Journal, Vol. 45 (1) https://doi.org/10.1520/GTJ20200323

APPENDIX 4

List of Key Acronyms in Open File Report

BC	British Columbia
BGS	British Geological Survey
BVLOS	Beyond Visual Line of Sight
CN	Canadian National Railways
CP	Canadian Pacific Railways
DEM	Digital Elevation Model
DInSAR	Differential Interferometric Synthetic Aperture Radar
DSM	Digital Surface Model
GCP	Ground Control Point
GPS	Global Positioning System
GSC	Geological Survey of Canada
ICL	International Consortium on Landslides
IMOU	Inter-Departmental Memorandum of Understanding
InSAR	Interferometric Synthetic Aperture Radar
IPL	International Program on Landslides
IUGS	International Union of Geological Sciences
LiDAR	Light Detection and Ranging
LoS	Line of Sight
MN	Manitoba
NRCAN	Natural Resources Canada
PRIME	Proactive Infrastructure Monitoring and Evaluation
RCM	RADARSAT Constellation Mission
RGHRP	Railway Ground Hazard Research Program
RPAS	Remote Piloted Aircraft Systems
RPM	Remote Predictive Mapping
RS2	RADARSAT 2
RTK-GNSS	Real Time Kinematic Global Navigation Satellite System
SAR	Synthetic Aperture Radar

S1	Sentinel 1
SFM	Structure from Motion
SK	Saskatchewan
SRTM	Shuttle Radar Topographic Mission
TC-IC	Transport Canada Innovation Centre
UA	University of Alberta
UAV	Unoccupied Aerial Vehicle
USASK	University of Saskatchewan
VTOL	Vertical Take Off and Landing